

INFORMATION TO USERS

The most advanced technology has been used to photograph and reproduce this manuscript from the microfilm master. UMI films the original text directly from the copy submitted. Thus, some dissertation copies are in typewriter face, while others may be from a computer printer.

In the unlikely event that the author did not send UMI a complete manuscript and there are missing pages, these will be noted. Also, if unauthorized copyrighted material had to be removed, a note will indicate the deletion.

Oversize materials (e.g., maps, drawings, charts) are reproduced by sectioning the original, beginning at the upper left-hand corner and continuing from left to right in equal sections with small overlaps. Each oversize page is available as one exposure on a standard 35 mm slide or as a 17" × 23" black and white photographic print for an additional charge.

Photographs included in the original manuscript have been reproduced xerographically in this copy. 35 mm slides or 6" × 9" black and white photographic prints are available for any photographs or illustrations appearing in this copy for an additional charge. Contact UMI directly to order.



300 North Zeeb Road, Ann Arbor, MI 48106-1346 USA

Order Number 8801699

**Studies of the interactions of chiral ruthenium(II) complexes
with DNA**

Danishefsky, Avis Tchiya, Ph.D.

City University of New York, 1987

Copyright ©1987 by Danishefsky, Avis Tchiya. All rights reserved.

U·M·I
300 N. Zeeb Rd.
Ann Arbor, MI 48106



PLEASE NOTE:

In all cases this material has been filmed in the best possible way from the available copy. Problems encountered with this document have been identified here with a check mark .

1. Glossy photographs or pages
2. Colored illustrations, paper or print _____
3. Photographs with dark background
4. Illustrations are poor copy _____
5. Pages with black marks, not original copy _____
6. Print shows through as there is text on both sides of page _____
7. Indistinct, broken or small print on several pages
8. Print exceeds margin requirements _____
9. Tightly bound copy with print lost in spine _____
10. Computer printout pages with indistinct print _____
11. Page(s) _____ lacking when material received, and not available from school or author.
12. Page(s) _____ seem to be missing in numbering only as text follows.
13. Two pages numbered _____. Text follows.
14. Curling and wrinkled pages _____
15. Dissertation contains pages with print at a slant, filmed as received
16. Other _____





Studies of the Interactions of Chiral Ruthenium(II) Complexes with DNA

by

Avis T. Danishefsky

A dissertation submitted to the Graduate Faculty in Biochemistry in
partial fulfillment of the requirements for the degree of Doctor of
Philosophy, The City University of New York.

1987

c 1987

Avis T. Danishefsky

All Rights Reserved

This manuscript has been read and accepted for the Graduate Faculty in Biochemistry in satisfaction of the dissertation requirement for the degree of Doctor of Philosophy.

August 11, 1987
Date

William Rooney
Chair of Examining Committee

August 11, 1987
Date

Trout Schultz
Executive Officer

Trout Schultz
Jacqueline Bosh
King L. Gyer
Charlotte Russell
Supervisory Committee

Abstract

Studies of the Interactions of Chiral Ruthenium(II) Complexes with DNA

by

Avis T. Danishefsky

Adviser: Professor Jacqueline K. Barton

We have investigated the interactions of chiral polypyridyl complexes of ruthenium(II) with DNA. The ultimate goal of these studies is to develop these, or similar complexes, as probes or modifiers of DNA with particular conformational or sequence specificities. Chiral complexes are employed because the relative affinity of two enantiomers can reflect the conformation of the helical DNA. Moreover, the well characterized spectroscopic characteristics of the ruthenium(II) complexes provide a handle by which the interactions of these molecules with DNA can be monitored.

Enhancement of the emission of $\text{Ru}(1,10\text{-phenanthroline})_3^{2+}$ and $\text{Ru}(4,7\text{-diphenylphenanthroline})_3^{2+}$ is observed upon binding to DNA. Emission titrations of $\text{Ru}(\text{phen})_3^{2+}$ with calf thymus DNA illustrate that greater enhancement is observed for the Δ enantiomer than for the Λ enantiomer, consistent with our model of an intercalative mode of binding. The degree of enantioselectivity observed was dependent on DNA base composition, which may reflect the different modes of binding of $\text{Ru}(\text{phen})_3^{2+}$ to these various sites as well as differences in structures of the binding sites.

We have also studied interactions of the complex, $\text{Ru}(\text{phen})_2\text{Cl}_2$ with DNA.

Coordination of ruthenium(II) to DNA lends a sequence selectivity to the binding as well as a greater degree of stability of the bound adduct as compared to that of the tris chelate complex.

Binding studies indicate a preference for G·C containing sequences. A binding preference for the Λ enantiomer was observed in most cases. Of the polynucleotides examined, only the alternating polymer poly(dG-dC)·poly(dG-dC) displayed a binding preference for the Δ enantiomer. Similar degrees of enantioselectivity in binding were observed for poly(dG)·poly(dC) and calf thymus DNA suggesting that the binding sites on these two polynucleotides are structurally similar. A model of the bound adduct is proposed based on these observations and on spectroscopic data.

Photochemical reactions of the ruthenium(II) complexes with DNA have also been observed. Irradiation of Ru(phen)₂Cl₂ in the presence of DNA increases the rate of binding, though the mode of binding appears to be similar to that of the thermal reaction. Photocleavage of DNA in the presence of Ru(phen)₃²⁺ and Ru(phen)₂Cl₂ has also been observed.

Acknowledgements

I wish to thank Professor Jacqueline K. Barton for suggesting these studies and directing their execution. More importantly, I gratefully acknowledge the guidance and encouragement which she so generously gave me throughout my graduate career.

I wish to acknowledge the many rewarding friendships I had the good fortune to make with my fellow graduate students in Dr. Barton's research group. I thank them all for encouragement, insight, and assistance in ways too numerous to mention. I shall always fondly recall our discussions on matters chemical and less exalted.

Dedicated, with much love and many thanks, to my parents

Table of Contents

<u>Topic</u>	<u>page</u>
Approval Page	iii
Abstract	iv
List of Tables	x
List of Figures	ix
List of Abbreviations	xvi
Chapter 1: Introduction	1
References	15
Chapter 2: Luminescence Studies of the Interactions of Tris Chelate Ruthenium(II) Complexes with DNA	
Introduction	19
Experimental Procedures	21
Results	30
Discussion	39
References	54
Chapter 3: Characterization of the Binding of Ru(phen) ₂ Cl ₂ to DNA	
Introduction	57
Experimental Procedures	58
Results	66
Discussion	100
References	112

8. Chapter 4: Photochemical Reactions of $\text{Ru}(\text{phen})_2\text{Cl}_2$ and $\text{Ru}(\text{phen})_3^{2+}$ with DNA

Introduction	115
Experimental Procedures	117
Results	120
Discussion	129
References	138

List of Tables

<u>Table</u>	<u>Page</u>
Chapter 1	
Table 1. Groove dimensions of nucleic acids	4
Chapter 3	
Table 1. Comparison of the molar ellipticities of $\text{Ru}(\text{phen})_3^{2+}$ and $\text{Ru}(\text{phen})_2\text{Cl}_2$ at 270 nm	73
Table 2. Enantiomeric preferences of the binding of $\text{Ru}(\text{phen})_2\text{Cl}_2$	75

List of Figures

<u>Figure</u>	<u>Page</u>
 Chapter 1	
1. Illustrations of DNA in the A, B, and Z conformation	2
2. Main chain torsional angles of DNA	3
3. Diagram of slide, twist, roll and propeller twist of nucleotides	4
4. Enantiomers of Ru(phen) ₃ ²⁺	14
5. Enantiomers of Ru(phen) ₂ Cl ₂	14
 Chapter 2	
1a. C.D. spectra of enantiomers of Ru(phen) ₃ ²⁺	24
1b. C.D. spectra of enantiomers of Ru(dip) ₃ Cl ₂	25
1c. C.D. spectrum of Ru(dip) ₃ ²⁺ in the presence of excess antimony- D-tartrate	27
2. Proton NMR spectra of Ru(dip) ₃ ²⁺ in the presence of Eu(tfc) ₃	28
3. Emission spectra of Ru(phen) ₃ ²⁺	31
4. Excited state decays of Ru(phen) ₃ ²⁺ in the presence and absence of DNA	33
5. Luminescence titration of enantiomeric Ru(phen) ₃ ²⁺ with calf thymus DNA	34
6. Emission spectra of enantiomeric Ru(phen) ₃ ²⁺ in the presence and absence of DNA	35

7. Luminescence titrations of enantiomeric $\text{Ru}(\text{phen})_3^{2+}$ with poly(dG-dC)·poly(dG-dC)	37
8. Luminescence titrations of enantiomeric $\text{Ru}(\text{phen})_3^{2+}$ with poly(dA-dT)·poly(dA-dT)	38
9. Emission spectra of $\text{Ru}(\text{dip})_3^{2+}$ free and bound to DNA	40
10. Luminescence titrations of $\text{Ru}(\text{dip})_3^{2+}$ with synthetic polynucleotides	41
11. Diagrams of $\text{Ru}(\text{phen})_3^{2+}$ intercalated into B-DNA.	42
12. Diagram of groove binding of the Λ enantiomer into B-DNA	46

Chapter 3

1. Proton NMR spectra of $\text{Ru}(\text{phen})_2\text{Cl}_2$ and $\text{Ru}(5,6\text{-dimethylphenanthroline})_2\text{Cl}_2$	60
2. Proton NMR spectra of $\text{Ru}(\text{phen})_2(\text{NH}_3)_2^{2+}$ and $\text{Ru}(\text{phen})_2(\text{py})_2^{2+}$	62
2a. Proton NMR spectrum of the major products of the reaction of $\text{Ru}(\text{phen})_2\text{Cl}_2$ with 2' deoxyguanosine	63
3. Time course of $\text{Ru}(\text{phen})_2\text{Cl}_2$ binding to calf thymus DNA	67
4. Proton NMR spectra of $\text{Ru}(\text{phen})_2\text{Cl}_2$ as a function of NaCl concentration	69
5a. C.D. spectrum of free $\text{Ru}(\text{phen})_2\text{Cl}_2$	70
5b. Enrichment of $\text{Ru}(\text{phen})_2\text{Cl}_2$ as a function of f_{bound}	70
6. Sequence preferences of $\text{Ru}(\text{phen})_2\text{Cl}_2$ binding to DNA	74
7. Effect of bound $\text{Ru}(\text{phen})_2\text{Cl}_2$ on the electrophoretic mobility of pBR322 DNA	77
8. C.D. spectra of poly(dG-dC)·poly(dG-dC) illustrating the effect	

of non-covalent binding of Ru(phen) ₂ Cl ₂ to this DNA	78
9. C.D. spectra of poly(dG-dC)·poly(dG-dC) illustrating the effect of coordination of the ruthenium complex to this DNA	79
10. C.D. spectra of poly(dG-dC)·poly(dG-dC) in Z-form illustrating the effect of coordination of the ruthenium complex to DNA	80
11. Resonance Raman spectra of Ru(phen) ₂ Cl ₂ free and bound to DNA and spectra of Ru(phen) ₂ NH ₃ ²⁺ and Ru(phen) ₂ (py) ₂ ²⁺	82
12a. Visible absorbance spectrum of Ru(phen) ₂ Cl ₂ before and after addition of DNA	83
12b. Effect of incubation with DNA over time on the visible absorbance spectrum of Ru(phen) ₂ Cl ₂	84
13. Visible absorbance spectra of complexes of the type Ru(phen) ₂ L ₂	85
14. Effect of chloro ligands on the visible absorbance spectrum of Ru(phen) ₂ Cl ₂ dissolved in aqueous solution	86
15. Visible absorbance spectra of Ru(phen) ₂ Cl ₂ dissolved in buffer R and in phosphate buffer	87
16. Visible absorbance spectra of Ru(phen) ₂ Cl ₂ after incubation with 2'-deoxyguanosine 5'-monophosphate and guanosine	88
17. Effect of the presence of Co(NH ₃) ₆ ³⁺ on the binding of Ru(phen) ₂ Cl ₂ to poly(dG-dC)·poly(dG-dC)	91
18. Absorbance spectra and C.D. spectra of B and Z DNA	93
19. Effect of the bound Ru(phen) ₂ Cl ₂ complex on the B to Z transition as monitored by the absorbance spectrum of the DNA	94

20. Effect of the bound $\text{Ru}(\text{phen})_2\text{Cl}_2$ complex on the B to Z transition as monitored by the C.D. spectrum of the DNA	95
21. Binding and enantiomeric enrichment of $\text{Ru}(\text{phen})_2\text{Cl}_2$, $\text{Ru}(5,6\text{-dimethylphen})_2\text{Cl}_2$, and $\text{Ru}(5\text{-phenylphen})_2\text{Cl}_2$ as a function of time of incubation with calf thymus DNA	96
22. Binding and enantiomeric enrichment of $\text{Ru}(\text{phen})_2\text{Cl}_2$, $\text{Ru}(5,6\text{-dimethylphen})_2\text{Cl}_2$, and $\text{Ru}(5\text{-phenylphen})_2\text{Cl}_2$ as a function of time of incubation with poly(dG-dC)·poly(dG-dC)	97
23. Effect of $\text{Ru}(\text{phen})_2\text{Cl}_2$ on the reaction of Exonuclease III with SV40 DNA	99
24. Proposed models of $\text{Ru}(\text{phen})_2\text{Cl}_2$ coordinated to B-DNA	102
Chapter 4	
1. Photophysical properties of $\text{Ru}(\text{bpy})_3^{2+}$	116
2. Effect of irradiation on the binding of $\text{Ru}(\text{phen})_2\text{Cl}_2$ to DNA	121
3. Effect of irradiation in the presence of $\text{Ru}(\text{phen})_2\text{Cl}_2$ on the electrophoretic mobility of SV40 DNA	123
4a. Difference C.D. spectrum of B-form poly(dG-dC)·poly(dG-dC) before and after irradiation in the presence of $\text{Ru}(\text{phen})_2\text{Cl}_2$	125
4b. Difference C.D. spectrum of Z-form poly(dG-dC)·poly(dG-dC) before and after irradiation in the presence of $\text{Ru}(\text{phen})_2\text{Cl}_2$	125
5. Racemization of $\text{Ru}(\text{phen})_2\text{Cl}_2$ as a function of time irradiated	126
6. Concentration of $\text{Ru}(\text{phen})_2\text{Cl}_2$ bound to DNA as a function of time irradiated	127

7. Cleavage of DNA in the presence of $\text{Ru}(\text{phen})_3^{2+}$ as a function of
time irradiated 128
8. Effect of the presence of D_2O on the photocleavage of DNA by
 $\text{Ru}(\text{phen})_3^{2+}$ 130
9. Effect of the presence of O_2 on the photocleavage of DNA by
 $\text{Ru}(\text{phen})_3^{2+}$ 131
10. Cleavage of DNA in the presence of $\text{Ru}(\text{phen})_2\text{Cl}_2$ as a function
of time of irradiation. 132

List of Abbreviations

DNA	deoxyribonucleic acid
A	adenine
G	guanine
T	thymine
C	cytosine
<u>cis</u> -DDP	<u>cis</u> -diamminedichloroplatinum(II)
form I DNA	covalently closed duplex DNA
form II DNA	nicked duplex DNA
GMP	2'-deoxyguanosine-5'-monophosphate
r_f	molar ratio of ligand to nucleotide
r_b	molar ratio of bound ligand to nucleotide
bpy	2,2'- bipyridine
dip	4,7-diphenyl-1,10-phenanthroline
EDTA	ethylenediaminetetraacetate
en	ethylenediamine
phen	1,10-phenanthroline
py	pyridine
CT	charge transfer
LF	ligand field
MLCT	metal to ligand charge transfer
k_r	radiative decay rate
k_{nr}	non-radiative decay rate

tris (buffer)	tris(hydroxymethyl)aminoethane
tfc	trifluoromethylhydroxymethylene--camphorato
cpm	counts per minute
C.D.	circular dichroism
W	watts
nm	nanometers

Chapter 1

Introduction

Investigations of the binding of small molecules and proteins to DNA have revealed that binding is often related to sequence dependent properties. For example, many intercalators display a binding preference for sequences containing G·C base pairs.^{1,2} Particular preferences have been observed for pyrimidine-3',5'-purine steps in many of these cases.^{3,4,5} On the other hand many DNA groove binders such as netropsin and structurally related antibiotics favor binding at A·T sequences.⁶ The importance of the DNA sequence for protein binding has been considered in terms of the hydrogen bonding capabilities of the functional groups on the bases by Seeman et. al.⁷ They concluded that formation of two hydrogen bonds between amino acid side chains and bases would lead to sequence specific recognition. Hydrogen bonding to, or electrostatic interactions with, various functional groups on the bases are means by which DNA binders can recognize DNA sequences. Base composition and sequence of the DNA also affect the conformation of the DNA. Therefore, in addition to sequence preferences that arise from hydrogen bonding and electrostatic interactions, conformational heterogeneities of the DNA may also contribute to specificities in ligand binding. The sequence dependencies of DNA conformations and their effect on the interactions of DNA with ligands are therefore areas of avid investigation. This chapter will begin with a review of recent findings on the conformations of DNA and their relation to base sequence. Proposals and evidence for the biological implications of the various conformations are then considered. Lastly, a description of some of the work involving small molecules as probes of DNA structure is discussed.

Several families of DNA conformations have been identified from fiber diffraction studies.^{8,9,10,11} Some of the major conformational families are illustrated in Figure 1. B-

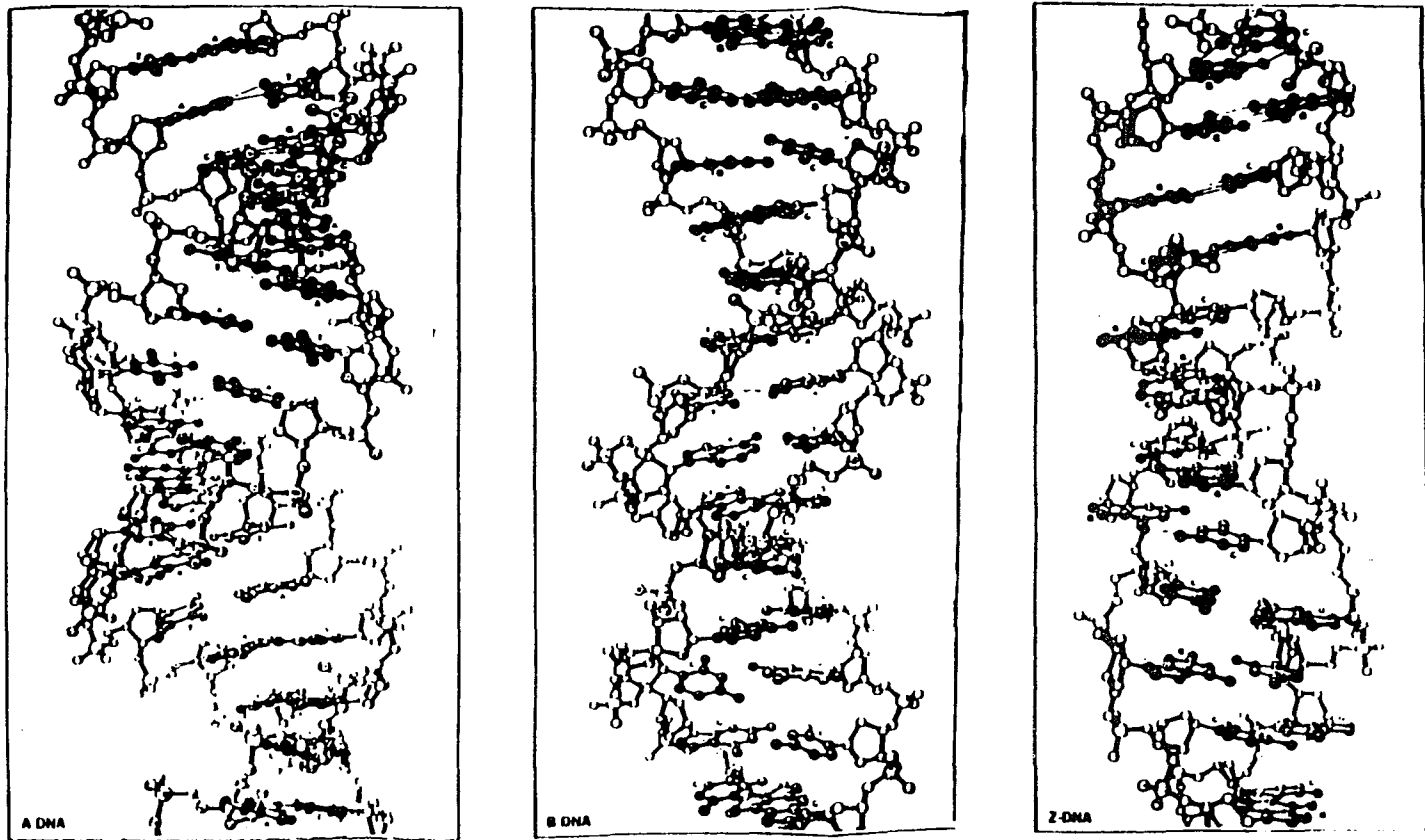


Figure 1. Illustrations of DNA in the A,B and Z conformations (from reference 12).

DNA is a right handed helix with an average of 10 base pairs per turn. The plane of the bases are approximately perpendicular to the helix axis. The B conformation has a narrow minor groove and a wide major groove of comparable depth. A-DNA is a shorter and wider helix. Its bases are canted toward the helix axis. It has a deep major groove and a shallow minor groove.

The differences between conformations can be described by the seven torsional angles shown in Figure 2.¹³

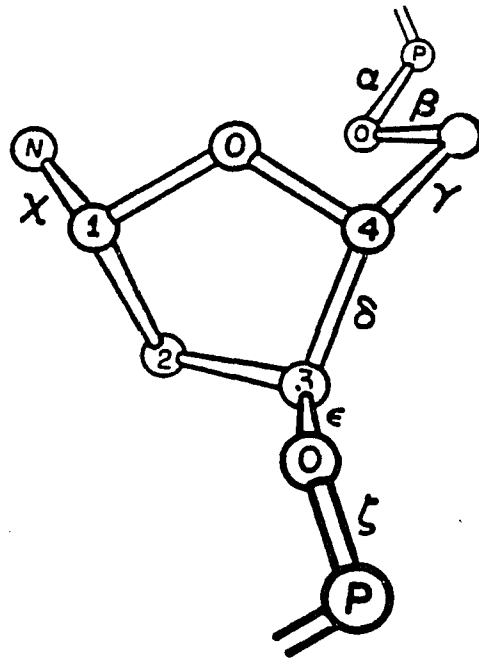


Figure 2. Main chain torsional angles of DNA.

Two particularly informative angles are χ and δ . The angle χ is the glycosyl angle between C1' and the nitrogen on the base. The conformation is termed syn when the base points toward the minor groove and anti when it points away from the groove. The angle δ identifies the conformation of the deoxyribose ring. Variations in main chain torsional angles are of course reflected in changes in the helix structure such as groove sizes, exposure of the phosphodiester

backbone and the distance and direction between a base and its neighbors. The range of groove sizes observed in the various DNA conformations is exemplified by the table below (from reference 16).

Table 1. Groove dimensions in nucleic acids

	Minor groove		Major groove	
	Depth (nm) [§]	Width (nm)	Depth (nm)	Width (nm)
A helix	0.28	11.0	1.35	0.27
B helix	0.75	0.57	0.85	1.17
Dodecamer†				
at central AATT	-	0.32	-	1.27
at end of ATT	-	0.70	-	1.06
d(GGATGGGAG) _n		0.83-0.97		0.93

Variations among DNA conformations can also be described by the parameters helical twist, propeller twist, slide and roll of the bases, illustrated in Figure 3. The helical twist is the projected angle between C1' and C1' looking down the helix axis. The propeller twist is the angle between hydrogen bonded bases with respect to each other. The slide is the translation of base pairs relative to each other down the long helix axis of the bases. The roll is the angle by which the base pairs open toward the minor groove.

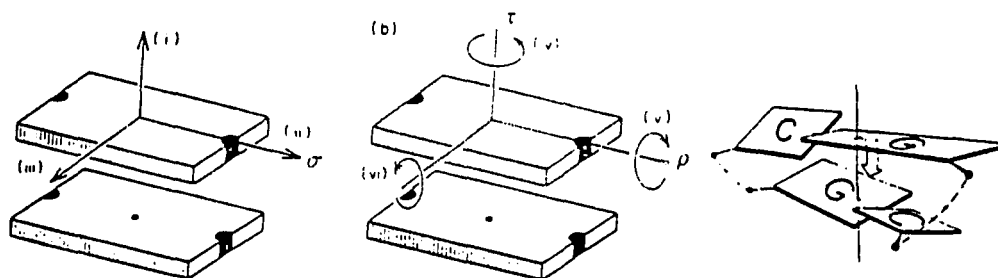


Figure 3. Diagram of slide (σ), twist (τ), roll (ρ) and propeller twist

Though most hydrated polynucleotides examined by fiber diffraction adopt the B conformation,¹⁷ varying environmental conditions can lead to preferences for other conformations.¹⁸ For example lowering the relative humidity causes a B to A transition in most cases. However, the propensity for a polynucleotide to adopt particular conformations was observed to be somewhat dependent on base sequence. For example, DNA of random sequence undergoes a B to A transition at a higher relative humidity than that at which poly(dA-dT)·poly(dA-dT)¹⁹ undergoes this transition. Poly(dG)·poly(dC) has a greater propensity than random sequence DNA to adopt the A conformation.²⁰ Poly(dA)·poly(dT) on the other hand appears never to adopt an A conformation.²¹ It has a strong preference for the B conformation but under conditions of low relative humidity may adopt a heteronomous conformation in which the dA strand is in an A like conformation and the dT strand is in a B-like conformation.²² Leslie et. al. have correlated the preference for the B conformation with the presence of A·T base pairs.²³

Fiber diffraction studies have yielded information about the heterogeneity of DNA in terms of overall families of conformations that can be adopted. However, it is impossible by this method to gain information on the local deviations from the average conformation of a polynucleotide. Information on local heterogeneities of DNA is instead being accrued from the more recent crystal structure analyses of oligonucleotides. Such analyses have been underway for about a decade. Crystal structures analyzed so far include those of the oligonucleotides: d(C-G-C-G),²⁴ d(C-G-C-G-C-G),²⁵ d(G-G-G-G-C-C-C-C),²⁶ d(G-G-A-T-A-T-C-C)²⁷, d(C-G-C-G-A-A-T-T-C-G-C-G)²⁸, d(G-G-A-T-G-G-G-A-G)²⁹ and d(G-G-C-C-G-G-C-C)³⁰. The alternating d(G-C) sequences were found to be in a Z conformation. This conformation is the only one that had not been previously defined by fiber diffraction. The Z conformation is that of a left handed helix. The characteristics of the grooves are in a sense exchanged with those of the A conformation in that the minor groove is deep and the major

groove is flattened. The repeating unit is a dinucleotide. The nucleotide conformations alternate between the syn and anti conformations of the χ angle for G and C nucleotides respectively. The conformation of the δ angle alternates as well.

The structural study of the dodecamer d(C-G-C-G-A-A-T-T-C-G-C-G) has exemplified the deviations in torsional angles from the average that can occur in B-DNA.³¹ For example the angle χ varies from -140° to -90° . The angle δ varies from 80° to 60° . One of the effects that these variations in the torsional angles have on the overall structure of the helix is in changes in the groove sizes. For example the center of the AATT region on the dodecamer has a minor groove .32 nm wide, while the end of this region has a minor groove .7 nm wide.³²

Aside from local deviations in conformation, another aspect of DNA structure elucidated by the crystal structure analyses is that of the solvent structure.³³ Seventy two ordered water molecules were observed surrounding the dodecamer. Particularly notable is an ordered arrangement of two layers of water molecules in the minor groove of the AT containing regions termed the spine of hydration. Water molecules ordered to this extent are not observed in GC rich regions, presumably because of disruption of the spine by the 2-NH₂ group on guanosine.

Effort has been directed toward the correlation of the various torsional angles within a conformation and the correlation of base sequences with deviations in torsional angles from the average values.³¹ For example, correlations were observed between χ and δ angles. As χ varies from -140° to -190° , δ varies from 80° to 160° degrees. Higher values for both of these dihedral angles were observed for purines than for pyrimidines. These observations were interpreted as arising from the need to alleviate steric hindrance between the base and sugar moiety, which occurs more severely for the 6-membered pyrimidine ring than for the five membered ring to which the sugar is bonded in purine bases. An interesting approach to the analysis of sequence dependent conformational deviations has been taken by Calladine.³⁴ In

this model, steric clashes occur between successive purines on opposite strands as a result of their propeller twists (see figure 2). These steric clashes can be alleviated by variations in the twist, roll, propeller twist and slide at these steps. (Corrections are also made to the steps immediately flanking those under consideration.) Dickerson has used this model to calculate theoretical values for these particular helical parameters given the sequence of the dodecamer.¹⁵ Theoretical and experimental values were compared for both B and A DNA. Correlation coefficients between theoretical and experimental values were .99 and .92 for the helical twist and roll, respectively in B-DNA. Correlations were also good for the δ angle and the propeller twist in B-DNA. In the A-DNA model, good correlation was found for the twist and roll for all the samples of A DNA analyzed by this method (including d(G-G-C-C), d(G-G-C-C-G-G-C-C) and d(G-G-T-A-T-A-C-C)) but not for the angle δ and the propeller twist. The corroboration or further elaboration of this model or the development of new models whose goal is to predict conformation based on sequence, awaits further data. Particularly, since the dodecamer is the only reported example of a B-DNA crystal, there is data on only 11 steps for B-DNA. Another aspect that may be very important to DNA conformation that is excluded from this model is the effect of flanking sequences further away from the nucleotide in question than the nearest neighbors.

Two questions arise concerning these DNA structural studies. 1. How accurately do structural determinations from crystallographic studies represent solution structures? 2. If the structural studies described are in fact related to the solution structures, what are the possible biological implications of the observed sequence dependence of the conformations? One experiment that was performed in order to address the first question was the reaction of a sequence, for which the crystal structure had been determined, with the endonuclease, DNaseI.³⁵ In these experiments a correlation was found between the rate of the reaction of DNase and the helical twist angle observed in the crystal form. Larger twist angles

corresponding to more accessible phosphodiester backbones are most easily cleaved. The result was taken to support the similarity between crystal and solution structures. On the other hand large scale transitions of the whole polynucleotide between one conformational family and the next may not always correspond between crystal structure and solution structure. For instance, poly(dG-dC)poly(dG-dC) in solution at physiological salt concentrations is in the B-conformation.³⁶ All crystal structures of this sequence however, are in the Z conformation.^{24,25} Except for the crystals containing alternating GC sequences which are in the Z conformation, and the dodecamer which is in the B conformation, all crystal structures reported so far have been in the A conformation. This finding is somewhat surprising and may be a function of crystal packing forces. The packing involves the hydrophobic interaction of the end base pair of one oligonucleotide with the minor groove of another, so that the long axes of the helices are perpendicular. Such a packing force may shift the conformational equilibrium of the DNA in favor of the A conformation.²⁷ An experiment which most directly proves the notion that oligonucleotides may adopt different conformations in solution than in the crystal structures is the study of the oligonucleotide d(G-G-A-T-A-T-C-C). This sequence was investigated by crystal structure analysis²⁷ and by NMR studies.³⁷ The conformation in the former studies was determined to be A while that in the NMR studies was determined to be B at least at the center steps. Thus, the observation of a particular conformation for crystal structures of particular oligonucleotides should probably be taken to indicate a propensity of that sequence to adopt that conformation, rather than an indication that the sequence will always adopt that conformation in solution.

There is evidence, some circumstantial and some direct, that the variety of conformations that DNA can adopt is exploited by nature. In order to argue that sequence dependent deviations from an average conformation may be biologically important it is necessary to show that proteins can recognize these deviations. It is of course easiest to address such a

question using proteins that do not have much sequence specificity. The studies by Lomonosoff et. al.³⁵ mentioned above indicate that DNase I is sensitive to the range of helical twist angles attainable within the B conformation . A good correlation was observed between the rate of reaction of this enzyme at each base step and the helical twist angle at that step observed in the crystal structures. In another study, DNase I was reacted with a sequence that contained a poly d(A)·d(T) tract and a poly d(G)·d(C) tract.³⁸ The enzyme did not react at the A·T tract or the G·C tract but it was reactive at the junction of these two tracts. This finding was interpreted as a sensitivity to the minor groove size which is believed to be larger than average for poly d(G)·d(C) and small for poly d(A)·d(T) but intermediate at the junction. In the same study restriction enzymes were observed to be sensitive to the flanking sequences around the consensus specific sequence, indicating that the flanking sequences were affecting the conformations of the specific sites in a way that the enzyme could recognize. Another example of the apparent sensitivity of an enzyme to the conformation of DNA (as opposed to its sequence) are the observations on the reactivity of mung bean nuclease. The DNA substrate sites for this enzyme were found to correspond to intergenic regions only with no obvious consensus sequence.³⁹

Another point that is important to address in order to investigate possible biological roles of various conformations is the frequency of occurrence in biological systems of families of DNA conformations other than B-DNA or the occurrence of sequences with a propensity to adopt conformations other than B-DNA. Z-DNA was originally observed in vitro only under extreme conditions such as high ionic strength or a dehydrated environment.⁴⁰ Subsequently it was determined that Z-DNA can exist in conditions of physiological ionic strength in supercoiled form⁴¹ and that under these conditions the conformation is sensitive to the ionic strength within physiological range.⁴² Alternating purine pyrimidine sequences have been

found in diverse eukaryotic genomes.⁴³ In vitro, the presence of Z-DNA sites has been implicated in enhancer sequences,⁴⁴ in polytene chromosomes⁴⁵ and at intergenic regions in plasmid DNA.⁴⁶

It has been noted that sequences with a propensity to adopt the A conformation tend to occur in transcription factors.⁴⁷ Whether this conformation exists under physiological conditions or whether it is requisite for these factors is unknown as yet. Roles for A-DNA that have been proposed include the importance of these structures for binding to RNA (which is also in the A conformation) or for promoting destacking or unwinding of the DNA.²⁷

Another interesting feature of DNA conformation that appears to have biological relevance is the ability for DNA to bend or circularize.⁴⁸ Poly d(A)·polyd(T) sequences at helical repeat distances have been observed to cause stable bending of the DNA. The phage λ origin is one example of a site at which such sequences have been identified.⁴⁹ These sequences appear to be important for wrapping around the O protein involved in replication. Though these sequences do not actually constitute the binding region to these proteins, their removal prevents replication. The ability to bend is also important for the wrapping of DNA around nucleosome particles.⁵⁰ Translational and rotational placement of nucleosome proteins on the DNA has been correlated with the ability of particular sequences of DNA to bend. The roll and twist angle of nucleotide steps as well as the groove sizes of the helices appear to be important in determining whether nucleosome particles will bind to the DNA.⁵¹

In recent years effort has been put into the design of DNA binding molecules that would bind to particular sequences and or conformations of DNA. The goal of such studies is to be able to identify, probe, or analyze particular sequences or conformations on DNA using these molecules. A mostly base sequence directed approach was taken by Dervan and coworkers. They have tethered Fe-EDTA to low molecular weight DNA binders (such as antibiotics and

anti viral agents) with sequence preferences.⁵² The Fe-EDTA in the presence of O₂ and a reducing agent generates hydroxy radicals which cleave the DNA.⁵³ The attached DNA binder provides sequence specificity. For example, Fe-EDTA-distamycin and related molecules cleave DNA near regions containing AT sequences. An Fe-EDTA moiety has also been tethered to oligonucleotides 16, 19 and 37 bases long,^{54,55} yielding molecules which specifically recognize the sequences complementary to the oligonucleotides and cleave DNA nearby these sequences.

Fe-EDTA in the presence of H₂O₂ has also been used alone to probe DNA conformations. The hydroxy radical formed leads to cleavage of DNA with no dependence on the identity of the base.⁵⁶ Burkhoff and Tullius monitored the cleavage pattern on kinetoplast DNA. (Kinetoplasts are small, stably curved DNAs containing long repeating AT tracts.) A sinusoidal cleavage pattern of this DNA at the A·T tracts was interpreted as a periodically changing shape of the minor groove, within these regions.⁵⁷

Sigman and coworkers have studied the binding and cleavage reaction of (phen)₂Cu⁺ in the presence of a reducing agent.⁵⁸ The efficiency of the reaction was observed to be a function of the conformation of the DNA.⁵⁹ DNA in the B conformation is the most efficiently cleaved. DNA in the A conformation is less efficiently cleaved and Z conformation DNA is not cleaved by the reagent. Cleavage studies were done on a series of mutations in the lac promoter region.⁶⁰ It was observed that various mutations had different hypersensitive sites to the reagent. These studies therefore indicate that the mutations effected the local conformation of the DNA.

Methods other than cleavage of DNA have also been used in designing probes or site specific binders. Helene and coworkers have studied the binding of a molecule containing acridine tethered to an oligonucleotide.⁶¹ The binding of the oligonucleotide could be

monitored by changes in the emission of the acridine. Moreover, a suitably placed acridine molecule enhanced the binding of the oligonucleotide to its complementary strand of the DNA.

Attempts have also been made to study the interaction of small peptides with DNA in order to model DNA protein interactions and ultimately design sequence specific DNA binding peptides.⁶² Based on the observation that many DNA binding proteins contain α -helical regions that bind to the major groove of the DNA,⁶³ an α -helical peptide was designed as a sequence non-specific DNA binder. The α -helical structure of the peptide was found to increase upon binding to the DNA. Binding of the peptide was also improved when hydrogen bonding side chains were added.

In Dr. Barton's laboratory we have employed small chiral metal complexes as conformational and sequence sensitive probes or modifiers of DNA. Except for their interactions with other chiral molecules, such as DNA, the chemistry of the two enantiomers of any of the metal complexes are obviously identical. The relative binding of two enantiomers can be affected by conformational characteristics of the DNA such as groove size or helicity. The chirality of the complex therefore lends a conformational sensitivity to the binding experiment. Depending on the particular complex employed, the metal center can impart to the molecule a spectroscopic handle, a redox active center or a means by which the probe can coordinate to the DNA. The first work in this area was done with $\text{Zn}(\text{phen})_3^{2+}$.⁶⁴ Binding of this complex to B-DNA shows a preference for the Δ enantiomer. Binding and enantiomeric discrimination were studied further with $\text{Ru}(\text{phen})_3^{2+}$ ⁶⁵ (Figure 4) and $\text{Co}(\text{phen})_3^{3+}$ ⁴⁶. Ruthenium(II) was chosen as the metal center in these studies because of the well characterized spectroscopic characteristics of ruthenium(II) polypyridyl complexes⁶⁶ (discussed further in Chapters 2 and 3). This complex absorbs and emits strongly in the visible region. Moreover, the spectroscopic properties are affected by DNA binding. Cobalt(III) compounds which undergo photoreduction reactions are effective photocleavers of

DNA. DNA cleavage reactions of $\text{Co}(\text{phen})_3^{3+}$ or related cobalt(III) complexes at particular sites on DNA can be monitored sensitively.^{46,70} Cleavage with the bulkier $\text{Co}(\text{dip})_3^{2+}$ complex has been used to map conformationally distinct sites on DNA. Whereas both enantiomers bind to Z-DNA, presumably because of the shallower groove size of this conformation, the Δ enantiomer binds to B-DNA. Specific cleavage was observed at intergenic regions on pBR322 and at particular control regions on SV40 DNA.

Recently, binding of $\text{Ru}(3,4,7,8\text{-tetramethylphenanthroline})_3^{2+}$ to DNA has also been monitored in our laboratory. It was observed that this complex binds to polynucleotides in the A conformation but not in the B conformation.⁷¹ Mapping of the cleavage sites of this complex on plasmid DNAs is currently in progress in our laboratory .

This thesis involves investigations of aspects of the binding of $\text{Ru}(\text{phen})_3^{2+}$ (Figure 4) and $\text{Ru}(\text{phen})_2\text{Cl}_2$ (Figure 5) to DNA. In Chapter 2 the use of luminescence assays to detect binding of $\text{Ru}(\text{phen})_3^{2+}$ to DNA is described. The sequence dependencies of luminescence and binding are considered. In Chapters 3 and 4 binding of $\text{Ru}(\text{phen})_2\text{Cl}_2$ to DNA is described. Unlike the tris(phenanthroline) metal complexes, this complex has two labile ligands, enabling the ruthenium(II) to coordinate to the DNA. Coordination lends stability as well as sequence preferences to the interactions with DNA. In Chapter 3 we consider the binding in terms of sequence preferences, enantiomeric preferences and effects on conformation of the DNA. Spectroscopic studies were done to try to characterize the type of site to which the ruthenium may be coordinated are also discussed. In Chapter 4 photoreactions of $\text{Ru}(\text{phen})_2\text{Cl}_2$ and $\text{Ru}(\text{phen})_3^{2+}$ with DNA are described. Photosubstitution and photocleavage reactions were observed.

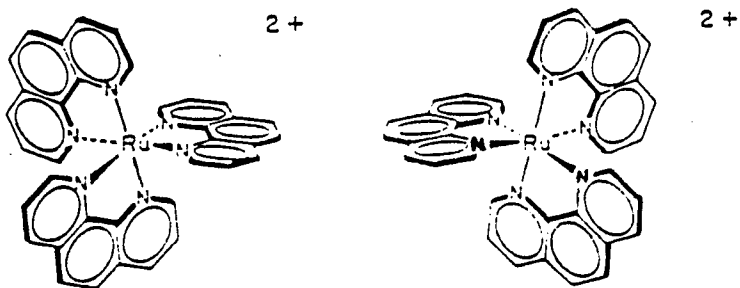


Figure 4. Enantiomers of $\text{Ru}(\text{phen})_3^{2+}$.

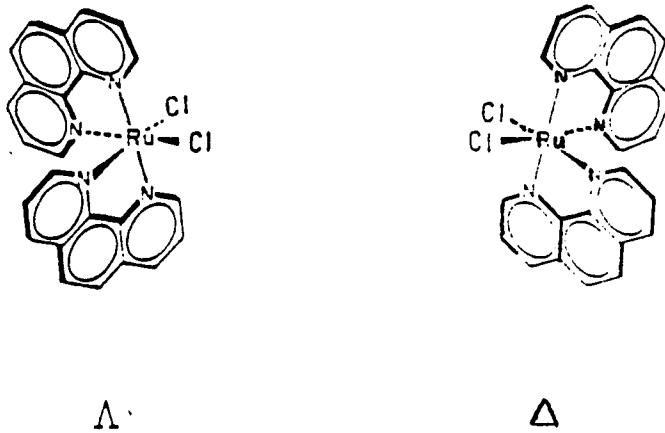


Figure 5. Enantiomers of $\text{Ru}(\text{phen})_2\text{Cl}_2$. The chloro ligands are labile in aqueous solution.

References

1. a) Muller, W., Crothers, D.M. (1975) Eur. J. Biochem. **54** 267-77. b) Muller, W., Buneman, H., Dattagupta, N. (1975) Eur. J. Biochem. **54** 279-91.
2. Feigon, J., Denny, W.A., Leupin, W., Kearns, D.R. (1984) J. Med. Chem. **27** 450-65.
3. Patel, D.J., Canuel, L.L. (1976) Proc. Nat. Acad. Sci. **73** 3343-47.
4. Phillips, D.R., Roberts, G.C.K. (1980) Biochemistry **19** 4795-801.
5. Reinhardt, C.G., Krugh, T.R. (1978) Biochemistry **17** 4845-54.
6. a) Braithwaite, A.W., Baguley, B.C. (1980) Biochemistry **19** 1101-6. Muller, W., Gautier, F. (1975) Eur. J. Biochem. **54** 385-94.
7. Seeman, N.C., Rosenberg, J.M., Rich, A. (1976) Proc. Nat. Acad. Sci. **73** 804-8.
8. Arnott, S., Hukins, D.W.L. (1973) J. Mol. Biol. **81** 93-105.
9. Arnott, S., Hukins, D.W.L. (1972) Biochem. Biophys. Res. Commun. **47** 1504-9.
10. Arnott, S., Selsing, E. (1975) J. Mol. Biol. **98** 265-69.
11. Arnott, S., Chandrasekaran, R., Hukins, D.W.L., Smith, P.J.C., Watts, L. (1974) J. Mol. Biol. **88** 523-33.
12. Geis, I. (1983) J. Biomol. Struct. Dyn. **1** 581-91.
13. Arnott, S. (1970) Prog. Biophys. Molec. Biol. **21** 265-319.
14. Calladine, C.R., Drew, H.R. (1984) J. Mol. Biol. **178** 773-82.
15. Dickerson, R.E. (1983) J. Mol. Biol. **166** 419-41.
16. Neidle, S., Pearl, L.H., Skelly, J.V. (1987) Biochem. J. **243** 1-13.
17. a) Hamilton, L.D., Barclay, R.K., Wilkins, M.H.F., Brown, G.L., Wilson, H.R., Marvin, D.A., Ephrussi-Taylor, H., Simmons, N.S. (1959) J. Biophys. Biochem. Cytol. **5** 397-403. b) Premilat, S., Albiser, G. (1975) J. Mol. Biol. **99** 27-36.
18. a) Wilkins, M.H.F. (1963) Science **140** 941. b) Ivanov, V.I., Minchenkova, L.E., Schyolkina, A.K., Poletayev, A.I. (1973) Biopolymers **12** 89-110. c) Ivanov, V.I., Minchenkova, L.E., Minyat, E.E., Frank-Kanminetski, M.D., Schyolkina, A.K. (1974) J. Mol. Biol. **87** 817-33.
19. Arnott, S., Selsing, E. (1974) J. Mol. Biol. **88** 509-21.
20. Arnott, S., Selsing, E. (1974) J. Mol. Biol. **88** 551-2.
21. Pilet, J., Blicharski, J., Brahms, H. (1975) Biochemistry **14** 1869-76.

22. Arnott, S., Chandrasekaran, R., Hall, I.H., Puigjaner, C.C. (1983) Nucleic Acids Res. **11** 4141-55.
23. Leslie, A.G.W., Arnott, S., Chandrasekaran, R., Ratliff, R.L. (1980) J. Mol. Biol. **143** 49-72.
24. a) Drew, H., Takano, T., Tanaka, S., Itakura, K., Dickerson, R.E. (1980) Nature **286** 567-73. b) Crawford, J.L., Kolpak, F.J., Wang, A. H.-J., Quigley, G.J., van Boom, J.H., van der Marel, G., Rich, A. (1980) Proc. Nat. Acad. Sci **77** 4016-20.
25. Wang, A. H.-J., Quigley, G.J., Kolpak, F.J., Crawford, J.L., Van Boom, J.H., Van der Marel, G., Rich, A. (1979) Nature **282** 680-86.
26. McCall, M., Brown, T., Kennard, O. (1985) J. Mol. Biol. **183** 385-96.
27. Shakked, Z., Rabinovitch, D., Kennard, O., Cruse, W.B.T., Salisbury, S.A., Viswamitra, M.A. (1983) J. Mol. Biol. **166** 183-201.
28. Wing, R., Drew, H., Takano, T., Broka, C., Tanaka, S., Itakura, K. Dickerson, R.E. (1980) Nature **287** 755-58.
29. McCall, M., Brown, T., Hunter, W.N., Kennard, O. (1986) Nature **322** 661-64.
30. Wang, A., H.-J., Fujii, S., van Boom, J.H., Rich, A. (1982) Proc. Nat. Acad. Sci. **79** 3968-72.
31. a) Dickerson, R.E., Drew, H.R. (1981) Proc. Nat. Acad. Sci. **78** 7318-22. b) Dickerson, R.E., Drew, H.R. (1981) J. Mol. Biol. **149** 761-86.
32. a) Dickerson, R.E., Kopka, M.L. (1985) J. Biomol. Struct. Dyn **3** 423-436. b) Fratini, A.V., Kopka, M.L., Drew, H.R., Dickerson, R.E. (1982) J. Biol. Chem. **257** 14686-707.
33. Drew, H.R., Dickerson, R.E. (1981) J. Mol. Biol. **151** 535-56.
34. Calladine, C.R. (1982) J. Mol. Biol. **161** 343-52.
35. Lomonosoff, G.P., Butler, P.J.G., Klug, A. (1981) J. Mol. Biol. **149** 745-760.
36. Pohl, F.M. (1976) Nature **260** 365-6.
37. Patel, D.J., Shapiro, L., Hare, D. (1986) Biopolymers **25** 693-706.
38. Drew, H.R., Travers, A.A. (1985) Nucleic Acids Res. **13** 4445-67.
39. McCutchan, T.F., Hansen, J.L., Dame, J.B., Mullins, J.A. (1984) Science **225** 625-8.
40. Pohl, F. M., Jovin, T.M. (1972) J. Mol. Biol. **67** 375-96.
41. Nordheim, A., Lafer, E.M., Peck, L.J., Wang, J.C., Stollar, B.D., Rich, A. Cell **31** 309-18.
42. Azorin, F., Nordheim, A., Rich, A. (1983) EMBO J. **2** 649-55.

43. Hamada, H., Petrino, M.G., Kakunaga, T. (1982) Proc. Nat. Acad. Sci. 79 6465-69.
44. Nordheim, A., Rich, A. (19) Nature 303 674-8.
45. Nordheim, A., Pardue, M.L., Lafer, E.M., Moller, A., Stollar, B.D., Rich, A. (1981) Nature 294 417-22.
46. Barton, J.K., Raphael, A.L. (19) Proc. Nat. Acad. Sci. 82 6460-4.
47. Rhodes, D., Klug, A. (1986) Cell 46 123-32.
48. a) Koo, H.S., Wu, H.M., Crothers, D.M. (1986) Nature 320 501-6. b) Ulanovsky, L., Bodner, M., Trifonov, E.N., Choder, M. (1986) Proc. Nat. Acad. Sci. 83 862-66.
49. Zahn, K., Blattner, F.R. (1987) Science 236 416-22.
50. a) Drew, H.R., Calladine, C.R., (1987) J. Mol. Biol. 195 143-73. b) Drew, H.R., Travers, A.A. (1985) J. Mol. Biol. 186 773-90. c) Simpson, R.T., Kunzler, P. (1979) Nucleic Acids Res. 6 1387-1415.
51. Calladine, C.R., Drew, H.R. (1986) J. Mol. Biol. 192 907-18.
52. Dervan, P.B. (1986) Science 232 464-471.
53. Hertzberg, R.P., Dervan, P.B. (1984) Biochemistry 23 3934-45.
54. Dreyer, G.V., Dervan, P.B. (1985) Proc. Nat. Acad. Sci. 82 968-72.
55. Chu, B.C.F., Orgel, L.E. (1985) Proc. Nat. Acad. Sci. 82 963-7.
56. Tullius, T.D., Dombrowski, B.A. (1985) Science 230 679-81.
57. Burkhoff, A.M., Tullius, T.D. (1987) Cell 48 935-943.
58. Sigman, D.S. (1986) Acc. Chem. Res. 19 180-6.
59. Pope, L.E., Sigman, D.S. (1984) Proc. Nat. Acad. Sci. 81 3-7.
60. Sigman, D.S., Spassky, A., Rimsky, S., Buc, H. (1985) Biopolymers 24 183-97.
61. Asseline, U., Delarue, M., Lancelot, G., Toulme, F., Thuong, N.T., Montenev-Garestier, T., Helene, C. (1984) Proc. Nat. Acad. Sci. 81 3297-301.
62. Walters, L., Kaiser, E.T. (1985) J. Am. Chem. Soc. 107 6422-6424.
63. a) Anderson, W.F., Takeda, Y., Ohlendorf, D.H., Matthews, B.W. (1982) J. Mol. Biol. 159 745-51. b) Pabo, C.O., Sauer, R.T. (1984) Ann. Rev. Biochem. 53 293-321.
64. Barton, J.K., Dannenberg, J.J., Raphael, A.L. (1982) J. Am. Chem. Soc. 104 4967-8.
65. Barton, J.K., Danishefsky, A., Goldberg, J. (1984) J. Am. Chem. Soc. 106 2172-6.

66. Barton, J.K., Raphael, A.L. (1984) J. Am. Chem. Soc. 106 2466-8.
67. Watts, R.J., (1983) J. Chem. Ed. 60 834-42.
68. a) Barton, J.K., Basile, L.A., Danishefsky, A.T., Alexandrescu, A. (1984) Proc. Nat. Acad. Sci. 81 1961-65.
69. Kumar, C.V., Barton, J.K., Turro, N.J. (1985) J. Am. Chem. Soc. 107 5518-23.
70. Muller, B.C., Raphael, A.L., Barton, J.K. (1987) Proc. Nat. Acad. Sci. 84 1764-68.
71. Mei, H.Y., Barton, J.K. (1986) J. Am. Chem. Soc. 108 7414-7416.

Chapter 2

Luminescence Studies of the Interactions of Tris Chelate Ruthenium(II) complexes with DNA.

Introduction

One of the reasons that the properties of small molecules that bind to DNA are currently under avid investigation,¹ is that these molecules can be used as stains or probes by which the DNA can be identified. Many of the known DNA binding molecules contain extended aromatic, heterocyclic systems. As a result of these structures they absorb visible light and often have excited states that decay by radiative pathways. Both of these properties are useful because they allow binding to the DNA to be monitored spectroscopically. Some dyes have been widely employed because of these properties². For example, the trypanocide ethidium bromide, which displays a marked increase in fluorescence upon binding to DNA³ is often used in research to locate DNA. Some dyes are specific as to where they bind on the DNA or what types of sites cause spectroscopic changes. Such discrimination can be particularly useful. For example acridine orange emits 535 nm light when bound to double stranded DNA and 640 nm light when bound to single stranded DNA⁴. This property renders it a useful tool for detecting these forms of DNA. Luminescent DNA binders, such as quinacridines⁵, or the mithramycin group of antibiotics⁶ have also been used to stain chromosomes. The binding or enhancement at particular sites causes the well known banding patterns on the chromosomes. The advantages of both luminescent properties and DNA site specificity in a DNA binding molecule has prompted researchers to synthetically combine these two aspects in a single molecule. One example is the linking of luminescent molecules to single stranded oligonucleotides.⁷ The binding properties of such molecules are being investigated.

In order to develop or use small molecules as probes it is desirable to understand what modes of binding they can undergo with DNA, what are the preferred binding sites on the DNA and what spectroscopic effects result from different sites or modes of binding. Many studies designed to answer such questions have been conducted with classical intercalators. Intercalation of planar aromatic compounds such as ethidium⁸ and acridine⁹ derivatives has been demonstrated by x-ray crystallographic studies. An intercalative mode of binding, first described by Lerman¹⁰, involves the insertion of an aromatic ring of the ligand between the base pairs of the DNA. It is known however, that more than one type of binding mode can occur for most of these chromophores. Preferences of one type of DNA binding site over another and non-intercalative types of binding may occur. This fact has been demonstrated by binding studies, involving spectroscopic methods, for ethidium^{2,11} and for acridine derivatives^{12,13}. Some questions still exist concerning which of these modes of binding contribute to emission enhancement.¹⁴ An outside mode of binding involving the interaction of the ligand with the groove of the helix has been depicted by the crystal structure of netropsin, an oligopeptide antibiotic, with DNA.¹⁵ Groove binding is also known to occur for the structurally related oligopeptide distamycin,¹⁶ for the mithramycin group of antibiotics¹⁷ and for steroidal diamines such as irhediamine A¹⁸. Simple electrostatic binding of charged dyes to the phosphates no doubt also occurs. It is to be expected that the modes of binding that occur will be somewhat dependent on the sequence composition of the DNA.

In this chapter investigations of the binding of the chiral inorganic complexes $[\text{Ru}(\text{phen})_3]\text{Cl}_2$ and $[\text{Ru}(\text{dip})_3]\text{Cl}_2$ to DNA by luminescence assays are described. The metal center imparts a spectroscopic handle to the molecule because of the intense metal to ligand charge transfer band. We take advantage, also, of the the chirality of the molecule by monitoring the difference in binding of the two enantiomers. This property is useful because the differential binding of the two enantiomers, in many cases, reflects the conformation of the

right handed helix. In the first sections below we investigate the overall effect of DNA on the luminescence of the two enantiomers, discuss the origin of the sensitivity of luminescence of these complexes to DNA and develop a luminescence assay to monitor binding. In the latter sections we investigate the effect of the different types of DNA binding sites on the luminescence of the two enantiomers, by employing synthetic polynucleotides with varying base compositions. This data together with data from experiments done by coworkers in our laboratory¹⁹ is used to propose a model of the way in which the observed variations in the luminescence of the complex reflect the nature of the binding and the way in which the nature of the binding reflects the DNA structure.

Experimental Procedures

Nucleic Acids.

Calf thymus DNA was purchased from Sigma Chemicals and purified by phenol extraction as described previously.²⁰ An extinction coefficient of $6600 \text{ M}^{-1} \text{ cm}^{-1}$ at 260 nm was used to determine nucleotide concentrations.²¹ The synthetic polynucleotides poly(dA-dT)·poly(dA-dT) and poly(dG-dC)·poly(dG-dC) were purchased from P.L. Biochemicals. Extinction coefficients of $6600 \text{ M}^{-1} \text{ cm}^{-1}$ ²² and $8400 \text{ M}^{-1} \text{ cm}^{-1}$ ²³, respectively, were used to determine concentrations of these polynucleotides. All nucleic acids were extensively dialyzed against buffer R (5mM Tris-HCl, 50mM NaCl, pH 7.5) prior to the luminescence experiments.

Syntheses of ruthenium(II) complexes.

The ruthenium starting materials used for the syntheses of the complexes was obtained from either of two sources. K_2RuCl_5 was purchased from Alfa products, and RuCl_3 was

received as a gift from Engelhard. The ligands, 1,10-phenanthroline and 4,7-diphenyl- 1,10-phenanthroline were purchased from Aldrich Chemicals. Syntheses were carried out as described by Lin et. al.²⁴ except that the final products were recrystallized using NaCl rather than HCl. (The latter caused formation of a large amount of a clear crystalline solid.)

Several types of analyses were done to ensure the purity of the products. An extinction coefficient of $3.02 \times 10^4 \text{ M}^{-1} \text{ cm}^{-1}$ was determined for the visible charge transfer band which is consistent with the reported literature value of $2.95 \times 10^4 \text{ M}^{-1} \text{ cm}^{-1}$ ²⁴. Moreover, the UV-visible absorbance spectra observed are identical with published spectra of the complexes.²⁵ A typical elemental analysis was as follows, found: C:68.44, H:4.87, N:6.53, calculated: C:68.7, H:4.64, N: 6.67. An NMR spectrum of the $[\text{Ru}(\text{Dip})_3]\text{Cl}_2$ complex is shown in Figure 2a.

The samples of $[\text{Ru}(\text{phen})_3]\text{Cl}_2$ used in the experiments described below were gifts from several laboratory coworkers. Spectral characteristics of these complexes were also consistent with those reported in the literature.

Resolution of $[\text{Ru}(\text{phen})_3]\text{Cl}_2$ and $[\text{Ru}(\text{Dip})_3]\text{Cl}_2$ enantiomers.

a. $[\text{Ru}(\text{phen})_3]\text{Cl}_2$.

Enantiomers of $[\text{Ru}(\text{phen})_3]\text{Cl}_2$ were obtained by successive recrystallizations with antimony d-tartrate purchased from Pfaltz and Bauer inc. This method of separation has been described previously.²⁶ Specifically, $[\text{Ru}(\text{phen})_3]\text{Cl}_2$ was dissolved in water and a solution of the tartrate salt was added. The precipitate was filtered and redissolved, both precipitate and filtrate were recrystallized and the process was repeated until a molar ellipticity approaching $606 \text{ M}^{-1} \text{ cm}^{-1}$ was obtained. Based on studies done by Mason and Peart^{27*} and studies done in our laboratory with chiral shift reagents²⁸, this value corresponds to the molar ellipticity of pure

* The $\Delta\epsilon$ value determined for enantiomeric $\text{Ru}(\text{phen})_3\text{Cl}_2$ in our laboratory was slightly larger than that determined in reference 26.

enantiomers. C.D. spectra of the $[\text{Ru}(\text{phen})_3]\text{Cl}_2$ enantiomers used in several of the luminescence experiments are shown in Figure 1a. The optical rotations are $606 \text{ M}^{-1} \text{ cm}^{-1}$ for the Λ enantiomer and $450 \text{ M}^{-1} \text{ cm}^{-1}$ for the Δ enantiomer. Absolute configurations were assigned analogously to those assigned for $[\text{Fe}(\text{phen})_3]\text{Cl}_2$ by crystallographic methods²⁹ and by exciton theory³⁰.

Consistent, reproducible results from the luminescence experiments were obtained only when the Sb-D tartrate was removed and chloride anions were substituted onto both enantiomers. Clearly, intensities of emission are extremely sensitive to small variations in the solution, such as the anion or the salt concentration. The anion exchange was accomplished by the use of anion exchange columns or successive precipitations in concentrated NaCl solutions. The removal of the tartrate anion can be easily monitored by the carbonyl stretch on the I.R. spectrum, or by the CD spectrum of tartrate, which is very strong below 240 nm. The presence of tartrate does not affect the C.D. spectrum of the ruthenium complex at wavelengths above 240 nm, as illustrated in Figure 1c. As an extra precaution, in the first luminescence experiments performed, solutions of a racemic mixture were compared to solutions of a 50/50 mixture of the resolved Δ and Λ enantiomers. This comparison ensured that no impurities were introduced into the enantiomeric solutions as a result of the separation procedure.

Partial resolution of the $[\text{Ru}(\text{phen})_3]\text{Cl}_2$ enantiomers could also be accomplished by use of a DNA-cellulose column (Sigma chemicals). However, this technique was not optimized and enantiomers obtained in this manner were not used in luminescence experiments.

b. $[\text{Ru}(\text{Dip})_3]\text{Cl}_2$

$[\text{Ru}(\text{Dip})_3]\text{Cl}_2$ enantiomers were resolved in a similar fashion to that used for the $[\text{Ru}(\text{phen})_3]\text{Cl}_2$ enantiomers. The differences between the two methods, arise because of the differences in solubilities of the two ligands. To resolve enantiomers of the $[\text{Ru}(\text{Dip})_3]\text{Cl}_2$, a

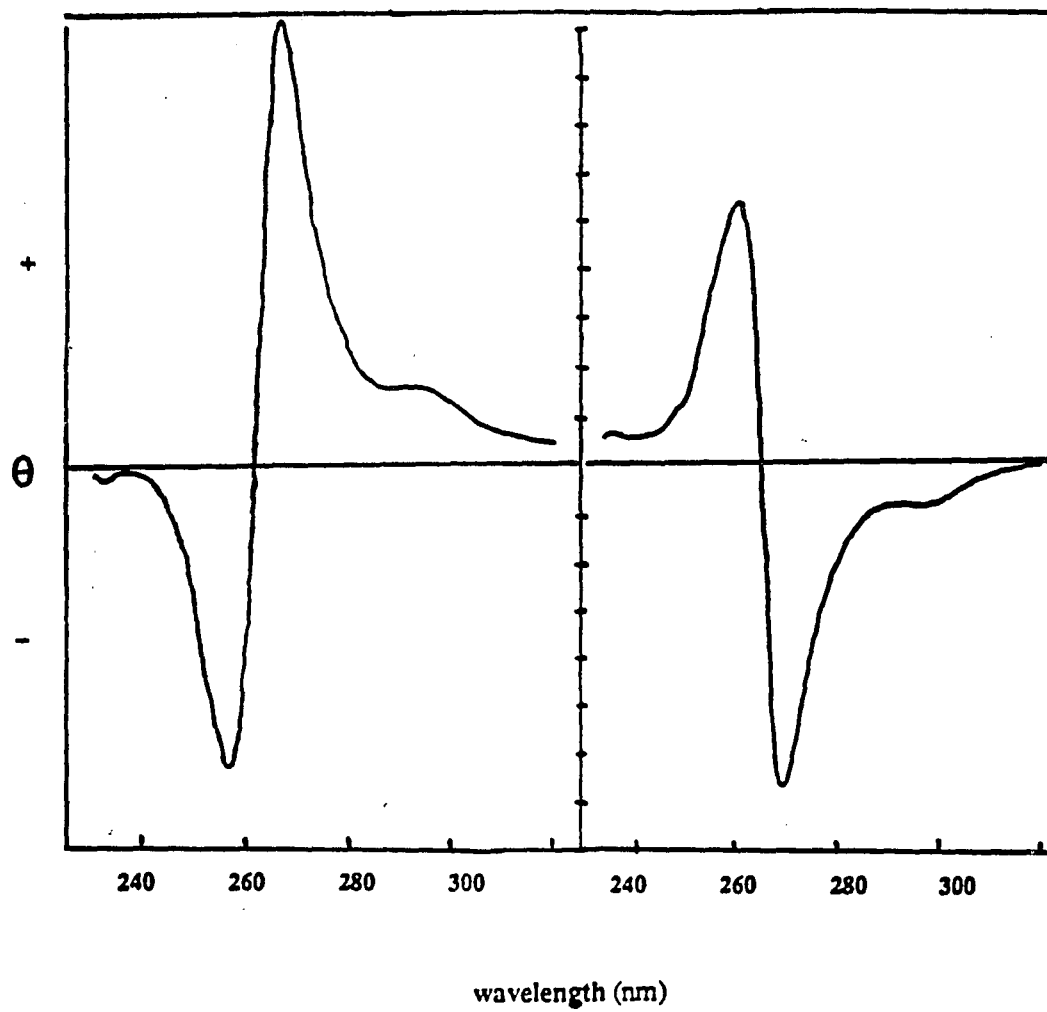


Figure 1a. C.D. spectra of enantiomers of $[\text{Ru}(\text{phen})_3]\text{Cl}_2$ ($10\mu\text{M}$) used in the luminescence titrations. (Instrument sensitivity = 20). right: spectrum of the solution enriched in the Δ enantiomer - 89% Δ , left: spectrum of the solution enriched in the Λ enantiomer - 100% Λ .

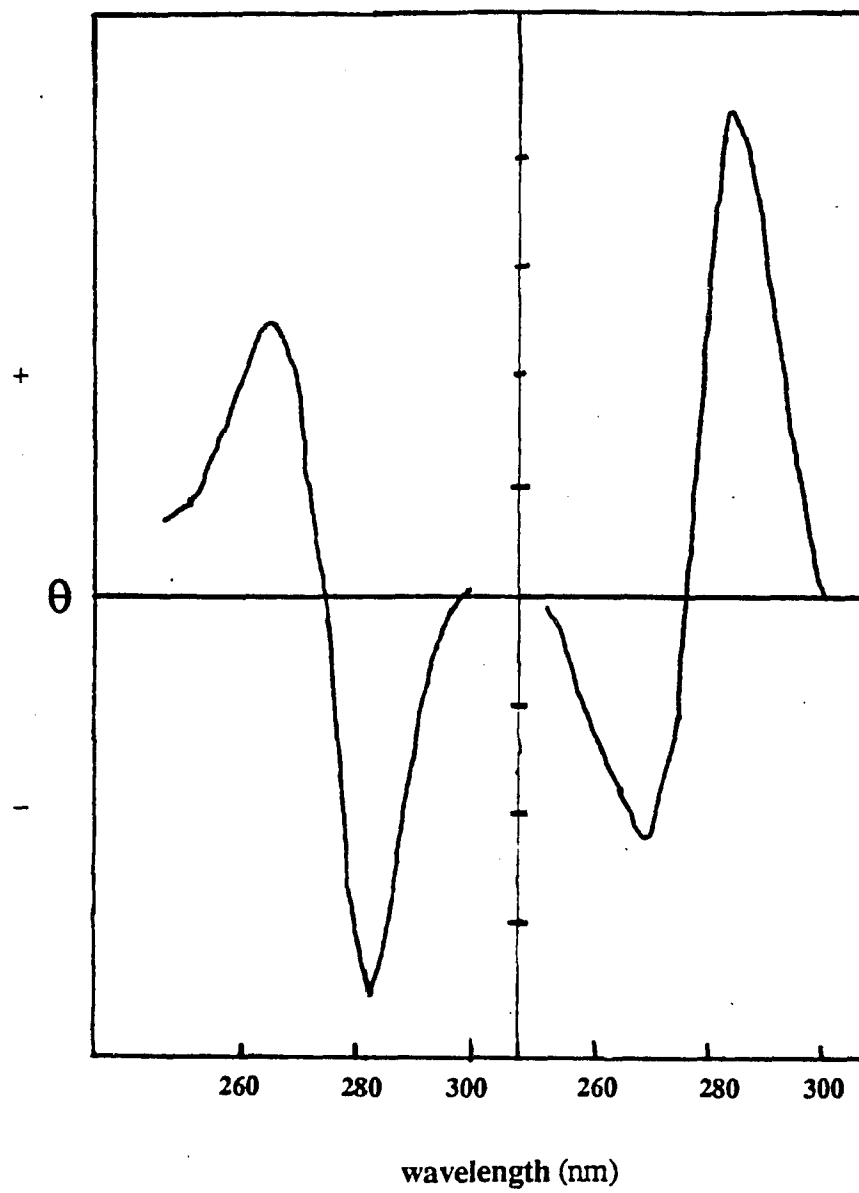


Figure 1b. C.D. spectra of enantiomers of $[\text{Ru}(\text{dip})_3]\text{Cl}_2$ (10 μM) used in the luminescence titrations

concentrated solution of the complex was prepared in ethanol to which an equal volume of water was added. To this clear solution, a concentrated solution of Sb-D-tartrate was added dropwise to obtain a final stoichiometry of approximately 1:1 $[\text{Ru}(\text{Dip})_3]\text{Cl}_2$ to tartrate. The precipitate, which developed either immediately or overnight was filtered and then redissolved by the addition of a few drops of nitromethane, several milliliters of ethanol and an equal volume of H_2O , in that order. The nitromethane was necessary to dissolve the complex which had limited solubility in ethanol. The Λ enantiomer tended to be enriched in the precipitate but this was dependent on pH as well as concentration of the solution. The separation was most efficient when no pH adjustments were made to the ethanol H_2O solutions (i.e. pH 5-7). An NMR spectrum of $[\text{Ru}(\text{Dip})_3]\text{Cl}_2$ in the presence of the chiral shift reagent, tris[3-(trifluoromethylhydroxymethylene)- α -camphorato]europium(III) is shown in Figure 2. The spectra of both a racemic mixture and a sample with an optical rotation of $235 \text{ M}^{-1} \text{ cm}^{-1}$ are shown. Using this method we assign the rotation of $[\text{Ru}(\text{Dip})_3]\text{Cl}_2$ to be approximately $300 \text{ M}^{-1} \text{ cm}^{-1}$.

The methods used to substitute chloride ions for tartrate ions described above for $[\text{Ru}(\text{phen})_3]\text{Cl}_2$ were not successful for $[\text{Ru}(\text{Dip})_3]\text{Cl}_2$ because of the insolubility of this complex. One alternative method for accomplishing the ion exchange was extraction of the complex into pentanol saturated with $\text{H}_2\text{O}/\text{HCl}$. The $[\text{Ru}(\text{Dip})_3]\text{Cl}_2$ partitioned almost exclusively into the pentanol phase whereas the tartrate salt was more soluble in the aqueous phase. Three or four extractions were usually sufficient to remove the tartrate salt.

Final recrystallizations from ethanol H_2O mixtures containing excess LiCl yielded very thin needle-like crystals of the Λ enantiomer. The less enantiomerically pure Δ complex was collected as powder.

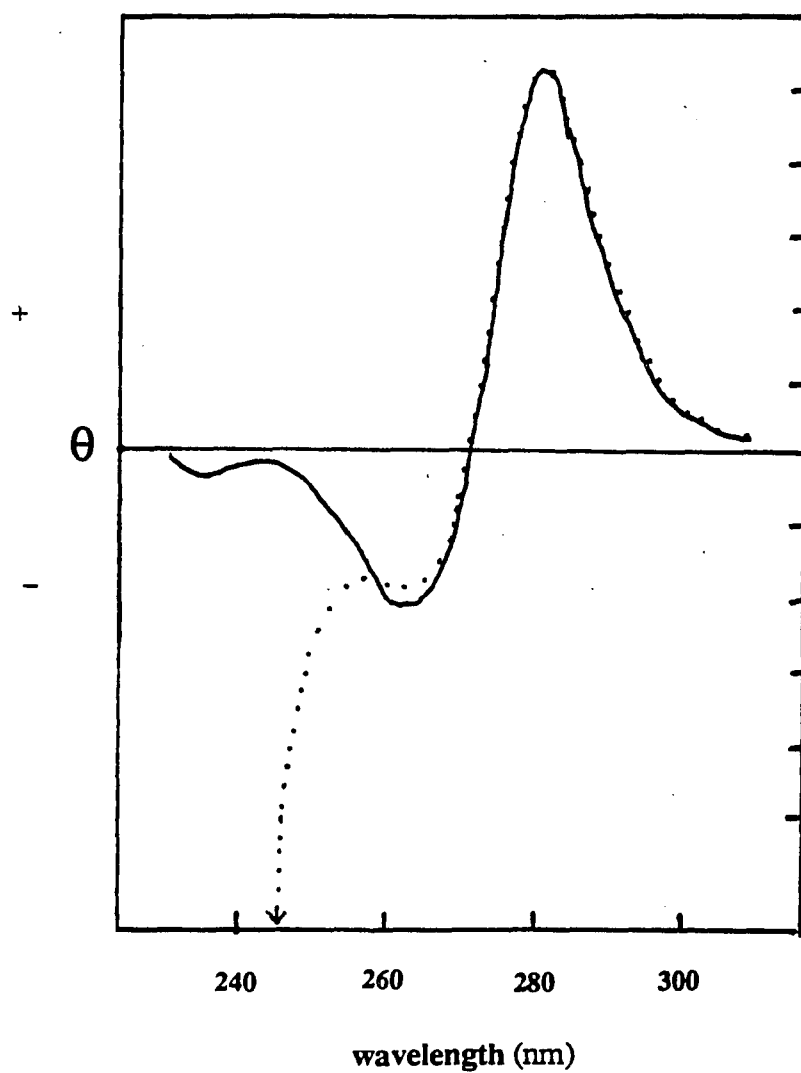


Figure 1c. C.D. spectrum of $[\text{Ru}(\text{dip})_3]\text{Cl}_2$ ($10\mu\text{M}$) in the presence (\cdots) and absence (\rightarrow) of excess Sb-D-tartrate. The excess tartrate was added to ensure an interaction with the ruthenium complex. The spectrum illustrates that there is practically no effect of the tartrate on the C.D. spectrum of $[\text{Ru}(\text{dip})_3]\text{Cl}_2$ at wavelengths above 240 nm. The optical rotation of tartrate itself becomes large at wavelengths below 240 nm.

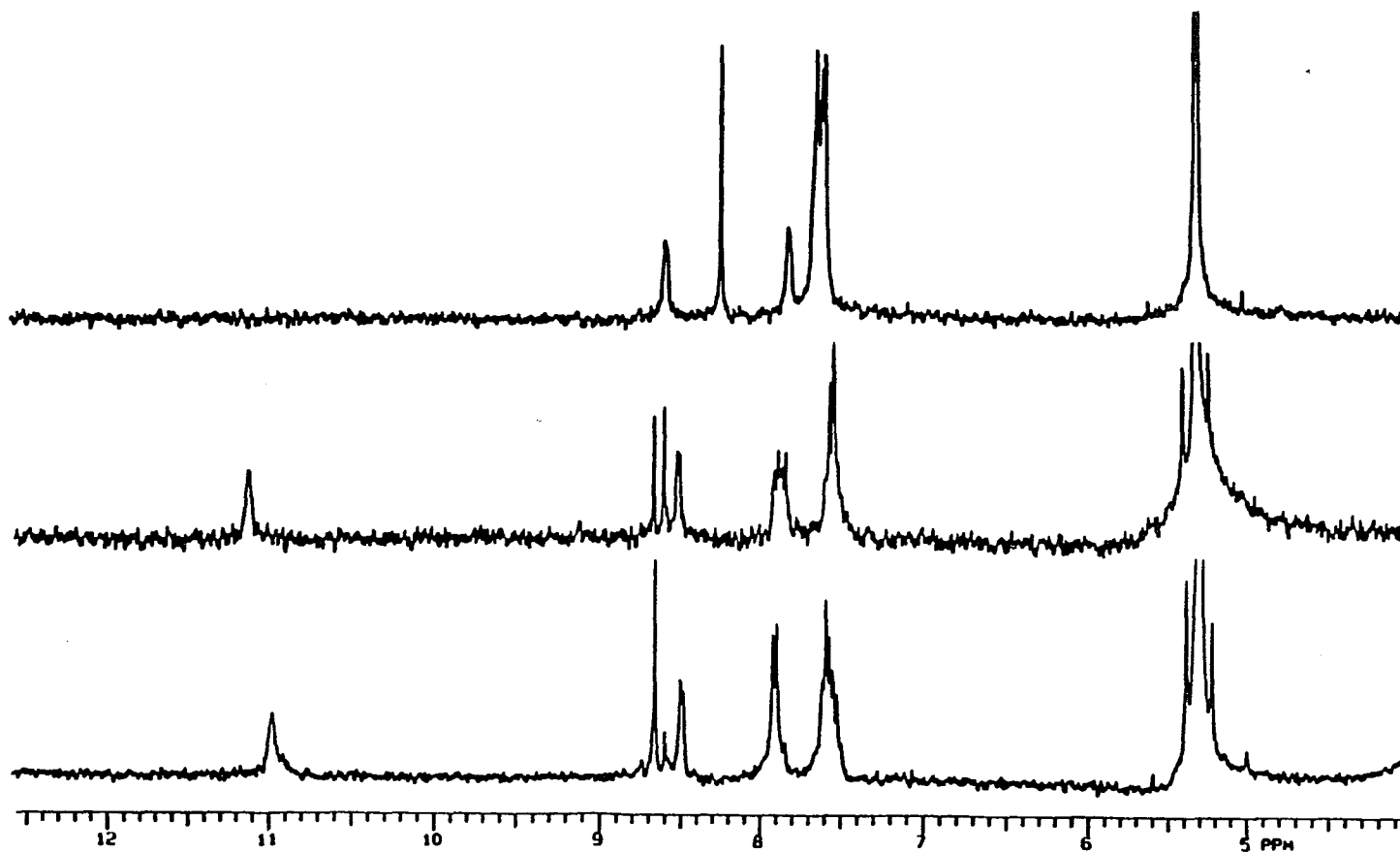


Figure 2. Proton NMR spectra illustrating the effect of the chiral shift reagent, $\text{Eu}(\text{tfc})_3$ on the spectrum of $[\text{Ru}(\text{dip})_3]\text{Cl}_2$. top: racemic mixture of $[\text{Ru}(\text{dip})_3]\text{Cl}_2$ in CD_2Cl_2 , middle: same as top spectrum with 5 mg. of the Eu shift reagent, bottom: enantiomerically enriched $[\text{Ru}(\text{dip})_3]\text{Cl}_2$ having a molar ellipticity of $235 \text{ M}^{-1} \text{ cm}^{-1}$, in the presence of $\text{Eu}(\text{tfc})_3$ in CD_2Cl_2 .

[Ru(phen)₃]Cl₂ emission spectra and titrations of [Ru(phen)₃]Cl₂ and [Ru(Dip)₃]Cl₂ with DNA

Titrations were performed on a Perkin-Elmer LS-5 spectrofluorimeter. Samples were excited at 460 nm, the isosbestic point in absorbance titrations, and emission was monitored at 595 nm. Both excitation and emission slit widths were set at 3 nm. The fluorimeter was fitted with a UV filter to counteract screening effects caused by the large absorbance in the UV region by the phenanthroline ligands and by the DNA in these experiments. The experiments were performed in ES quartz glass cells purchased from NSG Precision Cells Inc.

Titrations were performed by adding aliquots of DNA from a concentrated stock solution to a solution of [Ru(phen)₃]Cl₂ and the emission intensities were monitored. Since the DNA stock solution did not contain [Ru(phen)₃]Cl₂, intensities were always corrected for dilution effects. The intensity of the readings were somewhat unstable with time and were therefore recorded at a consistent time interval (1 minute) after the DNA was added. Spectra were recorded using a Perkin Elmer Data Station and the PECLS program. The concentrations of [Ru(phen)₃]Cl₂ in these experiments was either 3 μ M or 10 μ M. The latter was most convenient for observing binding but emission intensities were not linear with ruthenium concentrations in this region. (This non-linearity is more likely a function of the instrumentation than a property of the complex.)

[Ru(Dip)₃]Cl₂ emission titrations were carried out by methods similar to those described for [Ru(phen)₃]Cl₂ emission titrations, with the following changes. [Ru(Dip)₃]Cl₂ stock solutions were prepared in DMSO immediately prior to performing the experiment. Stock concentrations were such that the final DMSO concentration in the titration experiment was less than 0.3%. Given concentrations of DNA were mixed thoroughly in buffer within the fluorescence cell. The [Ru(Dip)₃]Cl₂ was then diluted to 3 μ M within the cuvette and mixed

slightly, just until the compound was observed to be evenly distributed throughout the cuvette. This sequence of events was necessary because the $[\text{Ru}(\text{Dip})_3]\text{Cl}_2$ complex is quite insoluble in aqueous solution and sticks to surfaces of cuvettes, pasteur pipettes etc.. Any excessive mixing or other disturbance of the solution exacerbates this situation. On the other hand, the presence of DNA solubilizes the $[\text{Ru}(\text{Dip})_3]\text{Cl}_2$ somewhat. Prior addition of DNA therefore allowed adequate mixing of the viscous, DNA stock solution without excessive disturbance of the $[\text{Ru}(\text{Dip})_3]\text{Cl}_2$ in addition to slightly increasing the solubility of the latter complex.

Excited state lifetime measurements

Lifetime measurements were performed on an Ortec 776 single photon counter and timer in line with an Apple Computer. The samples were excited with a PRA 510A nanosecond lamp and emission was observed at 593 nm. Measurements were made at ambient temperature. No attempt was made to purge the O_2 from the cell. The time per channel was equal to 1.64×10^{-8} seconds.

Results

Effect of DNA binding on emission properties of racemic $[\text{Ru}(\text{phen})_3]\text{Cl}_2$.

The following experiments were performed to determine the effect of binding to DNA on the luminescence properties of $[\text{Ru}(\text{phen})_3]\text{Cl}_2$.

Emission Spectra.

The emission spectra of $[\text{Ru}(\text{phen})_3]\text{Cl}_2$ in the free form and when bound to calf thymus DNA are shown in Figure 3. Addition of DNA to $[\text{Ru}(\text{phen})_3]\text{Cl}_2$ at the concentrations

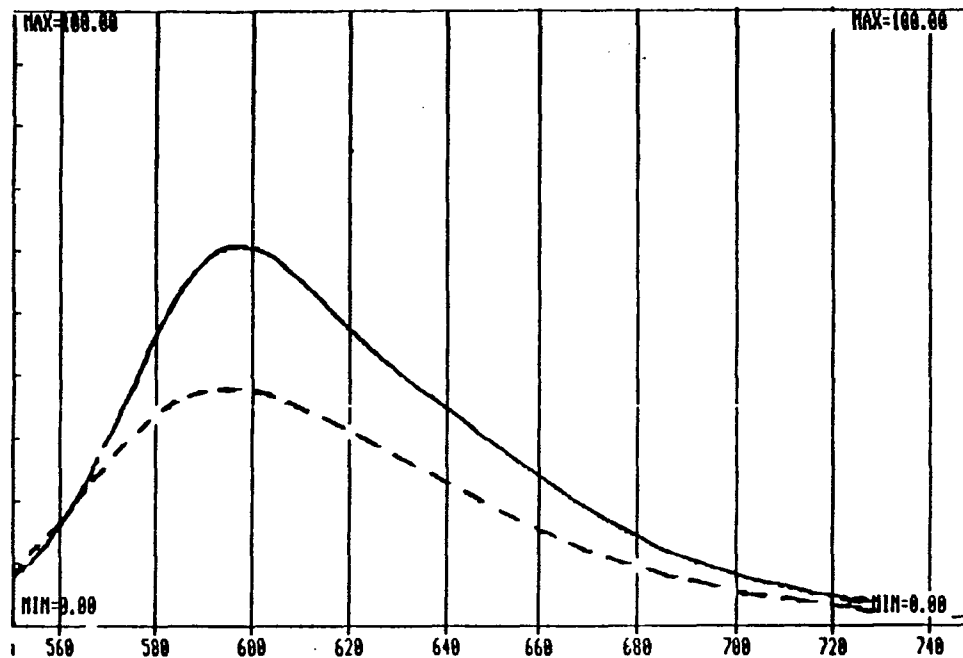


Figure 3. Emission spectra of racemic [Ru(phen)₃]Cl₂ free (- -) and in the presence of calf thymus DNA (-). The ruthenium and nucleotide concentrations were 10 μM and 200 μM respectively.

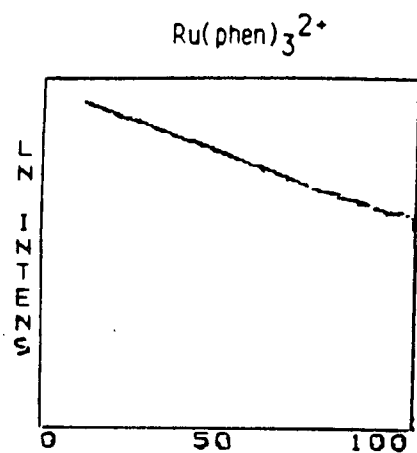
indicated causes an approximately two-fold enhancement of emission. A small red shift at the peak maximum, of 2-3 nanometers is observed as well.

Excited State Lifetimes.

The excited state lifetimes of $[\text{Ru}(\text{phen})_3]\text{Cl}_2$ measured are shown in Figure 4. A lifetime of 0.54 $\mu\text{seconds}$ was measured for free $[\text{Ru}(\text{phen})_3]\text{Cl}_2$, consistent with values reported in the literature.³¹ The decay curve is monoexponential, indicating one emitting species. In contrast, the decay curve of the bound form of $[\text{Ru}(\text{phen})_3]\text{Cl}_2$ was not monoexponential and clearly contained contributions from more than one species. The decay traces were not deconvoluted at this time. Rather, approximations were made by neglecting the first one to two microseconds of the curve thus reducing the contribution of the free form to the decay curve. By this approximation, the excited state lifetime was found to increase approximately three-fold as a result of binding to DNA. This value was subsequently corroborated by fitting the trace to a biexponential equation.^{19a}

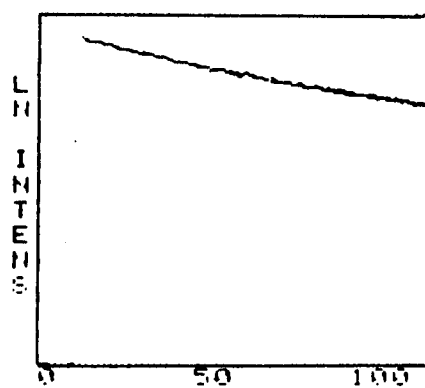
Emission titrations of $[\text{Ru}(\text{phen})_3]\text{Cl}_2$ enantiomers with calf thymus DNA.

In order to determine if the emission enhancement observed reflects an enantioselective mode of binding to calf thymus DNA an emission titration of the enantiomers of $[\text{Ru}(\text{phen})_3]\text{Cl}_2$ with calf thymus DNA was performed. Figure 5 illustrates that addition of DNA causes a gradual enhancement concomitant with binding. The observed enhancement is slightly greater for the Δ enantiomer than for the Λ enantiomer. At the DNA concentrations shown the emission of the Δ enantiomer is approximately 30% more enhanced than that of the Λ enantiomer. This value is consistent with the enantioselectivity observed from equilibrium dialysis data.³² The qualitative effect of DNA on the emission spectrum is the same for both enantiomers as shown in Figure 6.



CHANNEL NO
LIFETIME IS $5.4\text{E}-07\text{SEC}$
CORRELATION COEFFICIENT $-.998$

$\text{Ru}(\text{phen})_3^{2+}$ with calf thymus DNA



CHANNEL NO
LIFETIME IS $1.5\text{E}-06\text{SEC}$
CORRELATION COEFFICIENT $-.992$

Figure 4. Plots of the excited state decays of free $[\text{Ru}(\text{phen})_3]\text{Cl}_2$ (top) and $[\text{Ru}(\text{phen})_3]\text{Cl}_2$ in the presence of calf thymus DNA (bottom). Ru and DNA concentrations were $10\ \mu\text{M}$ and $300\ \mu\text{M}$ respectively. The time per channel was 1.64×10^{-8} seconds.

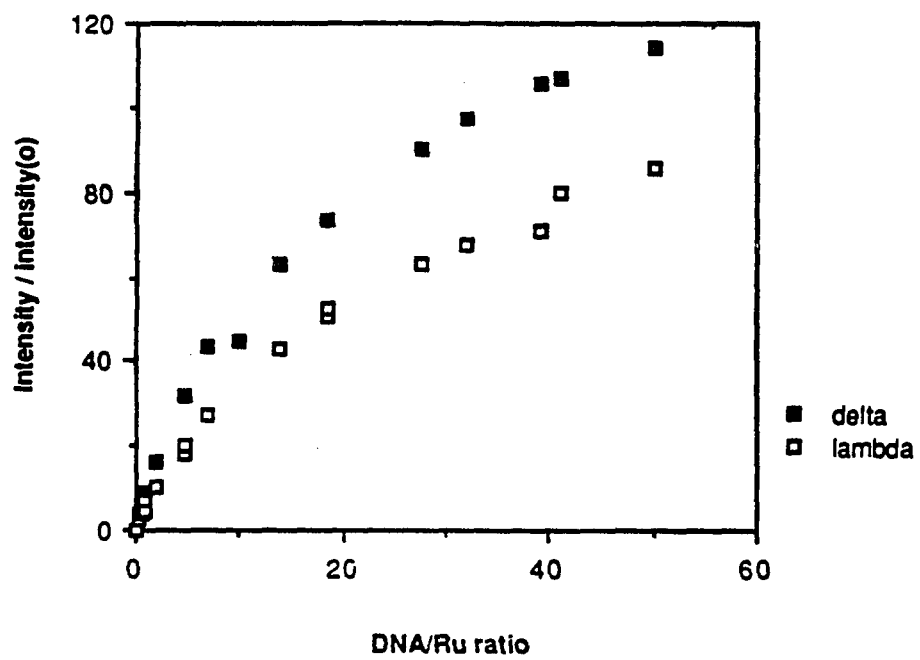


Figure 5. Luminescence titrations of enantiomeric $[\text{Ru}(\text{phen})_3]\text{Cl}_2$ with calf thymus DNA. $[\text{Ru}(\text{phen})_3]\text{Cl}_2$ concentration is equal to 10 μM .

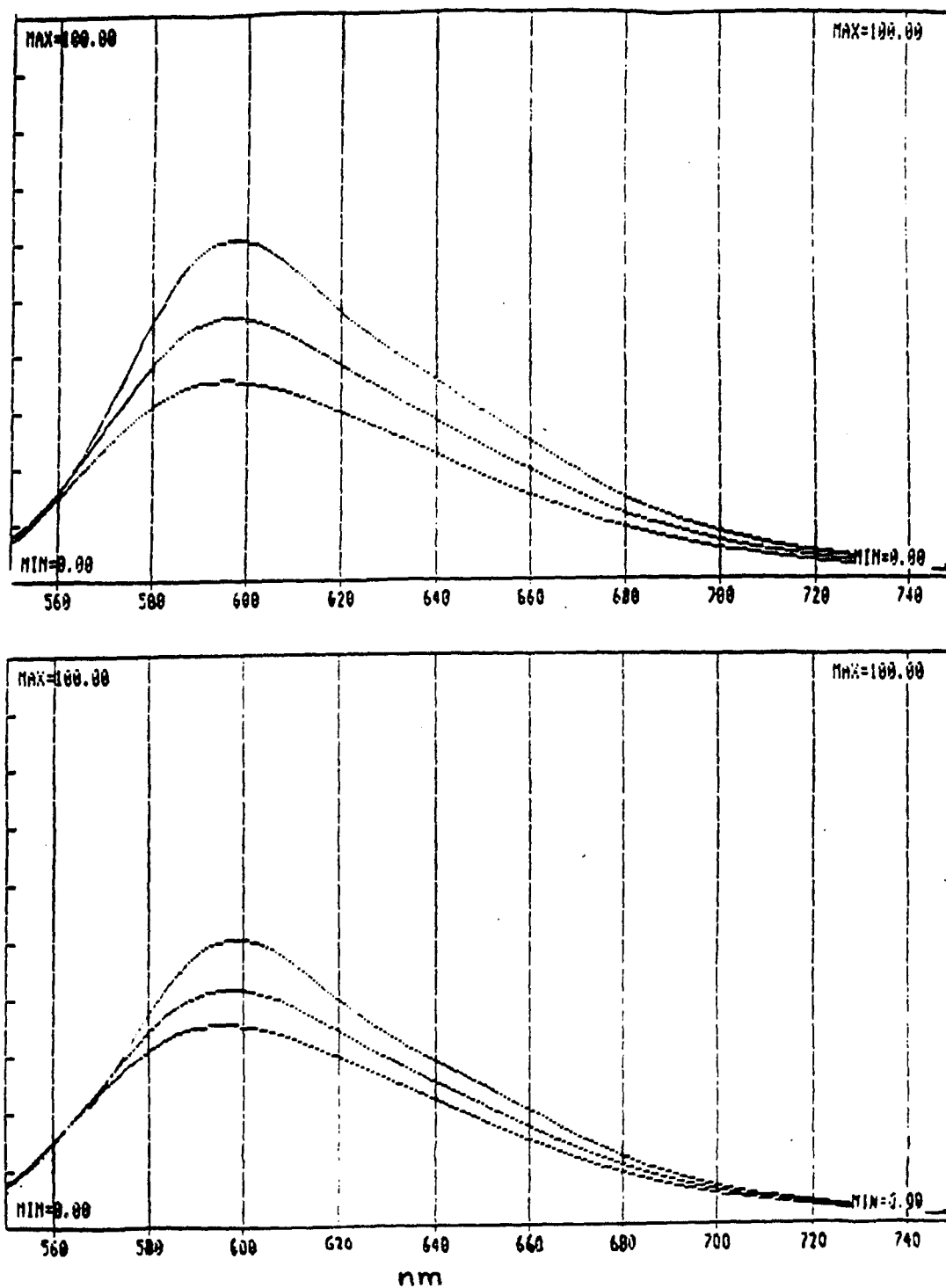


Figure 6. Emission spectra of Δ (top) and Λ (bottom) $[\text{Ru}(\text{phen})_3]\text{Cl}_2$ free and bound to calf thymus DNA. The nucleotide to ruthenium ratios for the spectra shown were 0:1, 7:1, and 15:1.

Sequence dependence of emission enhancement and enantioselectivity.

The experiments discussed in previous sections have demonstrated that the emission of $[\text{Ru}(\text{phen})_3]\text{Cl}_2$ is sensitive to the DNA and that the binding of $[\text{Ru}(\text{phen})_3]\text{Cl}_2$ to DNA can be monitored by luminescence titrations. It is useful to know whether these titrations are also sensitive to the particular nature of the site on the DNA. To address this question we monitored the emission of $[\text{Ru}(\text{phen})_3]\text{Cl}_2$ as a function of binding to synthetic polynucleotides, poly(dG-dC)·poly(dG-dC) and poly(dA-dT)·poly(dA-dT). Figure 7 and 8 illustrate emission titrations of enantiomers of $[\text{Ru}(\text{phen})_3]\text{Cl}_2$ with synthetic polynucleotides of various base compositions. (The poly(dA-dT)·poly(dA-dT) titrations were performed at a $[\text{Ru}(\text{phen})_3]\text{Cl}_2$ concentration of $3\mu\text{M}$. This concentration was preferred because the emission intensities of $[\text{Ru}(\text{phen})_3]\text{Cl}_2$ were found to be slightly non-linear with concentration. The emission of poly(dG-dC)·poly(dG-dC), however, was not enhanced enough at these concentrations, so a $[\text{Ru}(\text{phen})_3]\text{Cl}_2$ concentration of $10\mu\text{M}$ was used in this case. Titrations with calf thymus DNA were done at both these concentrations for comparison. The following results were observed:

1. Poly(dG-dC)·poly(dG-dC) is the most enantioselective in its enhancement of the emission of $[\text{Ru}(\text{phen})_3]\text{Cl}_2$ of the polynucleotides examined. Enhancement of the Δ enantiomer is observed but no enhancement of the Λ enantiomer is observed up to DNA to ruthenium ratios of 10:1.
2. Whereas the Δ enantiomer is preferred to the exclusion of the Λ enantiomer (as far as can be discerned from this experimental technique) in the case of poly(dG-dC)·poly(dG-dC), and is slightly preferred in the case of calf thymus DNA, enhancement by poly(dA-dT)·poly(dA-dT) is greater for the Λ enantiomer.
3. The degree of emission enhancement of $[\text{Ru}(\text{phen})_3]\text{Cl}_2$ by the various polynucleotides follows the order poly(dA-dT)·poly(dA-dT) > calf thymus DNA > poly(dG-dC)·poly(dG-dC).

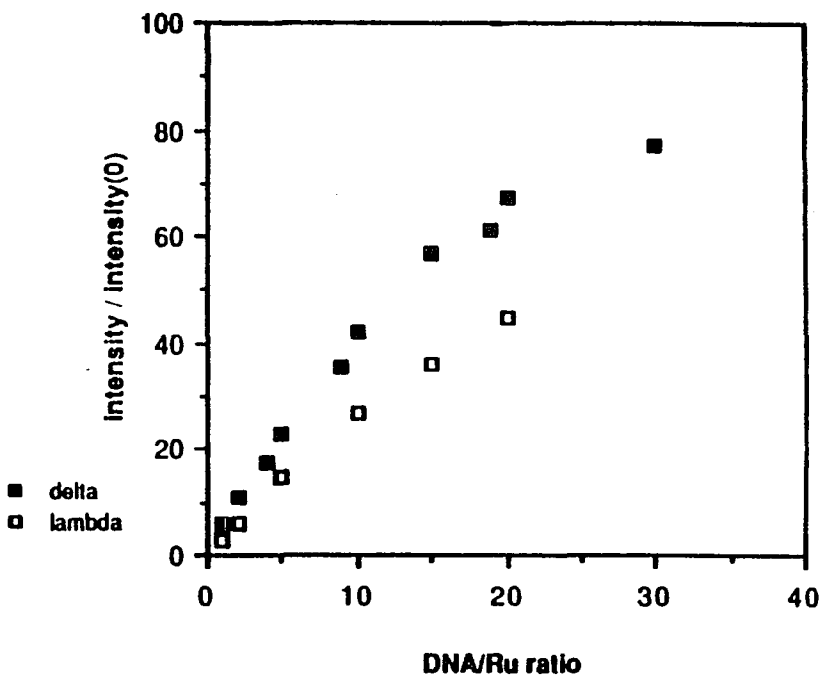
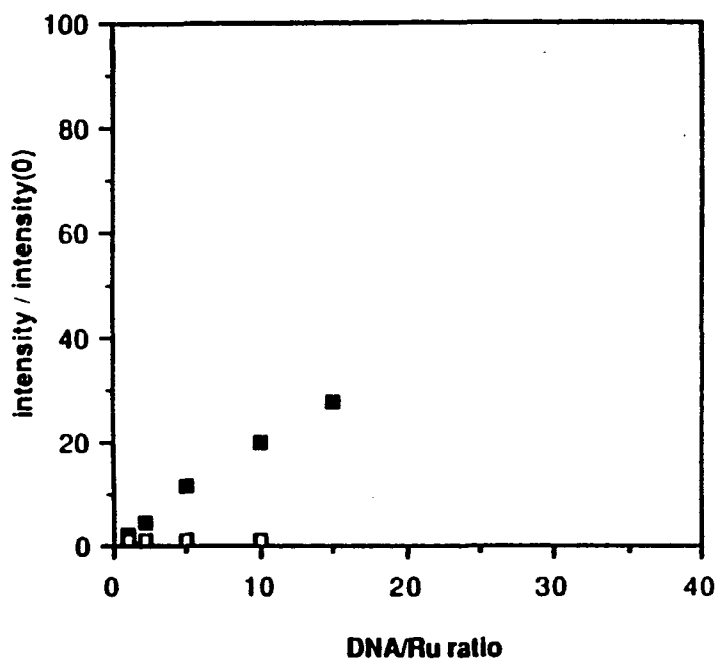


Figure 7. Luminescence titrations of enantiomeric $[\text{Ru}(\text{phen})_3]\text{Cl}_2$ with poly(dG-dC)poly(dG-dC) (left) and calf thymus DNA (right). The $[\text{Ru}(\text{phen})_3]\text{Cl}_2$ concentration was $10 \mu\text{M}$ for both titrations.

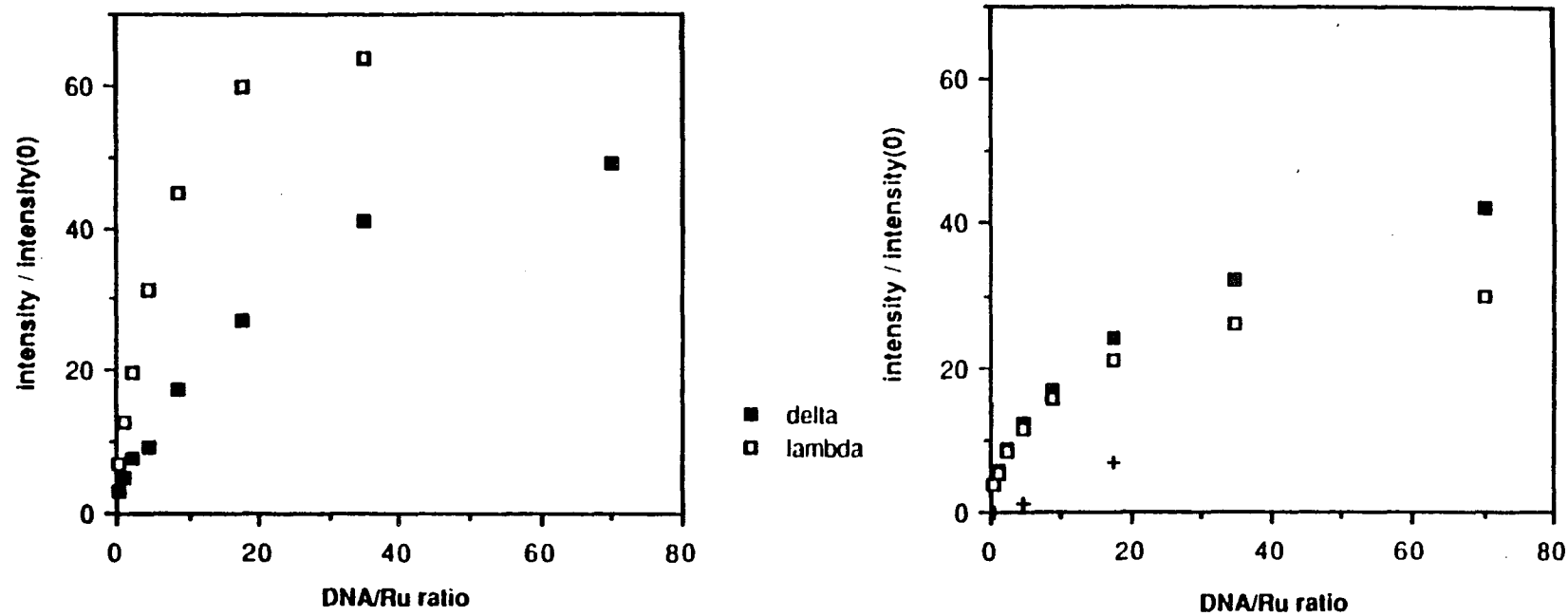


Figure 8. Luminescence titrations of enantiomeric $[\text{Ru}(\text{phen})_3]\text{Cl}_2$ with poly(dA-dT)poly(dA-dT) (left) and calf thymus DNA (right). Two points in a titration of the Δ enantiomer with poly(dG-dC)poly(dG-dC) are also shown for comparison (+). The $[\text{Ru}(\text{phen})_3]\text{Cl}_2$ concentration was $3 \mu\text{M}$ in all the titrations.

Effect of DNA on emission spectra of $[\text{Ru}(\text{Dip})_3]\text{Cl}_2$

An emission spectrum of free and bound $[\text{Ru}(\text{Dip})_3]\text{Cl}_2$ is shown in Figure 9 for a 2:1 ratio of DNA to ruthenium. The two fold increase in enhancement is similar to that seen for $[\text{Ru}(\text{phen})_3]\text{Cl}_2$ with calf thymus DNA. The 10 nm red shift in the case of $[\text{Ru}(\text{Dip})_3]\text{Cl}_2$ is larger than that seen for $[\text{Ru}(\text{phen})_3]\text{Cl}_2$.

Titration of enantiomers of $[\text{Ru}(\text{Dip})_3]\text{Cl}_2$ with calf thymus DNA

Emission titrations of $[\text{Ru}(\text{Dip})_3]\text{Cl}_2$ with calf thymus DNA are illustrated in Figure 10. The degree of enhancement is similar to that seen for $[\text{Ru}(\text{phen})_3]\text{Cl}_2$ but the maximum is reached very early in the titration i.e., below a ratio of 5:1 nucleotides to ruthenium. The figure illustrates that the emission enhancement of both enantiomers is nearly equal.

DNA sequence dependence of the emission enhancement of $[\text{Ru}(\text{Dip})_3]\text{Cl}_2$.

Titration of $[\text{Ru}(\text{Dip})_3]\text{Cl}_2$ with DNA were compared for calf thymus DNA poly(dG-dC)·poly(dG-dC) and poly(dA-dT)·poly(dA-dT). Graphs of these titrations are shown in Figure 11. The relative magnitudes of emission enhancements; poly(dA-dT)·poly(dA-dT) > calf thymus > poly(dG-dC)·poly(dG-dC), are similar to those observed for $[\text{Ru}(\text{phen})_3]\text{Cl}_2$. (Even larger differences among emission enhancements caused by the polynucleotides of various sequences were observed when conditions were varied slightly and 4% DMSO was used in the buffer.)

Discussion

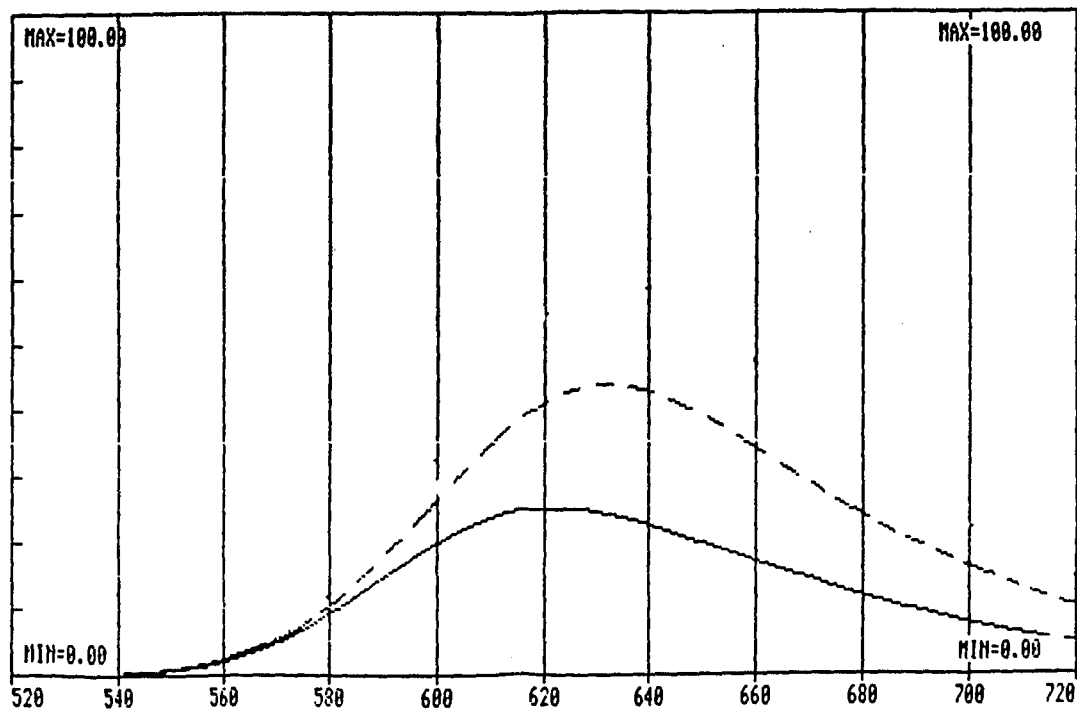


Figure 9. Emission spectra of racemic $[\text{Ru}(\text{dip})_3]\text{Cl}_2$, free (—) and in the presence of calf thymus DNA (--), at a ratio of 2:1 nucleotides to ruthenium

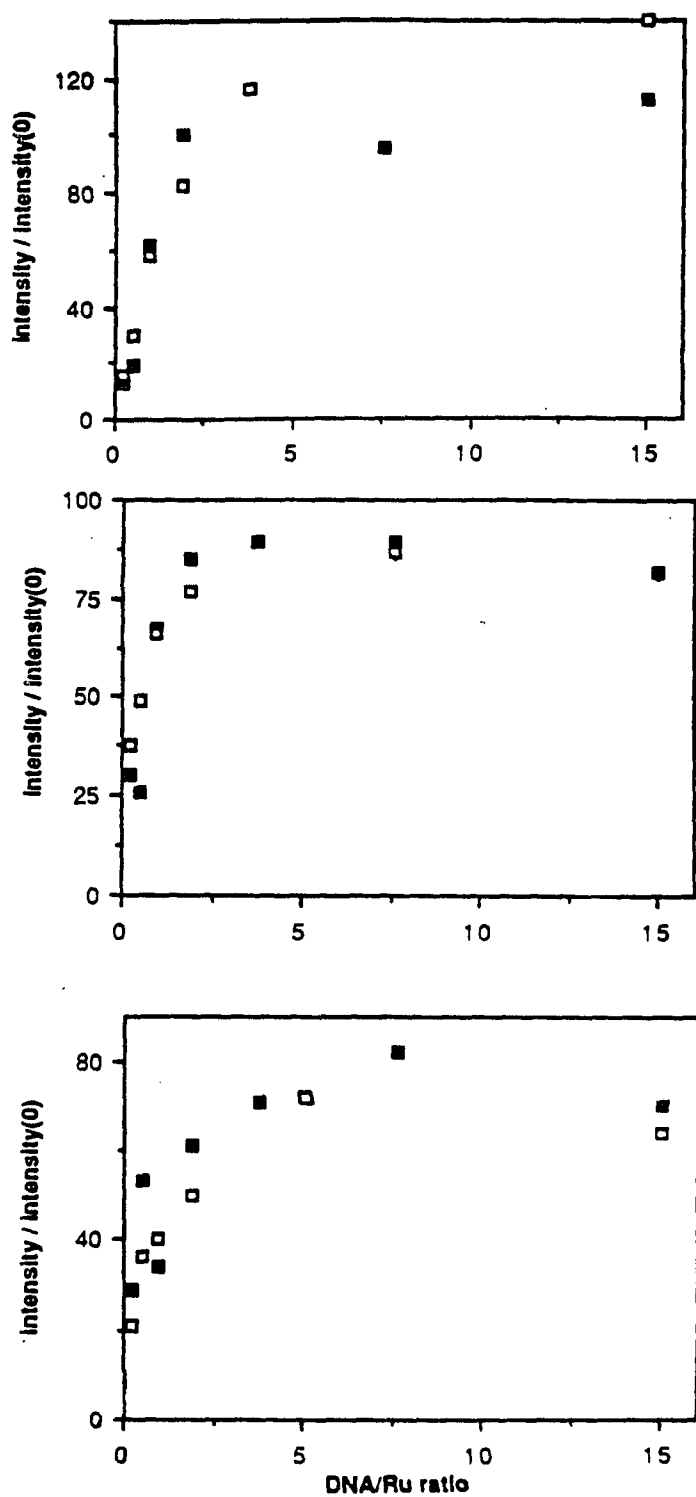


Figure 10. Luminescence titrations of enantiomeric $[\text{Ru}(\text{dip})_3]\text{Cl}_2$ with poly(dA-dT):poly(dA-dT) (top), calf thymus DNA (middle) and poly(dG-dC):poly(dG-dC) (bottom). Δ , \blacksquare ; Δ , \square .

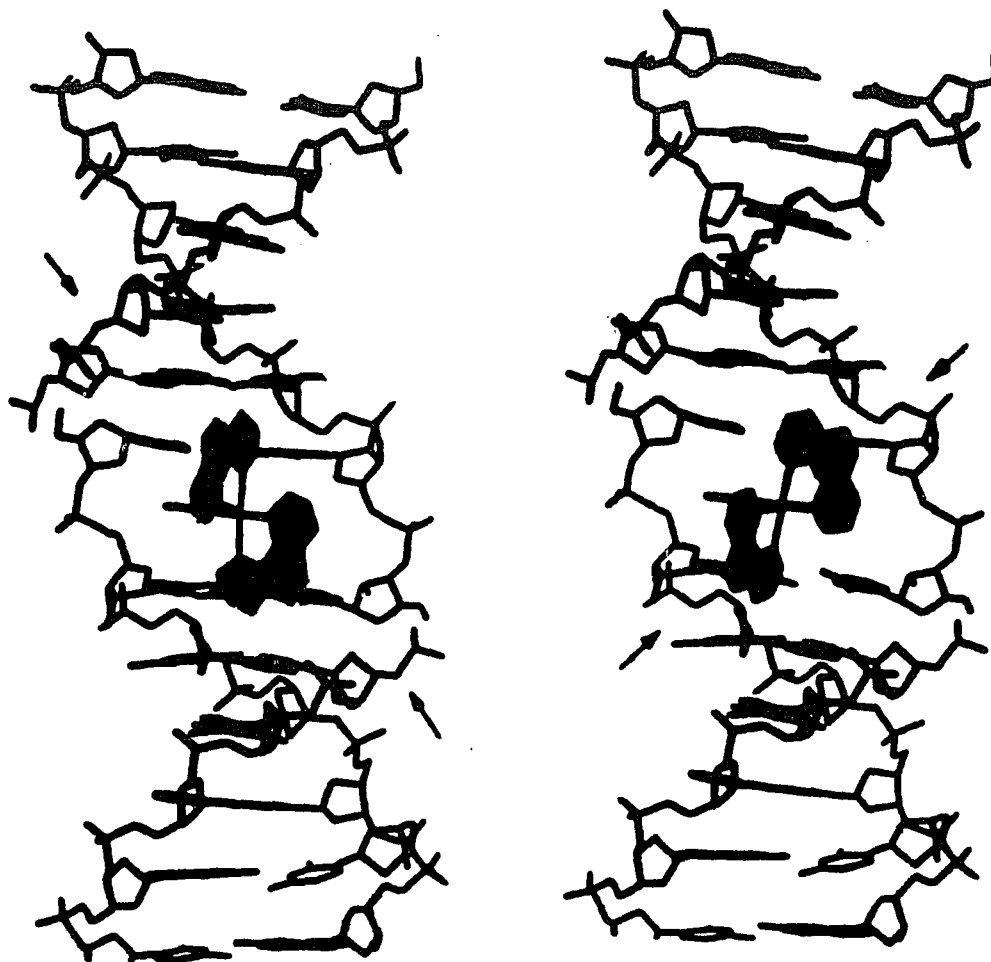


Figure 11. Diagrams of Λ (left) and Δ (right) $\text{Ru}(\text{phen})_3^{2+}$ with one phenanthroline ligand intercalated into B-DNA. When one ligand is intercalated the other two are positioned within the groove of the helix. The groove easily accommodates the two non-intercalating ligands of the Δ enantiomer. Binding of the Λ enantiomer is hindered somewhat by the interaction of the two non-intercalating ligands with the phosphodiester backbone.

Emission enhancement

Figure 3 illustrates the emission enhancement observed upon binding of $[\text{Ru}(\text{phen})_3]\text{Cl}_2$ to DNA. Emission spectra of $[\text{Ru}(\text{phen})_3]\text{Cl}_2$ have been extensively studied and this emission band has been assigned as a ^3CT to ground state.^{33,34}

The lifetime of the excited state of ruthenium polypyridyls has been found to be sensitive to the medium.^{31,35} The emission enhancement that we observe in the presence of DNA is consistent with these findings. Moreover, this sensitivity presents a handle for monitoring the binding of this molecule to DNA. It is therefore interesting to consider the basis for the effect of the medium on the emission of $[\text{Ru}(\text{phen})_3]\text{Cl}_2$. This topic has been addressed in the literature, though not yet fully answered. For example, some ruthenium polypyridyls have been found to have a faster rate of non-radiative decay in D_2O than in H_2O .³¹ This finding led to the suggestion that there is a charge transfer to solvent component to the relaxation and that this component accounts for the medium dependence. In other studies the non-radiative decay rate of the excited state has been observed to increase with higher solvent dielectric constant.³⁵ The dependence of the emission intensity of $[\text{Ru}(\text{phen})_3]\text{Cl}_2$ on the medium has been exploited in studies of the interaction of this molecule with micelles in aqueous solution.^{37,38} In those studies as well, it was found that interactions with micelles (or protection from the aqueous environment) enhances $[\text{Ru}(\text{phen})_3]\text{Cl}_2$ emission. In any case, interactions with the aqueous solvent seem to be important in affecting the emission intensity.

Excited state lifetime measurements

An emission enhancement such as that discussed in the above section can theoretically arise from either a smaller rate of non-radiative decay or a faster rate of radiative decay, according to the equation $\Phi = k_r / (k_r + k_{nr})$. (Φ =quantum yield of emission, k_r =radiative decay rate, k_{nr} =non-radiative decay rate) A faster rate of radiative decay would be expected to be accompanied by an

electronic change in the ground or excited state. Since the absorbance and emission spectra of $[\text{Ru}(\text{phen})_3]\text{Cl}_2$ in the bound and free forms are qualitatively similar (Figure 3 and reference 32), it seemed likely that the observed emission enhancement was due to a decreased rate of non-radiative decay.

To further investigate this question we examined the effect of DNA binding on the excited state lifetime of the complexes. A faster radiative decay rate would be reflected by a shorter radiative lifetime while a smaller non-radiative decay rate would result in a longer lifetime. The three-fold increase in the observed lifetime is consistent with a slower rate of non-radiative decay. Exclusion of the polar H_2O molecules (as discussed above) is likely to be at least partially responsible for this phenomenon.

Emission titrations of enantiomers of $[\text{Ru}(\text{phen})_3]\text{Cl}_2$ with calf thymus DNA.

Figure 5 illustrates the emission enhancement of $[\text{Ru}(\text{phen})_3]\text{Cl}_2$ as a function of calf thymus DNA concentration. The degree of enhancement is slightly larger for the Δ enantiomer than for the Λ enantiomer. This finding is consistent with equilibrium dialysis experiments done in our laboratory by Jon Golberg in which 20+ 10% more binding was observed for the Δ enantiomer over the Λ enantiomer with calf thymus DNA.³² The consistency between the results of the equilibrium dialysis experiments and the luminescence titration experiments demonstrates that increased enhancement reflects increased binding. This explanation is at least part and perhaps most of the overall scheme. It may be a slight oversimplification, however, since it has been shown in our laboratory by methods involving luminescence quenchers¹⁹ that there is more than one mode of binding for each enantiomer and that not all modes always lead to emission enhancement. (See below.) Nevertheless, the agreement between the equilibrium dialysis experiments and the luminescence titrations leads us to propose that in the case of titrations with calf thymus DNA, molecules bound by modes that do not lead to

luminescence enhancement are either not a large fraction of the overall bound population, or occur to equal extents for both enantiomers.

Equilibrium dialysis and spectroscopic methods complement each other in terms of the information that they yield. Equilibrium dialysis yields information about overall binding whereas luminescence experiments yield information about particular modes of binding. There are also other advantages and disadvantages to each of these experiments. A binding constant was obtained from equilibrium dialysis but not from luminescence titrations. Mainly, this is because the emission intensity of the bound $[\text{Ru}(\text{phen})_3]\text{Cl}_2$ remains unknown. At DNA concentrations large enough to have all the ruthenium bound, other factors, such as solution viscosity also affect emission enhancement. (These other factors are not large, but even small artifactual effects make it difficult to ascertain a binding constant by this method¹⁴.) On the other hand, in some sense the sensitivity of the luminescence experiment is greater than that of the equilibrium dialysis experiment. Enantioselectivity could only be determined in the dialysis experiments by a difference method in which the optical rotation of the unbound $[\text{Ru}(\text{phen})_3]\text{Cl}_2$ in the dialysate was measured. Experiments in which the two enantiomers were separately dialysed against the DNA were not sensitive enough to detect small differences in binding. Furthermore, the luminescence titrations present a simpler, less time consuming method for determining qualitative binding and enantioselectivity.

The preference in binding of the Δ enantiomer to calf thymus DNA is best interpreted in terms of an intercalation model. The Δ enantiomer preferentially intercalates into the DNA. Intercalation of the Λ enantiomer is less favored because of steric repulsions between the non-intercalated ligands and the helix backbone. This model is illustrated in Figure 12. The intercalation model is based on several types of experimental evidence: DNA unwinding angles measured by gel electrophoresis are similar to those of other intercalators.³² Luminescence depolarization values are greater for the bound Δ enantiomer than for the bound

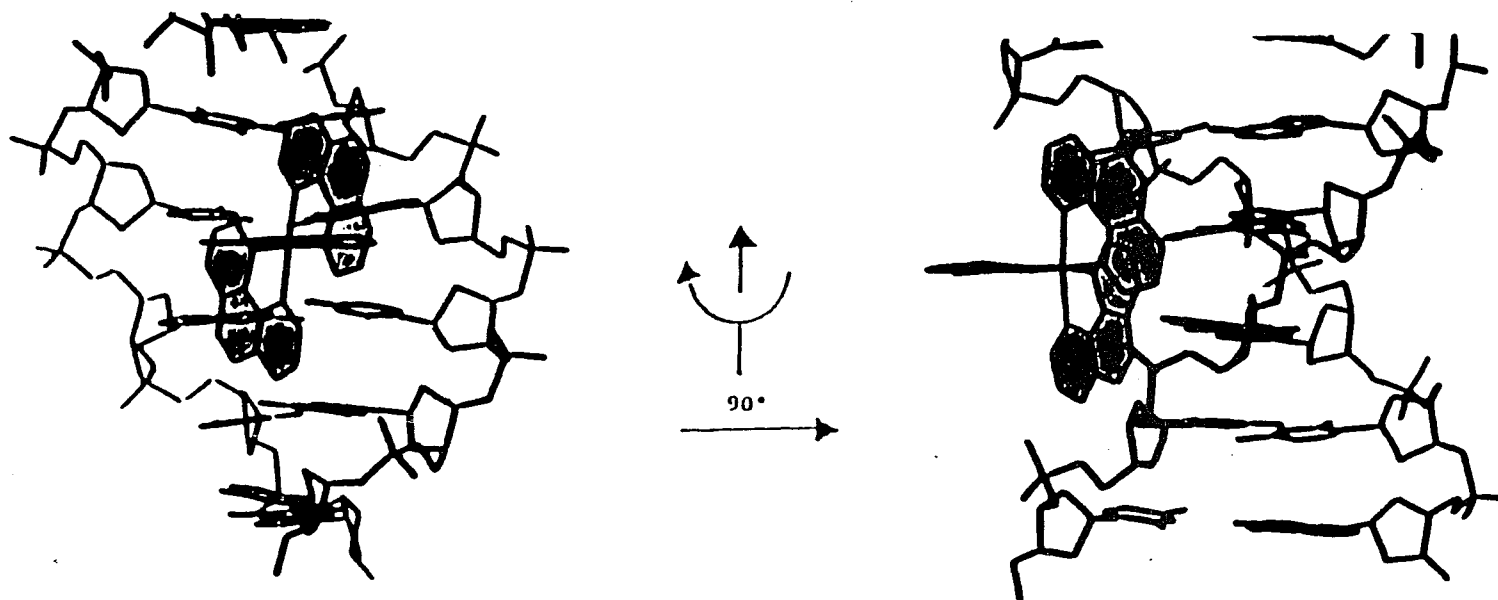


Figure 12. Illustration of the groove binding of the A enantiomer into B-DNA. Left, view facing the groove; right, view from the side of the groove.

Λ enantiomer. The bound Δ $[\text{Ru}(\text{phen})_3]\text{Cl}_2$ enantiomer is more inaccessible to solvent than the bound Λ enantiomer as shown by luminescence quenching experiments. Linear dichroism measurements consistent with one phenanthroline ligand perpendicular to the helix axis have been observed for $[\text{Ru}(\text{phen})_3]\text{Cl}_2$ ³⁹ and $[\text{Fe}(\text{phen})_3]\text{Cl}_2$ ⁴⁰.

The classical examples of intercalators involve extensive overlap of the ligand with the bases. However extensive overlap may not be necessary for a favorable stacking interaction. This point is noteworthy since because extensive overlap is not possible for $[\text{Ru}(\text{phen})_3]\text{Cl}_2$ because of the steric hindrance of the non-intercalating ligands. In a study done by Bugg et. al.⁴¹ seventy crystal structures of nucleotides and nucleosides were examined. A common packing motif, which prevailed through many complexes which were not structurally similar in other respects, was the partial overlap of rings or the overlap of a bond moment with a polarizable system. (Extensive overlap of aromatic rings was not a common motif.) Bugg et. al. attribute the favorability of this interaction to a dipole-induced dipole interaction. Other studies have also led to the conclusion that the interaction between the polar nucleotide and a polarizable ligand is important in complex formation.

Sequence dependence of enhancement

Emission titrations of $[\text{Ru}(\text{phen})_3]\text{Cl}_2$ with DNA (Figures 7 and 8) have shown that there is greatest emission enhancement of $[\text{Ru}(\text{phen})_3]\text{Cl}_2$ with poly(dA-dT)·poly(dA-dT), least for poly(dG-dC)·poly(dG-dC) and intermediate for calf thymus DNA. Three types of explanations can be invoked to account for the observed sequence dependence of the magnitude of emission enhancement:

1. Enhancement may simply reflect the quantity of binding.

2. Various modes of binding occur for the different sequences and these modes may differ in the degree of emission enhancement that they cause.

3. The different electronic structures of the bases or different solvent structures surrounding the bases may cause varying degrees of quenching in a sequence dependent manner. This explanation differs from the second in that differences in binding modes need not be invoked.

To address the first possibility we compare the binding constants, of the various polynucleotides to $[\text{Ru}(\text{phen})_3]\text{Cl}_2$, obtained by equilibrium dialysis.¹⁹ These values are charted below.

<u>DNA</u>	<u>$K(M^{-1})$</u>
poly(dG-dC)·poly(dG-dC)	4000
calf thymus DNA	6200
poly(dA-dT)·poly(dA-dT)	9200

The binding constants correlate with the degrees of emission enhancement observed. However it is not clear that the variations in binding affinity totally account for the variations in emission enhancement.

The second proposal, that there are different modes of binding for poly(dG-dC)·poly(dG-dC) and poly(dA-dT)·poly(dA-dT), is supported by the fact that the enantioselectivity of Δ over Λ observed for calf thymus DNA and poly(dG-dC)·poly(dG-dC) is reversed for poly(dA-dT)·poly(dA-dT) (Figure 8).

The third possibility for the variations in enhancement is that they arise from the nature of the polynucleotide itself. For example, different sequences have different water structures around them and such differences could affect intensity of emission. Moreover, particular base specific electronic interactions have been observed to quench other luminescent intercalators.⁴² For example, in the cases of proflavine⁴³ and acriflavine⁴⁴, enhancement, or

no effect is seen on dye emission when bound to poly(dA-dT)·poly(dA-dT) , but binding to poly(dG-dC)·poly(dG-dC) causes quenching. Authors explained this observation by a charge transfer interaction between the guanine and the dye, since metallation⁴⁵ or methylation⁴⁶ of the guanine inhibits this quenching in certain cases. A similar phenomenon might be occurring in the case of [Ru(phen)₃]Cl₂.

In order to determine if either different modes of binding or various degrees of emission enhancement by the different polynucleotides are causing the variations in the emission intensities observed in the titration experiments it would be useful to know the emission intensity at the end point of the titration. However, as mentioned above values for the end points were not obtainable from these titrations because at the DNA concentrations necessary to bind all the ruthenium, the viscosity and scattering effects render the emission intensity values unreliable. In lieu of the titration end point values we can compare the emission lifetimes (determined by C.V. Kumar in our laboratory) of the bound forms of racemic [Ru(phen)₃]Cl₂ in the presence of the three types of polynucleotides. The values of the observed lifetimes (from reference 19) are listed below.

<u>DNA</u>	<u>excited state lifetime of bound form (μsec)</u>
poly(dA-dT) · poly(dA-dT)	1076
poly(dG-dC) · poly(dG-dC)	708
calf thymus DNA	1600 (avg. value)

Based on these values and on those for the binding constants listed above, the relatively lower emission enhancements observed in the titrations with poly(dG-dC) · poly(dG-dC) result from both a lower binding constant with [Ru(phen)₃]Cl₂ and a lower increase in emission intensity of the bound form as compared to the other polynucleotides. The relatively larger increase in emission intensity of the ruthenium complex that we observe in the titrations with poly(dA-

dT) · poly(dA-dT) however must result only from an increase in the binding constant. This fact is clear because the lifetime of the excited state of [Ru(phen)₃]Cl₂ bound to poly(dA-dT) · poly(dA-dT) is actually lower than that of the ruthenium complex bound to calf thymus DNA. A combination of the three reasons mentioned should therefore be invoked to explain the sequence dependence of the emission enhancement observed in the titration experiment.

Sequence dependence of enantioselectivity.

In addition to the sequence dependence of the emission enhancement, Figures 7 and 8 also illustrates a sequence dependence of enantioselectivity. The selective enhancement of the Δ enantiomer over the Λ enantiomer follows the order poly(dG-dC)·poly(dG-dC) > calf thymus DNA > poly(dA-dT)·poly(dA-dT). In the titration of [Ru(phen)₃]Cl₂ with poly(dG-dC)·poly(dG-dC) only the emission of the Δ enantiomer is enhanced. In binding to calf thymus DNA, a slight enhancement of the emission of the Δ enantiomer over that of the Λ enantiomer is seen and in binding to poly(dA-dT)·poly(dA-dT), a greater enhancement is observed for the emission of the Λ enantiomer is preferred. The preference of poly(dG-dC)·poly(dG-dC) for the Δ enantiomer can be explained by the intercalation model described above for calf thymus DNA. To explain why poly(dA-dT)·poly(dA-dT) prefers the Λ enantiomer we describe another mode of binding. A mode of binding other than intercalation has also been defined based on experiments done by C.V. Kumar and J. Goldberg in our laboratory. This binding mode is enantioselective. Based on emission quenching experiments, it renders the [Ru(phen)₃]Cl₂ less accessible to solvent yet does not always cause emission enhancement. It displays lower values for luminescence depolarization. This binding mode has been assigned as a surface bound or groove bound mode.¹⁹ That is, the ligands have surface interactions with the groove of the helix. From model building studies it

seems that this mode of binding should be preferred by the Λ enantiomer (see Figure 11). We propose that groove binding is preferred in the case of poly(dA-dT)·poly(dA-dT).

These proposals are interesting in light of observations described in the literature which indicate that intercalators tend to bind at G·C containing sequences while groove binders prefer A·T containing sequences. Intercalation involves the insertion of planar aromatic ligands between the base pairs of DNA.¹⁰ Classical examples of intercalators are ethidium bromide⁷ and acridines.⁸ The interaction between a polar nucleotide and a polarizable ligand appear to be important for intercalation. Almost all intercalators studied so far display a preference for G·C. The G·C preference has been rationalized for intercalators in the acriflavine family by Muller and Crothers.^{47,48} It has been found that GC base pairs are more polar than AT base pairs⁴⁹ and would therefore be expected to be more preferred in the stacking interaction. It may then be true that an intercalation process is inherently a GC preferred type of interaction. DNA groove binding ligands have also been described in the literature. Most groove binders involve some hydrogen bonding to functional groups in the groove, but hydrogen bonding is not essential, as groove binders have been studied which have no hydrogen bonding capabilities.⁴⁹ Netropsin is an example of a groove binder whose structure has been solved.⁵⁰ The crystal structure of the groove binder netropsin has led to interesting proposals concerning what sorts of interactions favor groove binding. It has been suggested that the aromatic rings of groove binders oriented to match the walls of the helix,⁵¹ provide favorable surface interactions. This notion has further been used to explain the A·T preference that has been noted for groove binders.⁵⁰ Whereas aromatic rings can lie flat on the surface of the minor groove on A·T base pairs, the protruding amino group in the minor groove of G·C base pairs precludes such an interaction for this sequence. The

enantioselectivities we observe with $\text{Ru}(\text{phen})_3^{2+}$ may be a reflection of the sequence preferences of these two binding modes.

Another point to note from Figures 7 and 8 is that enhancement of $\text{poly}(\text{dG-dC})\cdot\text{poly}(\text{dG-dC})$ is the most enantioselective of the DNAs examined. Only the emission of the Δ enantiomer is enhanced. Emission of the Λ enantiomer is constant with $\text{poly}(\text{dG-dC})\cdot\text{poly}(\text{dG-dC})$ concentration. One explanation for the higher degree of enantioselectivity observed for $\text{poly}(\text{dG-dC})\cdot\text{poly}(\text{dG-dC})$ as compared to the other polynucleotides is a higher degree of rigidity for the G-C base pairs. Each G-C base pair contains three hydrogen bonds as opposed to two hydrogen bonds for A-T base pairs. Moreover, stacking energies for G-C base pairs have been calculated to be larger than those for A-T base pairs.⁵² In accord with the notion of decreased flexibility contributing to a higher degree of enantiomeric selectivity for the binding reaction with $\text{poly}(\text{dG-dC})\cdot\text{poly}(\text{dG-dC})$, we note that selectivity for the Δ enantiomer is also enhanced in the binding reaction with calf thymus DNA as a function of increasing salt concentration.¹⁹ Increasing salt concentration is expected to render the helix more stable and less flexible. Calf thymus DNA, most likely, consists of some sites more similar in nature to $\text{poly}(\text{dG-dC})\cdot\text{poly}(\text{dG-dC})$ and some sites more similar to $\text{poly}(\text{dA-dT})\cdot\text{poly}(\text{dA-dT})$ rendering the pattern of emission enhancement intermediate between that of the two synthetic polynucleotides.

The luminescence titration data for $\text{poly}(\text{dG-dC})\cdot\text{poly}(\text{dG-dC})$ is mostly consistent with the data from the equilibrium dialysis experiments. By both of these methods $\text{poly}(\text{dG-dC})\cdot\text{poly}(\text{dG-dC})$ was found to be the most enantioselective polynucleotide and to have the largest preference for the Δ enantiomer at this salt concentration. However, the enantioselectivity is seen more strikingly in the luminescence titrations. In the equilibrium dialysis experiments, a 3-4:1 preference of the Δ : Λ enantiomer was observed. In the

luminescence titrations no enhancement was observed for the Λ enantiomer. As mentioned in a previous section, there are apparently some modes of binding that do not contribute to the luminescence enhancement. The binding of the Λ enantiomer to poly(dG-dC)·poly(dG-dC) is clearly one example. This observation suggests that for poly(dG-dC)·poly(dG-dC) the Λ and Δ enantiomers are quite different in their modes of binding and perhaps the Λ enantiomer is completely precluded from intercalation.

In summary, emission titrations are a simple method by which to monitor enantioselectivity in binding to DNA. The data from these titrations together with data from binding experiments and emission lifetime determinations can be explained by a model which involves the preferential intercalation of the Δ enantiomer into calf thymus DNA and poly(dG-dC)·poly(dG-dC) and preferential groove binding of the Λ enantiomer with poly(dA-dT)·poly(dA-dT). (These preferences of course refer to net binding. Both enantiomers of $\text{Ru}(\text{phen})_3^{2+}$ bind to all the polynucleotides examined and more than one mode of binding may occur for each case.)

Emission enhancement of $[\text{Ru}(\text{dip})_3]\text{Cl}_2$ with DNA. Figures 9 and 10 illustrate the enhancement of $[\text{Ru}(\text{dip})_3]\text{Cl}_2$ as a function of DNA concentration. No large difference is observed between the enhancement of the two enantiomers. This observation is in contrast to the results obtained by absorbance titrations⁵³ done by L. Basile and luminescence quenching experiments¹⁹ done by C.V. Kumar in our laboratory. These experiments demonstrated exclusive binding of the Δ enantiomer to B DNA. It appears that because of the hydrophobicity of this complex, a non-specific type of binding is dominating the emission enhancement effect. A sudden, sharp increase in $[\text{Ru}(\text{dip})_3]\text{Cl}_2$ enhancement as compared to $[\text{Ru}(\text{phen})_3]\text{Cl}_2$ enhancement is also seen in studies in which these complexes were bound to

micelles.³⁸ This is probably also a reflection of the extreme hydrophobicity of this complex.

The methods which can better discriminate between different binding modes are clearly necessary to detect the differences in binding of these two enantiomers.

References

1. Neidle, S., Pearl, L.H., Skelly, J.V. (1987) Biochem. J. **243** 1-13.
2. Le Pecq, J.-B. (1974) In Biochemical Fluorescence: Concepts #2 ed. Chen, R.F., Edelhoch, H., chapter 18. Marcel Dekker Inc.
3. Le Pecq, J.-B., Paoletti, C. (1967) J. Mol. Biol. **27** 87-106.
4. Ichimura, I., Zama, M., Fujita, H. (1971) Biochim. Biophys. Acta **240** 485-95.
5. Caspersson, T., Zech, L.M., Johanssen, C., Modest, E.J. (1970) Chromosoma **30** 215-27.
6. Caspersson, T., Zech, L.M., Modest, E.J., Foley, G.E., Wagh, U., Simonason, E. (1969) Exp. Cell Res. **58** 128-40.
7. Toulme, J.J., Krisch, H.M., Loreau, N., Thuong, N.T., Helene, C. (1986) Proc. Nat. Acad. Sci. **83** 1227-31.
8. a) Tsai, C.C., Jain, S.C., Sobell, H.M. (1977) J. Mol. Biol. **114** 301-15. b) Jain, S.C., Tsai, C.C., Sobell, H.M. (1977) J. Mol. Biol. **114** 317-31.
9. a) Berman, H.M., Stallings, W., Carrell, H.L., Glusker, J.P. (1979) Biopolymers **18** 2405-29. b) Jain, S.C., Sobell, H.M. (1972) J. Mol. Biol. **68** 1-20.
10. Lerman, L.S. (1961) J. Mol. Biol. **3** 18-30.
11. a) Reinhardt, C.G., Krugh, T.R. (1978) Biochem. **17** 4845-54. b) Kastrup, R.V., Young, M.A., Krugh, T.R. (1978) Biochem. **17** 4855-65. c) Ryan, D.P., Crothers, D.M. (1984) Biopol. **23** 537-62.
12. Muller, W., Crothers, D.M. (1968) J. Mol. Biol. **35** 251-90.
13. a) Fredericq, E., Houssier, C. (1972) Biopol. **11** 2281-308. b) Li, H.J., Crothers, D.M. (1969) J. Mol. Biol. **39** 461-77.
14. Zimmerman, H.W. (1986) Angew. Chem. **25** 115-30.
15. Kopka, M.L., Yoon, C., Goodsell, D., Pjura, P., Dickerson, R.E. (1985) Proc. Nat. Acad. Sci. **82** 1376-80.
16. a) Luck, G., Triebel, H., Waring, M., Zimmer, C. (1974) Nucl. Acid. Res. **1** 503-30.

- b) Wartell, R. M., Larson, J.E., Wells, R.D. (1974) J. Biol. Chem. 249 6719-31.
17. Waring, M. (1970) J. Mol. Biol. 54 247-79.
18. a) Patel, D.J., Canuel, L.L. (1979) Proc. Nat. Acad. Sci. 76 24-28. b) Waring, M.J., Henley, S.M. (1975) Nucl. Acid Res. 2 567-86.
19. a) Kumar, C.V., Barton, J.K., Turro, N.J. (1985) J. Am. Chem. Soc. 107 5518-23.
b) Barton, J.K., Goldberg, J.M., Kumar, C.V., Turro, N.J. (1986) J. Am. Chem. Soc. 108 2081-88.
20. Smith, D., Martinez, A.M., Ratliff, R.C. (1970) Anal. Biochem. 38 85-89.
21. Felsenfeld, G., Hirschman, S.Z. (1965) J. Mol. Biol. 13 407-27.
22. Inman, R.B., Balwin, R.C. (1962) J. Mol. Biol. 5 172-84.
23. Wells, R.D., Larson, J.E., Grant, R.C.c Shortle, B.E., Cantor, C.R. (1970) J. Mol. Biol. 54 465-97.
24. Lin, C.T., Bottcher, W., Chou, M., Creutz, C., Sutin, N.J. (197?) J. Am. Chem. Soc. 98 6536 - 544 .
25. Watts, R.J., Crosby, G.A. (197) J. Am. Chem. Soc. 93 3184-88.
26. Gillard, R.D., Hill, R.E. (1974) J. Chem. Soc. Dalt Trans. 1217-36.
27. Mason, S.F., Peart, B.J. (1973) J. Chem. Soc. Dalton Trans. 949-55.
28. Barton, J.K., Nowick, J. (1984) J. Chem. Soc. Chem. Comm. 1650.
29. McCaffrey, A.J., Mason, S.F., Norman, B.J. (1969) J. Chem. Soc. A 1428.
30. Zalkin, A., Templeton, D.H., Tatzuo, U. (1973) Inorg. Chem. 12 1641-6.
31. Van Houten, J., Watts, R.J. (1975) J. Am. Chem. Soc. 97 3843-4 and references within.
32. Barton, J.K., Danishefsky, A., Goldberg, J. (1984) J. Am. Chem. Soc. 106 2172-65.
33. a) Lyttle, F.E., Hercules, D.M. (1969) J. Am. Chem. Soc. 91 253-7. b) Klassen, D.M., Crosby, G.A. (1968) J. Chem. Phys. 48 1853-8.
34. Demas, J.N., Taylor, D.G. (1979) Inorg. Chem. 18 3177-9.
35. Caspar, J.V., Meyer, T.J. (1983) J. Am. Chem. Soc. 105 5583-90.
36. Meyer, T.J. (1986) Pure Appl. Chem. 58 1193-1206.
37. Hauenstein, B.L., Dressick, W.J., Buell, S.L., Demas, J.N., DeGraff, B.A. (1983) J. Am. Chem. Soc. 105 4251-55.
38. Mandal, K., Hauenstein, B.L., Demas, J.N. (1983) J. Phys. Chem. 87 328-331.

39. Yamagishi, A. (1983) J. Chem. Soc. Chem. Comm. 572-3.
40. Hard, T., Norden, B. (1986) Biopolymers 25 1209-28.
41. Bugg, C.E., Thomas, J.M., Sundralingam, M., Rao, S.T. (1971) Biopolymers 10 175-249.
42. Schreiber, J.P., Daune, M.P. (1974) J. Mol. Biol. 83 487-501.
43. Thomes, J.C., Weill, G., Daune, M. (1969) Biopolymers 8 647-59.
44. Tubbs, R.K., Ditmars, W.E.J., Van Winkle, Q. (1964) J. Mol. Biol. 9 545-57.
45. Prusik, T., Kolubayev, T., Morelli, M.J., Brenner, H.C. (1979) J. Photochem. 10 315-21.
46. Ramstein, J., Leng, M. (1972) Biochim. Biophys. Acta 281 18-32.
47. Muller, W., Crothers, D.M. (1975) Eur. J. Biochem. 54 267-77.
48. Muller, W., Buneman, H., Dattagupta, N., (1975) Eur. J. Biochem. 54 279-291.
49. Braithwaite, A.W., Baguley, B.C. (1980) Biochemistry 19 1101-6.
50. Kopka, M.L., Yoon, C., Goodsell, D., Pjura, P., Dickerson, R.E. (1985) Proc. Nat. Acad. Sci. 82 1376-80.
51. Dervan, P. (1986) Science 232 464-71.
52. a) Ornstein, R.L., Rein, R., Breen, D.L., McElroy, R.D. (1978) Biopolymers 17 2341-360. b) Yoth, O., Tagashira, Y. (1981) Biopolymers 20 1033-42.
53. Barton, J.K., Basile, L.A., Danishefsky, A.T., Alexandrescu, A. (1984) Proc. Nat. Acad. Sci. 81 1961-65.

Chapter 3

Characterization of the Binding of Ru(phen)₂Cl₂ to DNA

Introduction

In chapter 2 we discussed the interactions of the chiral metal complex, Ru(phen)₃²⁺ with DNA. This work with Ru(phen)₃²⁺ as well as studies with the larger complex Ru(dip)₃²⁺ illustrate the advantage of using chiral complexes as probes. The chemistry of any two enantiomers is obviously the same except for their interactions with another chiral molecule such as DNA. The differences in binding between the two enantiomers can reflect the structure of the DNA.

Many transition metals bind to DNA at more or less specific sites.² For example, many of the soft transition metals that have been studied coordinate to N-7 of guanosine as a preferred site on DNA. This is the case for example in the extensively studied antitumor drug, cis-diamminedichloroplatinum(II).³ It is also the case for certain ruthenium(II) and ruthenium(III) ammine complexes.⁴

It has been noticed in recent years by several groups that a DNA sequence with a GpG step is often involved in binding to certain types of DNA regulatory proteins. Examples are SpI⁵, large T antigen⁶ and TFIIIA⁷. It has been proposed that short stretches of guanines within regulatory regions may adopt an A conformation. This proposal has been supported by the solution of the structure of the sequence GGATGGGAG⁸, part of the DNA binding site of the TFIIIA protein. With the ultimate goal of developing a molecule to probe or modify sites containing such GpG steps it is interesting to study such sequences in terms of their binding to small inorganic molecules.

As a first effort to try to design a molecule with a preference for guanine nucleotides while

maintaining the chirality of the complex, we studied the interaction of $\text{Ru}(\text{phen})_2\text{Cl}_2$ with DNA. The chloride ions are labile in aqueous solution and the metal is therefore able to coordinate to the DNA. Coordination of the metal is expected to lend a sequence sensitivity to the binding. Moreover, the interactions of the phenanthroline ligands with the DNA impart an enantioselectivity to the reaction which should reflect the structure of the adduct.

Coordination also lends a greater stability to this interaction than to those of the tris(phenanthroline) metal complexes with DNA.

In this chapter we describe some of the characteristics of the binding of $\text{Ru}(\text{phen})_2\text{Cl}_2$ to DNA. We first discuss the DNA sequence preferences and enantiomeric preferences of the binding. A preference for G·C containing sequences is observed. In contrast to the non-covalent binding of $\text{Ru}(\text{phen})_3^{2+}$ with DNA, a preference for binding of the Λ enantiomer is observed in most cases. Since covalent binders can affect the conformation of the DNA, the effect of binding of $\text{Ru}(\text{phen})_2\text{Cl}_2$ on DNA conformation was also investigated. Based on these observations and on spectroscopic data we propose a possible model for binding of $\text{Ru}(\text{phen})_2\text{Cl}_2$ to DNA.

Experimental Procedures

Preparation of DNA

Calf thymus DNA was purchased from Sigma Chemicals and purified by phenol extraction.⁹ Synthetic polynucleotides were purchased from P.L. Biochemicals. All DNAs were dialyzed extensively against buffer R (5 mM Tris-HCl, 50 mM NaCl, pH7.5) prior to the binding experiments. The extinction coefficients used to determine the nucleotide

concentrations were as follows: calf thymus DNA, $6600 \text{ M}^{-1} \text{ cm}^{-1}$ at 260 nm^{10} ; poly(dG)·poly(dC), $7400 \text{ M}^{-1} \text{ cm}^{-1}$ at 253 nm^{11} ; poly(dG-dC)·poly(dG-dC), $8400 \text{ M}^{-1} \text{ cm}^{-1}$ at 255 nm^{11} ; poly(dA)·poly(dT), 6000 at 260 nm^{11} ; poly(dA-dT)·poly(dA-dT), 6600 at 262 nm^{12} . SV40 plasmid DNA was purchased from Bethesda Research Laboratories.

Z-DNA was prepared by dialyzing a 1 mM stock solution of poly(dG-dC)·poly(dG-dC) against pH 7.5 buffer containing 5 mM tris-HCl, 10 mM NaCl. The stock solution was then diluted into the same buffer already containing 30 uM $\text{Co}(\text{NH}_3)_6^{3+}$. Final concentrations of the DNA used in these experiments was $100\text{-}150 \text{ uM}$. Higher concentrations of poly(dG-dC)·poly(dG-dC) tended to aggregate under these conditions.

Synthesis of Ru(II) complexes

RuCl_3 was received as a gift from Engelhardt Inc. The ligand, 1,10-phenanthroline was purchased from Aldrich Chemicals. Derivatized phenanthroline ligands were purchased from G. Frederick Smith Chemical Company. The synthesis of $\text{Ru}(\text{phen})_2\text{Cl}_2$ was similar to the one described by Sullivan et. al.¹³ for $\text{Ru}(\text{bpy})_2\text{Cl}_2$. The complex was prepared by the addition of stoichiometric phenanthroline to RuCl_3 already dissolved in DMF and refluxing for 2 to 3 hrs. To purify the complex, DMF was pumped off, the remaining solid was dissolved, by heating, in an ethanol/ H_2O solution and the purified product was precipitated overnight or longer from a 50:50 ethanol H_2O solution containing excess LiCl. Direct light was avoided during the synthesis and the subsequent purification steps were carried out in dim light or in foil wrapped glassware. A typical elemental analysis was as follows, found: C: 50.47%, N:10.6%, H: 3.41%; calculated: C:50.7%, N:9.9%, H:3.54%. An ϵ of $10,800 \pm 500 \text{ M}^{-1} \text{ cm}^{-1}$ ¹⁴ at 490 nm in ethanol was used to determine concentrations of the metal complex. The NMR spectrum of this compound shown in Figure 1 is consistent with its structure. The synthesis of $\text{Ru}(5,6\text{-dimethylphenanthroline})_2\text{Cl}_2$ and $\text{Ru}(5\text{-phenylphenanthroline})_2$ was

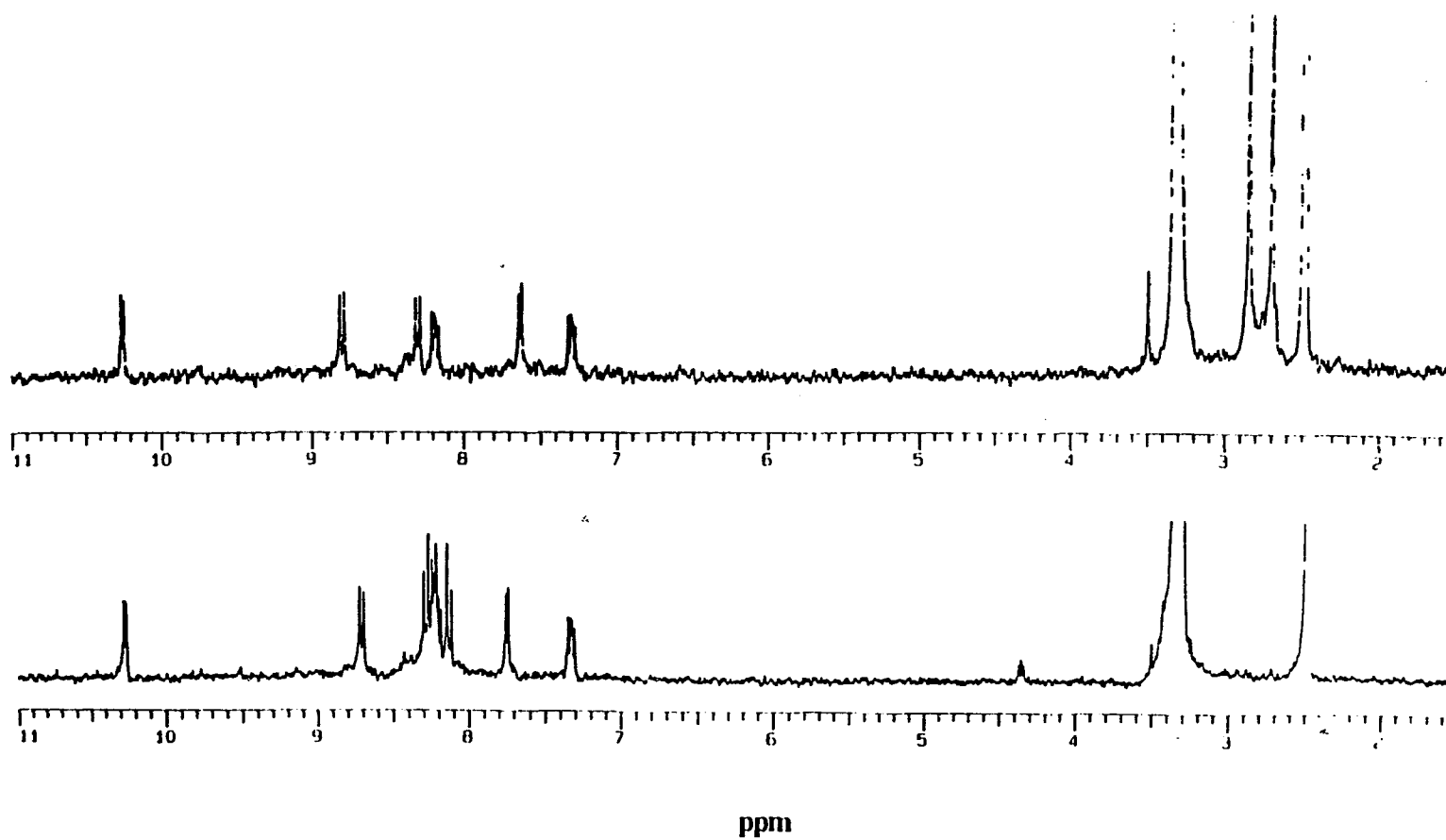


Figure 1. 300 MHz proton NMR spectra of Ru(5,6-dimethylphen)₂Cl₂ (top) and Ru(phen)₂Cl₂ (bottom) in d⁶DMSO. reference: DMSO at 2.49 ppm.

carried out analogously to that of $\text{Ru}(\text{phen})_2\text{Cl}_2$. The extinction coefficients determined for the two compounds in ethanol were $10,800 \pm 500 \text{ M}^{-1} \text{ cm}^{-1}$ at 500 nm and $11,500 \pm 500 \text{ M}^{-1} \text{ cm}^{-1}$ at 505 nm respectively.

$\text{Ru}(\text{phen})_2(\text{NH}_3)_2^{2+}$, $\text{Ru}(\text{phen})_2(\text{en})^{2+}$, $\text{Ru}(\text{phen})_2(\text{py})_2^{2+}$ and $\text{Ru}(\text{phen})_2\text{pyCl}^{2+}$ were synthesized as described by Bryant et. al.¹⁵ for the analogous bpy compounds starting from $\text{Ru}(\text{phen})_2\text{Cl}_2$. NMR spectra of these compounds are shown in Figure 2. The identities of the first two compounds were further corroborated by mass spectrometry analyses (molecular ion weights were 521 and 496 for $\text{Ru}(\text{phen})_2(\text{en})^{2+}$ and $\text{Ru}(\text{phen})_2(\text{NH}_3)_2^{2+}$ respectively) and elemental analyses (C:N ratios found were 3.7 and 3.4 for $\text{Ru}(\text{phen})_2(\text{en})$ and $\text{Ru}(\text{phen})_2(\text{NH}_3)_2$ respectively).

Attempts were also made to synthesize a $\text{Ru}(\text{phen})_2^{2+}$ complex with one or two guanosines coordinated to the metal. This was done by refluxing a 2:1 ratio of guanosine to $\text{Ru}(\text{phen})_2\text{Cl}_2$ in methanol/ H_2O for several hours. The reaction mixture was loaded on to a Sephadex CM-25 carboxymethylcellulose column and eluted with a NaNO_3 gradient which ranged from .05M to 2M in concentration. An NMR spectrum of the major band eluted from this column is shown in Figure 2a. The mass spec of this mixture contained peaks corresponding to $\text{Ru}(\text{phen})_2(\text{deoxyguanosine})$ (728) and $\text{Ru}(\text{phen})_2(\text{deoxyguanosine})\text{Cl}$ (764).

Agarose gel electrophoresis

Agarose gels of SV40 DNA bound to $\text{Ru}(\text{phen})_2\text{Cl}_2$ were run in 1% agarose type V purchased from Sigma Chemicals. The running buffer contained 50 mM Tris-HCl, 18mM NaCl, 18mM Na acetate, pH 7.0. Gels were run on a BRL Model H-6 "baby gel" at 40-50volts for 2-3 hours. DNA bands were visualized by staining with ethidium bromide solution.

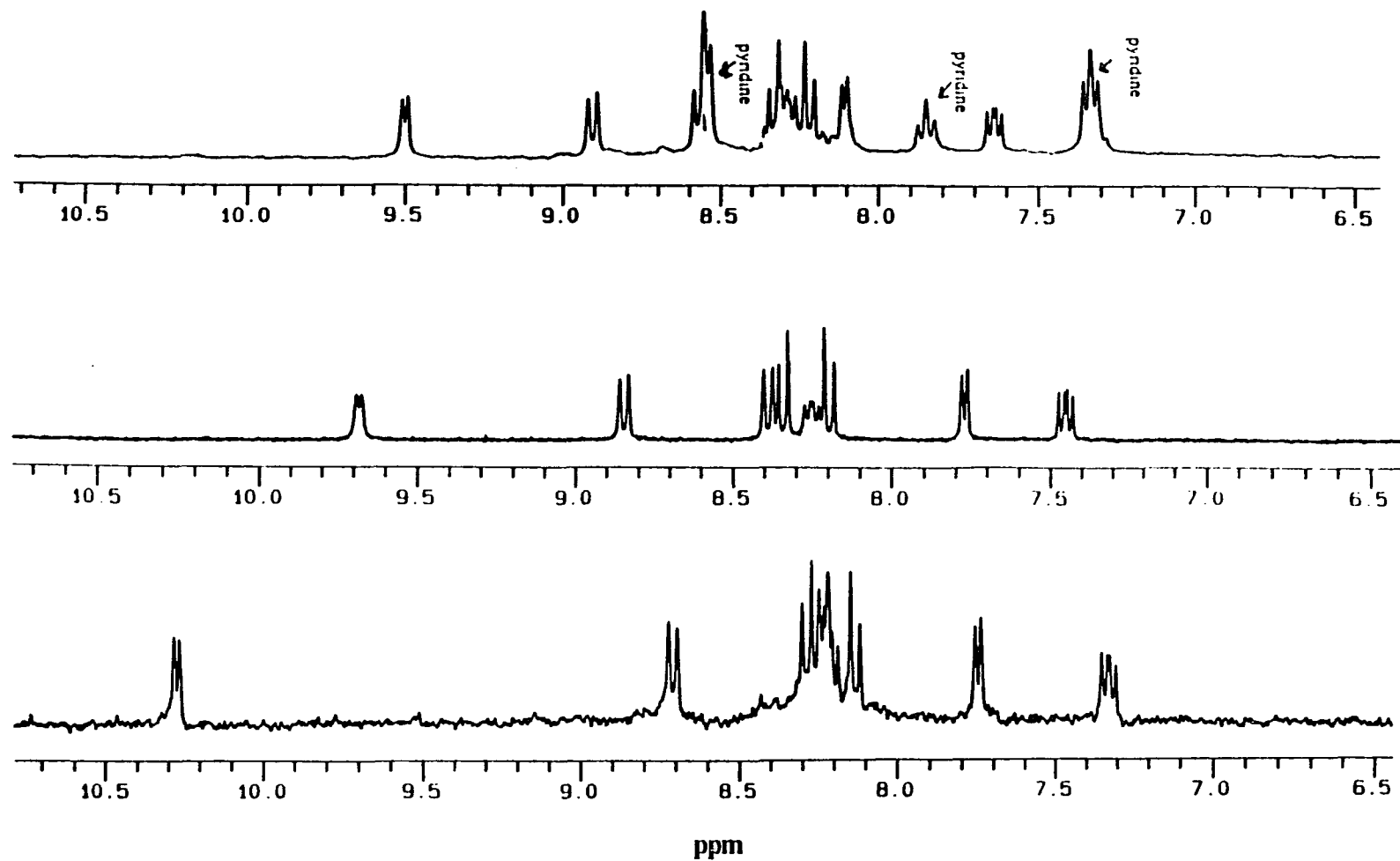


Figure 2. 300 MHz proton NMR spectra of $\text{Ru(phen)}_2(\text{py})_2^{2+}$ (top), $\text{Ru(phen)}_2(\text{NH}_3)_2^{2+}$ (middle), and $\text{Ru(phen)}_2\text{Cl}_2$ in $d^6\text{DMSO}$. reference: DMSO at 2.49 ppm.

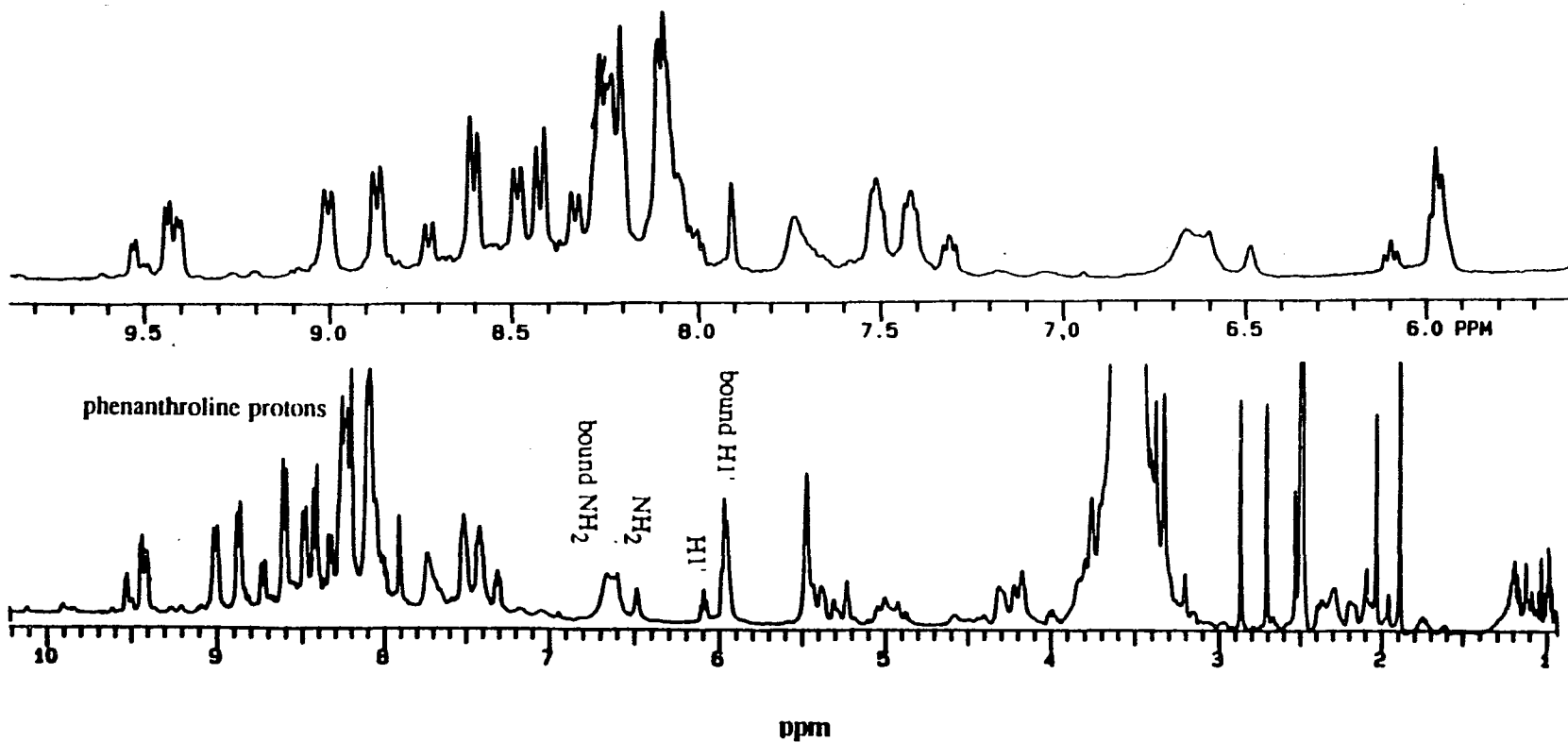


Figure 2a. Proton NMR spectrum of the major products of the reaction of $\text{Ru}(\text{phen})_2\text{Cl}_2$ with 2' deoxyguanosine

Spectroscopic instrumentation

Absorbance spectra were recorded on a Cary 219 spectrophotometer. C.D. spectra were recorded on either a Jasco J-40 recording spectropolarimeter or Jasco J-500A spectropolarimeter in line with a Jasco DP-500N data processor. Resonance Raman spectra were obtained by excitation of the sample at 441.6 nm with a Liconix He/Cd laser (40mW). The collection and analysis of data was identical to that described by Kumar et. al. ¹⁶

DNA sequencing experiments

The DNA fragment used in the sequencing experiments was obtained by digesting SV40 DNA with the restriction enzymes Bgl I (which cuts at the 5242 site) and Asp 718 (which cuts at the 299 site). Both enzymes were purchased from Boehringer Mannheim Biochemicals. The labelling of the 5' end of the DNA and the gel electrophoresis procedures were carried out as described in reference 17. The labelling reaction was performed subsequent to the Bgl I reaction and prior to the Asp 718 reaction. The fragment was purified on a 5% polyacrylamide gel (acrylamide: bis acrylamide 29:1) with bromphenol blue as a marker. The piece of the gel containing the fragment was identified by exposure to x-ray film, cut out of the gel, sliced into tiny pieces and left overnight at 4° C covered with buffer containing 500 mM Na acetate and 1 mM EDTA, pH 8. The solution was separated from the gel pieces through glass wool, loaded onto a NAP-10 purification column (P.L. Biochemicals) , eluted with H₂O and immediately frozen at -70° C and lyophilized. The fragment was stored lyophilized at -70° C and resuspended in buffer R immediately prior to the binding experiments.

Binding reactions were carried out by incubating Ru(phen)₂Cl₂ with the DNA fragment initially containing 30 cpm per sample. Calf thymus DNA at 1mM concentration was used as carrier. After the incubation period, the DNA was precipitated and resuspended in buffer

appropriate for the exonuclease reaction. ExonucleaseIII reactions were performed exactly as described by Bowler and Lippard.¹⁸

DNA sequencing was done according to the procedure of Maxam and Gilbert.¹⁹

Determination of the direction and magnitude of the rotation of Ru(phen)₂Cl₂

In order to prepare enantiomeric Ru(phen)₂Cl₂ a racemic mixture of this complex was incubated with DNA in buffer R at a 5 to 1 nucleotide to ruthenium ratio for 90 minutes, after which the DNA and the bound ruthenium complex was precipitated with ethanol. A 5-6 fold excess of phenanthroline was added to the free Ru(phen)₂Cl₂ in the supernatant and the solution was heated at 80° C +10 C for 3 hours. At that point optically active Ru(phen)₃²⁺ had been formed and hardly any Ru(phen)₂Cl₂ remained. The heated solutions were kept scrupulously in the dark. Control samples contained Ru(phen)₂Cl₂ refluxed without added phenanthroline and Ru(phen)₂Cl₂ kept at ambient temperature in the dark for 3 hours. The concentration of the samples at the end of the 3 hours was determined based on their visible absorbance spectra. C.D. spectra of the solutions were taken in order to determine the sign and magnitudes of the optical rotations at 270nm.

Calculation of enantiomeric selectivity from binding data

Solutions of Ru(phen)₂Cl₂ incubated with DNA for varying lengths of time were ethanol precipitated to remove DNA and bound ruthenium complex. C.D. spectra were taken of the free Ru(phen)₂Cl₂ in the supernatant. Enantiomeric selectivity of the reaction was calculated using the equation:

$$\% \text{selectivity} = \text{rotation observed} / (\text{concentration bound} \times \text{rotation of pure enantiomer}).$$

The concentration bound was determined by visible absorbance spectra.

Results

Binding of $\text{Ru}(\text{phen})_2\text{Cl}_2^*$ to calf thymus DNA

The binding of $\text{Ru}(\text{phen})_2\text{Cl}_2$ to DNA over time was monitored by incubating DNA with $\text{Ru}(\text{phen})_2\text{Cl}_2$ and ethanol precipitating the DNA and the bound $\text{Ru}(\text{phen})_2\text{Cl}_2$ after various time intervals. The concentration of free $\text{Ru}(\text{phen})_2\text{Cl}_2$ in the supernatant was measured by the visible absorbance band of the complex. ($\text{Ru}(\text{phen})_3^{2+}$ which cannot coordinate to the DNA shows no binding to DNA by this assay.) The time course of the binding reaction to calf thymus DNA is shown in Figure 3. When a solution with a 5:1 nucleotide to ruthenium ratio is incubated at room temperature, the reaction nears completion at an r_{bound} value of about .05 after approximately 3 hours. The final r_{bound} value was found to vary with the ruthenium concentration and the ruthenium to DNA ratio used in the experiment. Both higher ruthenium concentrations and higher ruthenium to nucleotide ratios result in higher r_{bound} values.

Further details concerning the nature of the reactants

The experiments described in this section address the following questions: 1. In the buffer system used (5mM tris 50mM NaCl pH 7.5) what is the identity of the two non-phenanthroline ligands? These ligands are labile and could be chloro groups, hydroxyl groups

* $\text{Ru}(\text{phen})_2\text{Cl}_2$ refers to the solid form of the complex. Once dissolved in aqueous solution aquo ligands partially or totally replace the chloride ligands.

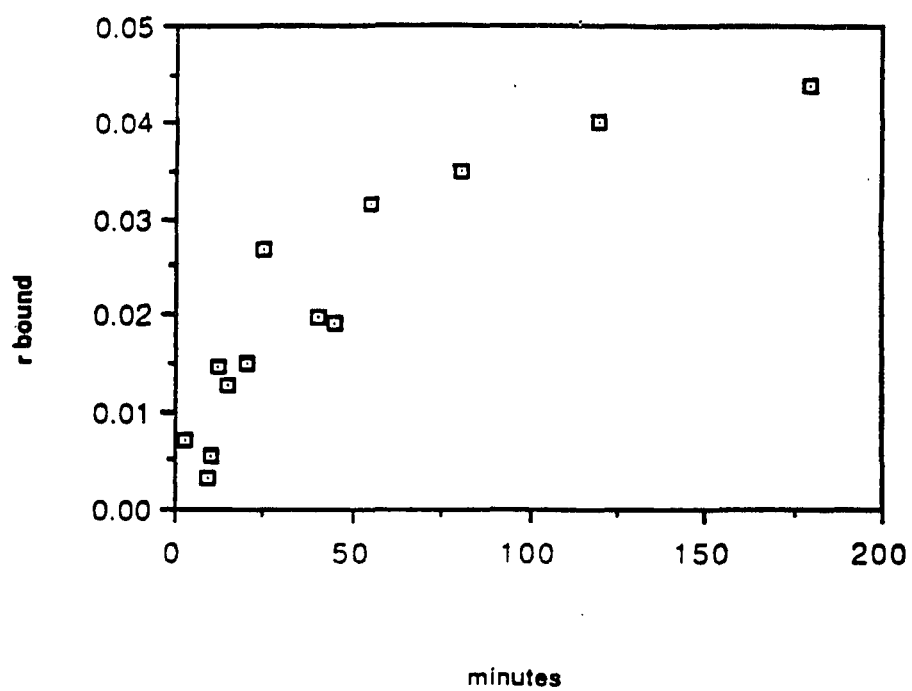


Figure 3. Time course of Ru(phen)₂Cl₂ binding to calf thymus DNA in buffer R. Concentrations bound at each point were measured by ethanol precipitation of the DNA with the bound Ru complex and measuring the absorbance of the free Ru(phen)₂Cl₂ left in solution.

or water molecules. 2. Does the nature of this leaving group ligand affect the enantioselectivity of the reaction?

It has been observed that when $\text{Ru}(\text{phen})_2\text{Cl}_2$ is dissolved by heating in aqueous solution one or two of the chloride ligands dissociate.²⁰ To determine if one of the non-phenanthroline ligands is a chloride ion in our buffer system NMR spectra were taken of $\text{Ru}(\text{phen})_2\text{Cl}_2$ in D_2O with increasing chloride concentrations. These spectra are shown in Figure 4. In D_2O the complex retains C_2 symmetry as seen by the eight peaks that appear in the spectrum. As the chloride concentration is increased some of the peaks begin to split. This splitting is most easily interpreted as chloride ions coordinating to the ruthenium in place of the D_2O to form $[\text{Ru}(\text{phen})_2\text{D}_2\text{OCl}]^+$ or $[\text{Ru}(\text{phen})_2\text{Cl}_2]$. At a concentration of 50 mM NaCl the downfield peaks are split with only about one half of the area corresponding to the peaks originally present in the D_2O spectrum. The non-phenanthroline ligands in our buffer system are then a mixture of chloride and solvent ligands. The pK for the analogous $\text{Ru}(\text{bpy})_2(\text{H}_2\text{O})_2^{2+}$ complex was determined to be approximately 9.²¹ Hydroxyl groups are therefore not expected to be the leaving groups on most of the complexes. The presence of aquo or chloro ligands on the ruthenium complex is also reflected in its visible absorbance spectra, as shown in Figure 20. No differences in enantioselectivities were observed between binding experiments performed in chloride containing buffer as compared to those in which the binding reaction took place in nitrate containing buffer.

Enantioselectivity of $\text{Ru}(\text{phen})_2\text{Cl}_2$ binding to calf thymus DNA

In order to determine the enantioselectivity of the binding reaction to DNA, the optical rotation of the $\text{Ru}(\text{phen})_2\text{Cl}_2$ left free in solution was measured for various time points during the reaction. In Figure 5 the optical rotation at 270 nm of the free $\text{Ru}(\text{phen})_2\text{Cl}_2$ is plotted versus the r value. This data illustrates that until an r value of approximately .04 is reached,

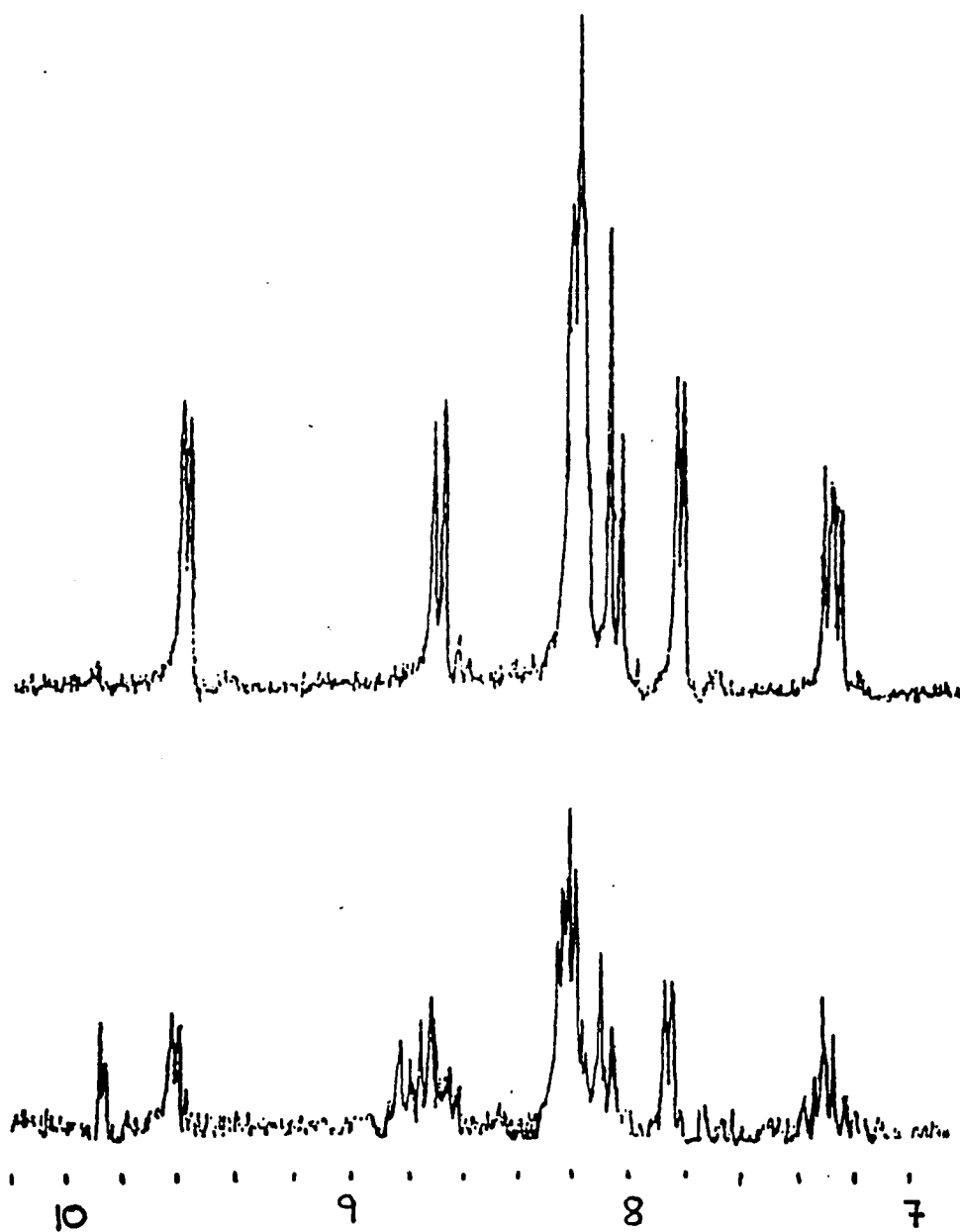


Figure 4. NMR spectra of Ru(phen)₂Cl₂ in D₂O with no excess NaCl (top) and 30' after addition of 50 mM NaCl (bottom).

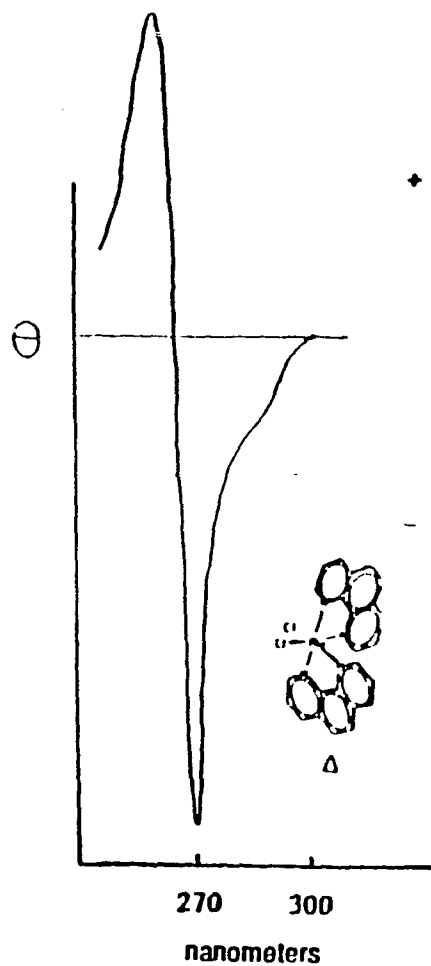


Figure 5a. C.D. spectrum of $\text{Ru}(\text{phen})_2\text{Cl}_2$ left free in solution after ethanol precipitation of the DNA with the bound ruthenium complex. The spectrum is of the Δ enantiomer indicating a preference in binding of the Δ enantiomer to calf thymus DNA.

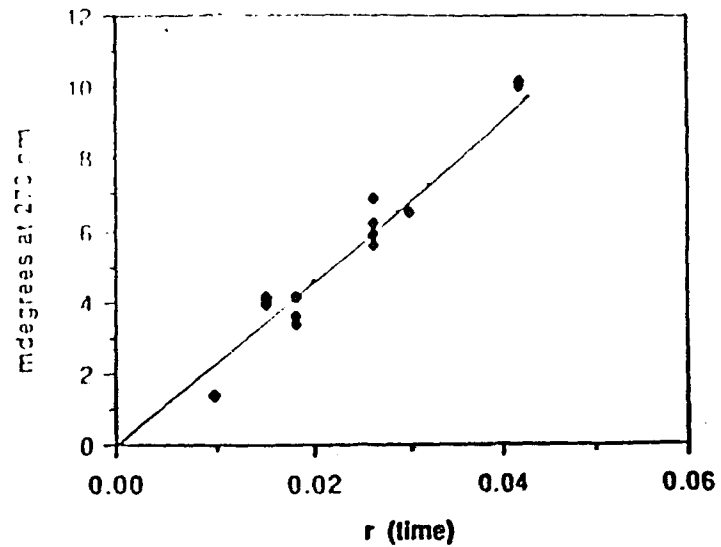


Figure 5b. Enrichment of the free $\text{Ru}(\text{phen})_2\text{Cl}_2$ solution in the Δ enantiomer as a function of r_{bound} .

the enantioselectivity is constant . From the slope of the line we calculate that there is approximately a 2.6 to 1 preference for binding of the Λ enantiomer over the Δ enantiomer to calf thymus DNA.** This value was calculated using $\Delta\epsilon_{270} = +280 \text{ M}^{-1} \text{ cm}^{-1}$ for Λ $\text{Ru}(\text{phen})_2\text{Cl}_2$ which was determined as described in the following section.

Equilibrium dialysis experiments of $\text{Ru}(\text{phen})_2\text{Cl}_2$ with calf thymus DNA

$\text{Ru}(\text{phen})_2\text{Cl}_2$ also interacts non-covalently with DNA . A certain enantiomeric preference in a non-covalent binding mode could conceivably set up a higher local concentration of the preferred enantiomer near the DNA thereby causing this enantiomer to be favored for coordination. In order to determine if this was the case in our experiments, equilibrium dialysis experiments of $\text{Ru}(\text{phen})_2\text{Cl}_2$ versus calf thymus DNA were performed. The enantioselectivity of the non-covalent mode of binding was determined by dialysing $\text{Ru}(\text{phen})_2\text{Cl}_2$ versus calf thymus DNA and measuring the optical activity of the dialysate. The dialysate was enriched in the Λ enantiomer indicating a preference for the Δ enantiomer similar to that observed for $\text{Ru}(\text{phen})_3^{2+}$. The enantioselectivity observed in such an experiment reflects both covalent and non-covalent modes of binding. A preference in binding the Δ enantiomer is observed. This finding indicates that the selectivity for the Λ enantiomer observed for the covalent binding mode does not simply result from a higher local concentration of this enantiomer near the DNA .

** Specifically, the enantioselectivity of the binding reaction with calf thymus DNA was calculated as follows: As shown in the graph in figure 4, at an r value of .02 the ellipticity in mdegrees of the solution of the unbound ruthenium complex at 270 nm was approximately 4.5. Since the ratio of ruthenium to DNA incubated was 50:250 uM, when the r_{bound} value equals .02, 5uM of the ruthenium complex is bound to the DNA. The samples were ethanol precipitated and this increased the volume of the samples 4x, so that the concentration of the sample of which the C.D. was measured was 1.25uM. (Pathlengths were equal to 1 cm.)

$$4.5\text{mdegree}/1.25\text{uM}=4.05\times 10^6 \text{ mdeg/uM}$$

The ellipticity of pure enantiomeric $\text{Ru}(\text{phen})_2\text{Cl}_2$ is estimated to be $.9\times 10^7$ mdegrees for a uM solution.

$$4.05\times 10^6/.9\times 10^7 = 42\% = 72\% \Lambda / 28\% \Delta = 2.57$$

Determination of the sign and magnitude of the optical rotation of $\text{Ru}(\text{phen})_2\text{Cl}_2$

In order to determine the enantioselectivities of the binding reaction discussed above it is, of course, necessary to know the sign and magnitude of the optical rotation of enantiomeric $\text{Ru}(\text{phen})_2\text{Cl}_2$. Since these values are known for $\text{Ru}(\text{phen})_3^{2+}$ ²² they could be determined for $\text{Ru}(\text{phen})_2\text{Cl}_2$ by synthesizing $\text{Ru}(\text{phen})_3^{2+}$ from enantiomerically enriched $\text{Ru}(\text{phen})_2\text{Cl}_2$. The synthesis was carried out by heating the $\text{Ru}(\text{phen})_2\text{Cl}_2$ solution in the presence of 5-fold excess phenanthroline. Complete absence of light is required to prevent racemization of the heated solution.

Table 1 lists the results of one such experiment. The sign of the rotation is the same for $\text{Ru}(\text{phen})_2\text{Cl}_2$ as for $\text{Ru}(\text{phen})_3^{2+}$. (It is known that this reaction occurs by a dissociative mechanism not involving inversion.) The magnitude of the rotation of $\text{Ru}(\text{phen})_2\text{Cl}_2$ at 270 nm is 2.2x less than that of $\text{Ru}(\text{phen})_3^{2+}$. Since $\Delta\epsilon_{270}$ has previously been determined to be approximately $600 \text{ M}^{-1}\text{cm}^{-1}$, for $\text{Ru}(\text{phen})_3^{2+}$, the $\Delta\epsilon$ of $\text{Ru}(\text{phen})_2\text{Cl}_2$ is calculated to be $280 \text{ M}^{-1} \text{ cm}^{-1}$ (+ 20%). This value is consistent with that calculated by Bosnich.²³

Sensitivity of binding and enantioselectivity to the DNA sequence

The DNA sequence sensitivity of the $\text{Ru}(\text{phen})_2\text{Cl}_2$ binding reaction was investigated using synthetic polynucleotides. Figure 6 illustrates the time course of the binding reaction of $\text{Ru}(\text{phen})_2\text{Cl}_2$ to DNA of varying sequences. More binding is observed to G·C containing sequences than to A·T containing sequences. The greatest amount of binding observed is to the homopolymer poly(dG)·poly(dC). The enantiomeric discrimination for the binding reactions with each of these sequences was determined in the same manner as that described above for calf thymus DNA. These preferences are compared in Table 2. Of the polynucleotides examined, the one with enantioselectivity closest to that of calf thymus DNA

Table1. Comparison of the optical rotations of Ru(phen)₃²⁺ and Ru(phen)₂Cl₂ at 270 nm.

	<u>sample concentration(μM)</u>	<u>rotation(mdegrees at 270nm)</u>	<u>rotation(mdegrees)/concentration(μM)</u>
1	11 ⁺¹	8.25	.76 ^{+.09}
2	13.75 ^{+.25}	10.75	.78 ^{+.01}
3	10 ⁺¹	17.5	1.8 ^{+.01}

sample 1, Ru(phen)₂Cl₂ heated at 80 C in ethanol/ H₂O for 3h; sample 2, Ru(phen)₂Cl₂ kept at ambient temperature in ethanol/H₂O for 3h; sample 3, same as sample 1 with 5x excess phenanthroline

Degrees are related to molar ellipticity by the equation: $O = 2.303 (A_L - A_R)180/4\pi = 33\Delta A$

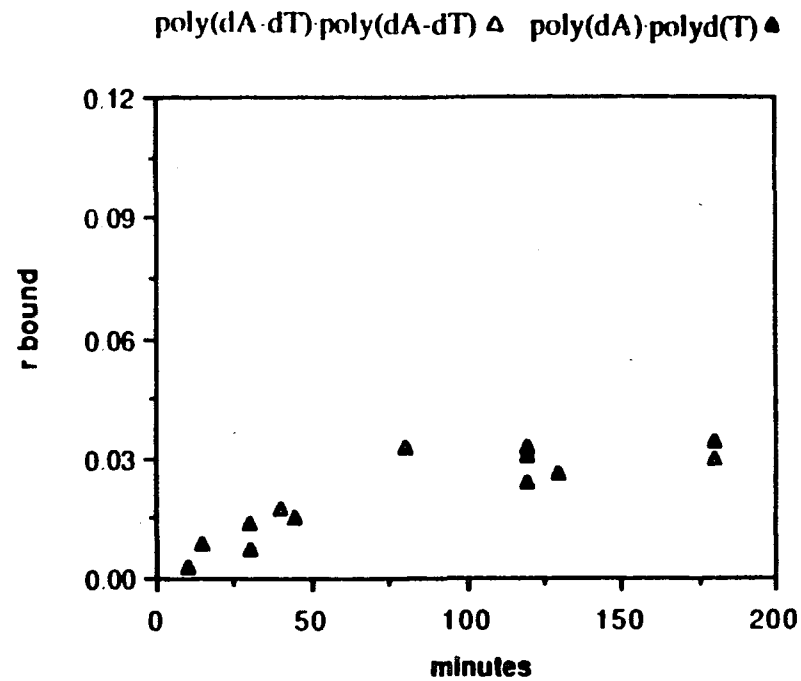
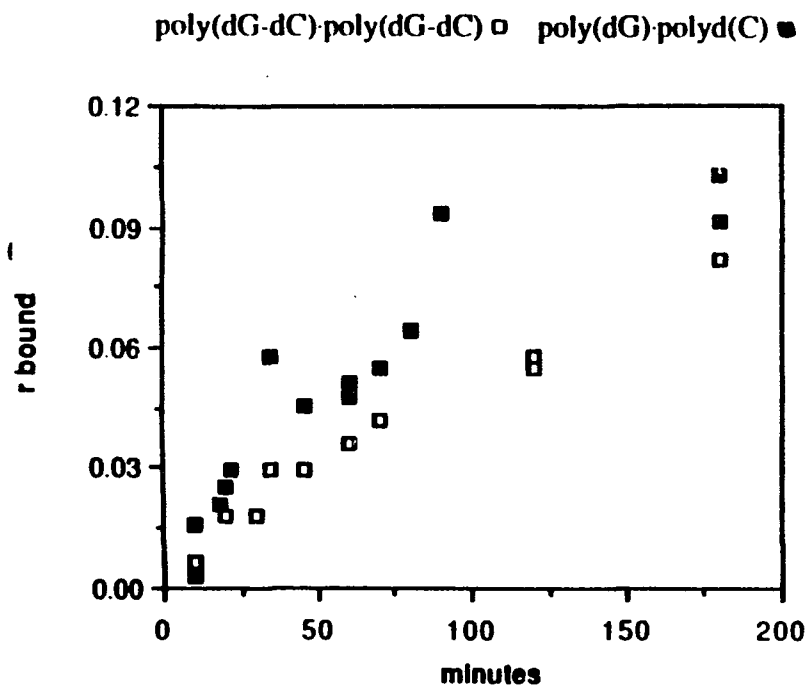


Figure 6. Sequence preferences of $\text{Ru}(\text{phen})_2\text{Cl}_2$ binding to DNA. left: poly(dG)-poly(dC) ■ poly(dG-dC)-poly(dG-dC) □ right: poly(dA)-poly(dT) ▲ poly(dA-dT)-poly(dA-dT) △ More binding is observed for the GC containing sequences. The greatest amount of binding occurs with the homopolymer poly(dG)-poly(dC).

Table 2. Enantiomeric preferences of the binding of Ru(phen)₂Cl₂ to DNA.

<u>DNA</u>	<u>r at 1 hr.</u>			<u>Δ/Δ bound</u>
	total	Λ	Δ	
Calf thymus DNA	.034	.0245	.0095	2.6
poly(dG)·poly(dC)	.049	.035	.014	2.4
poly(dG-dC)·poly(dG-dC)	.039	.016	.023	.7
poly(dA)·poly(dT)	.020	.011	.0091	1.4
poly(dA-dT)·poly(dA-dT)	.020	.011	.0091	1.4
poly(dG-dA)·poly(dC-dT)	Λ preference			

Enantioselectivities were calculated from plots similar to that shown in Figure 2, using a $\Delta\epsilon$ value of $280 \text{ M}^{-1} \text{ cm}^{-1}$ for enantiomeric Ru(phen)₂Cl₂.

is poly(dG)poly(dC), suggesting a similarity in the binding site for the two polymers. Less enantioselectivity is observed in the binding reactions with the A·T containing sequences.

Only the alternating sequence poly(dG-dC) poly(dG-dC) prefers the Δ enantiomer.

Effect of Ru(phen)₂Cl₂ binding on the conformation of the DNA

The effect that the coordination of Ru(phen)₂Cl₂ to the DNA, has on the conformation of the DNA was investigated by gel electrophoresis experiments. Figure 7 illustrates the results of an experiment in which pBR322 DNA, which had been incubated with Ru(phen)₂Cl₂ for varying time intervals was run on an agarose gel. It can be seen that as a function of incubation time, unwinding occurs for the supercoiled band and increased mobility occurs for the nicked band. These results also illustrate the slow dissociation rate of the metal complex from the DNA, as expected for a mode of binding involving the coordination of the metal to DNA. In contrast, for Ru(phen)₃²⁺ no effect on the mobility of DNA can be observed on an agarose gel unless the complex is dissolved within the gel. If the Ru(phen)₃²⁺ complex is simply incubated with the DNA prior to running the gel, it dissociates from the DNA once on the gel and travels to the opposite pole. (Some dissociation occurs in the case of Ru(phen)₂Cl₂ as well. This is known because the amount of unwinding was observed to be dependent on such factors as the length of the gel and the voltage at which it was run. This dissociation is slow enough however that the unwinding effect can still be observed.)

Consistent with the notion of a conformational change occurring to the DNA, we observe changes in the C.D. spectra both immediately and over the time course of binding to DNA. These spectra are shown in Figures 8, 9 and 10. Experiments performed to determine the effect of the ruthenium complex on the transition between the B and Z conformations in particular are discussed below.



Figure 7. Effect of bound $\text{Ru}(\text{phen})_2\text{Cl}_2$ on the mobility of pBR-322 DNA in agarose gel electrophoresis. From left to right, incubation times of the Ru complex with the DNA were: 0hr., .5hr., 1hr., 2hr., 6hr., 15hr. and 22hr.

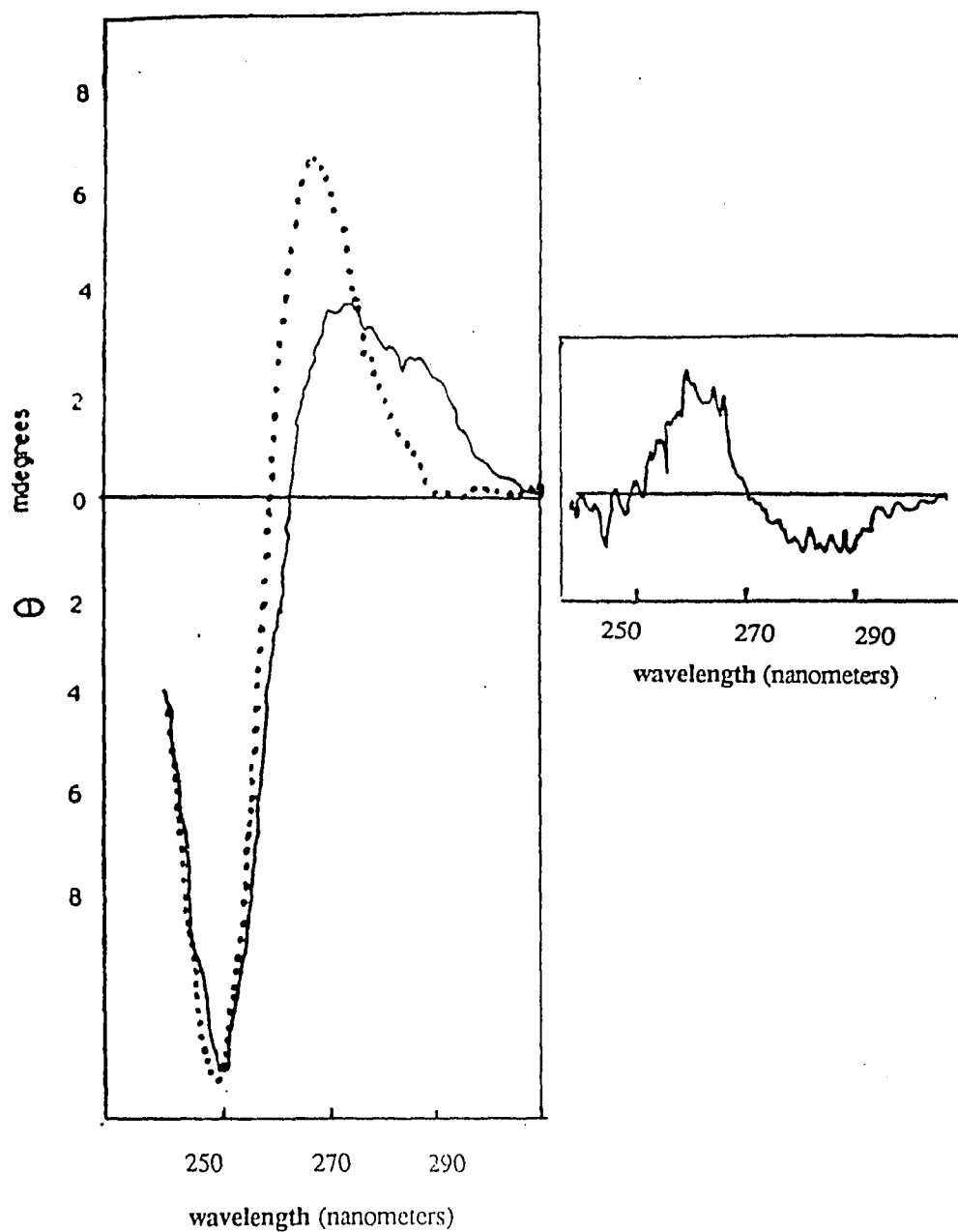


Figure 8. C.D. spectra of B-DNA illustrating the effect that the binding of the Ru complex has on the spectrum. Left: 100 uM poly(dG-dC)·poly(dG-dC) in the B-form (10mM NaCl, pH 7.5) — and the same DNA immediately after addition of 20uM Ru(phen)₂Cl₂ ····· Right: difference C.D. spectrum of the DNA before and after the addition of the ruthenium complex.

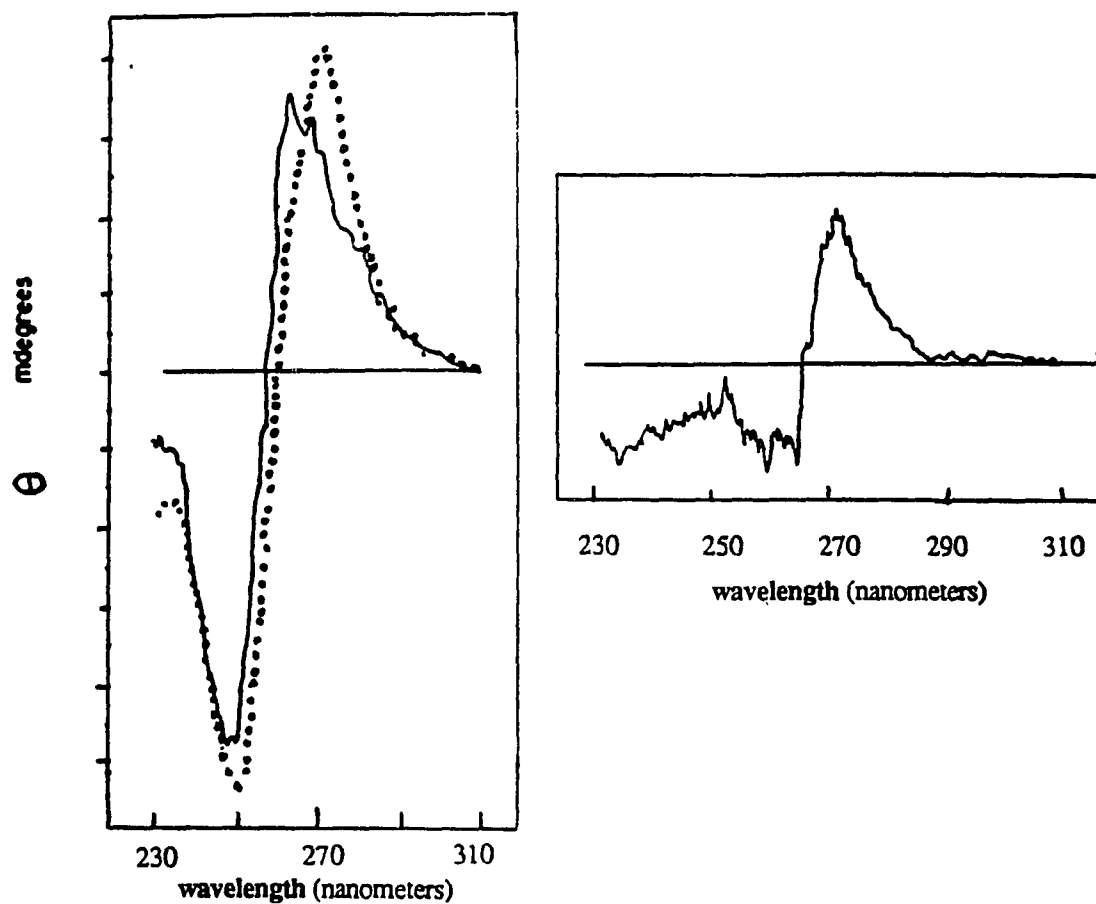


Figure 9. Effect over time of the binding of Ru(phen)₂Cl₂ on the C.D. spectrum of poly(dG-dC)·poly(dG-dC) in B-DNA conditions (10mM NaCl, pH7.5). Left: the polynucleotide immediately after the addition of Ru(phen)₂Cl₂ — and after 3 hours of incubation with the Ru complex - - - . Right: difference C.D. spectrum. Concentrations are the same as those in figure 8.

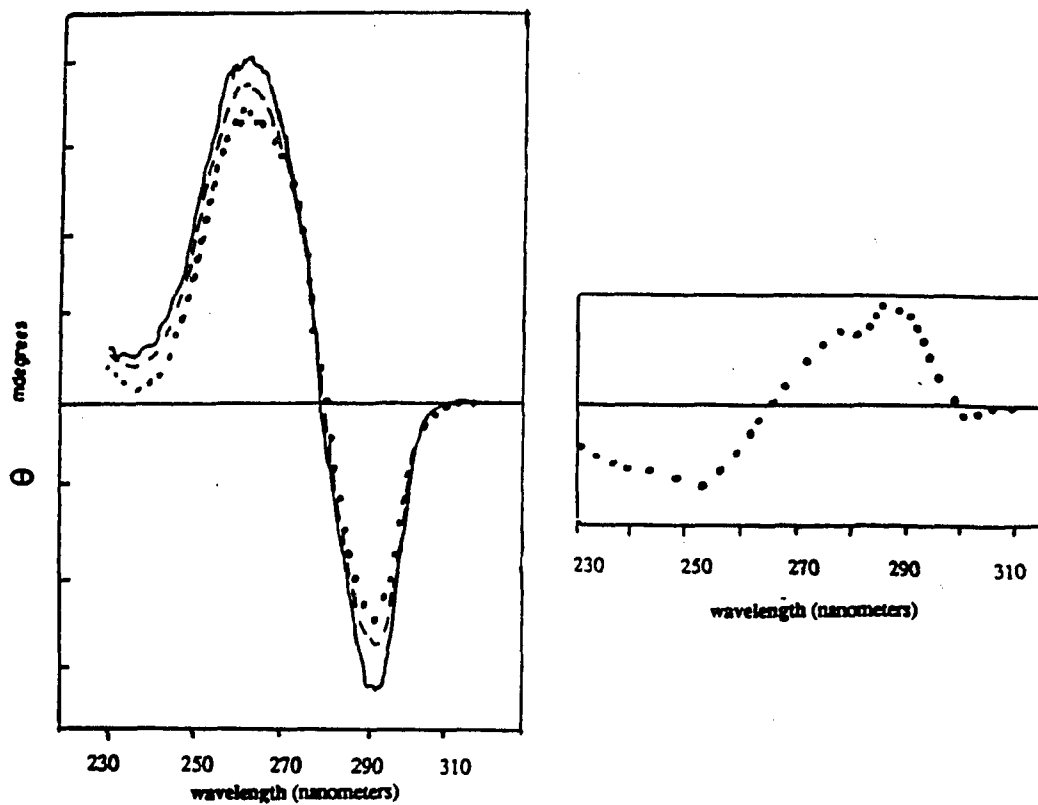


Figure 10. Effect over time of the binding of $\text{Ru}(\text{phen})_2\text{Cl}_2$ on the C.D. spectrum of Z-DNA. Left: 100 μM poly(dG-dC)-poly(dG-dC) converted to Z-DNA by the addition of 20 μM $\text{Co}(\text{NH}_3)_6^{3+}$ at various time points after the addition of 20 μM $\text{Ru}(\text{phen})_2\text{Cl}_2$: immediately after $\text{Ru}(\text{phen})_2\text{Cl}_2$ addition ———, 3 hrs after $\text{Ru}(\text{phen})_2\text{Cl}_2$ addition - - - and 18 hours after $\text{Ru}(\text{phen})_2\text{Cl}_2$ addition ·····. Right: the difference C.D. spectrum.

Resonance Raman Spectra of Ru(phen)₂L₂ Complexes

Attempts were made to identify the type of site on DNA to which Ru(phen)₂Cl₂ binds by comparing the resonance raman spectra for Ru(phen)₂Cl₂ bound to DNA with those of Ru(phen)₂py₂²⁺, Ru(phen)₂(NH₃)₂²⁺ and free Ru(phen)₂Cl₂. These compounds were chosen to represent binding of the metal to an endocyclic nitrogen or to an amine - both possible ligands on the DNA. The spectra of these compounds are shown in Figure 11. The largest peaks are seen at 1630, 1578, 1515, and 1450 cm⁻¹. Smaller peaks are seen at 1303, 1209, and 1146cm⁻¹. There are no significant shifts in these peaks among the various model compounds, though there may be some small changes in intensities. Not surprisingly, the peaks in the spectrum of [Ru(phen)₂Cl₂] bound to DNA are similar to the peaks observed for the model compounds. The attempts to use resonance Raman spectroscopy to elucidate the nature of the adduct were unsuccessful because of the apparent insensitivity of the spectrum to the non- chromophoric ligands.

Absorbance spectra of Ru(phen)₂Cl₂ bound to DNA and related complexes

The effect that DNA binding has on the visible absorbance spectrum of Ru(phen)₂Cl₂ is shown in Figures 12a and 12b. The immediate effect is a decrease in absorbance and a red shift, (12a) reminiscent of the effect seen with Ru(phen)₃²⁺. Over time, the band is blue shifted.(12b) For comparison, absorbance spectra of Ru(phen)₂L₂ (in which L₂ represents various known ligands) and absorbance spectra of Ru(phen)₂Cl₂ in various buffers are illustrated in Figures 13-15 . Addition of GMP or of guanosine to Ru(phen)₂Cl₂ also has the effect of blue shifting the spectrum over the course of several hours as shown in Figure 16. Unlike the effects of binding to DNA, no immediate red shift is observed in these cases. Attempts were also made to purify the major product of a reaction of Ru(phen)₂Cl₂ with

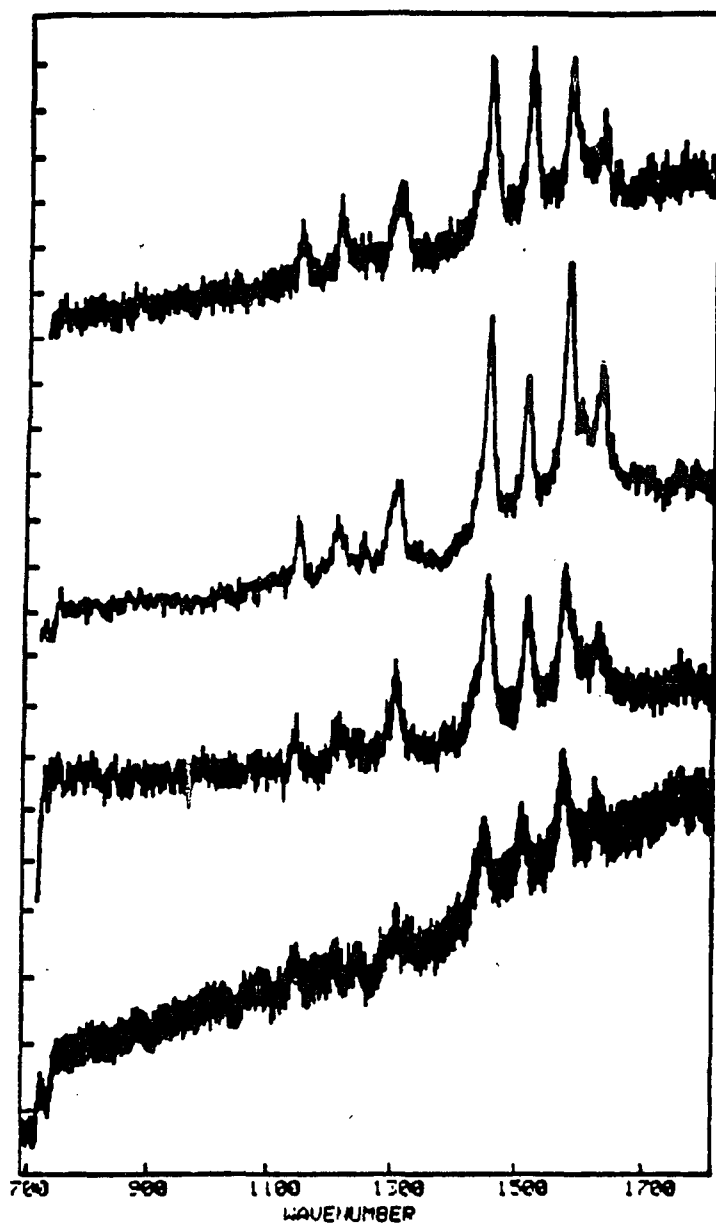


Figure 11. Resonance raman spectra (from top to bottom) of $\text{Ru}(\text{phen})_2\text{Cl}_2$, $\text{Ru}(\text{phen})_2(\text{py})_2^{2+}$, $\text{Ru}(\text{phen})_2(\text{NH}_3)_2^{2+}$ and $\text{Ru}(\text{phen})_2\text{Cl}_2$ bound to calf thymus DNA.

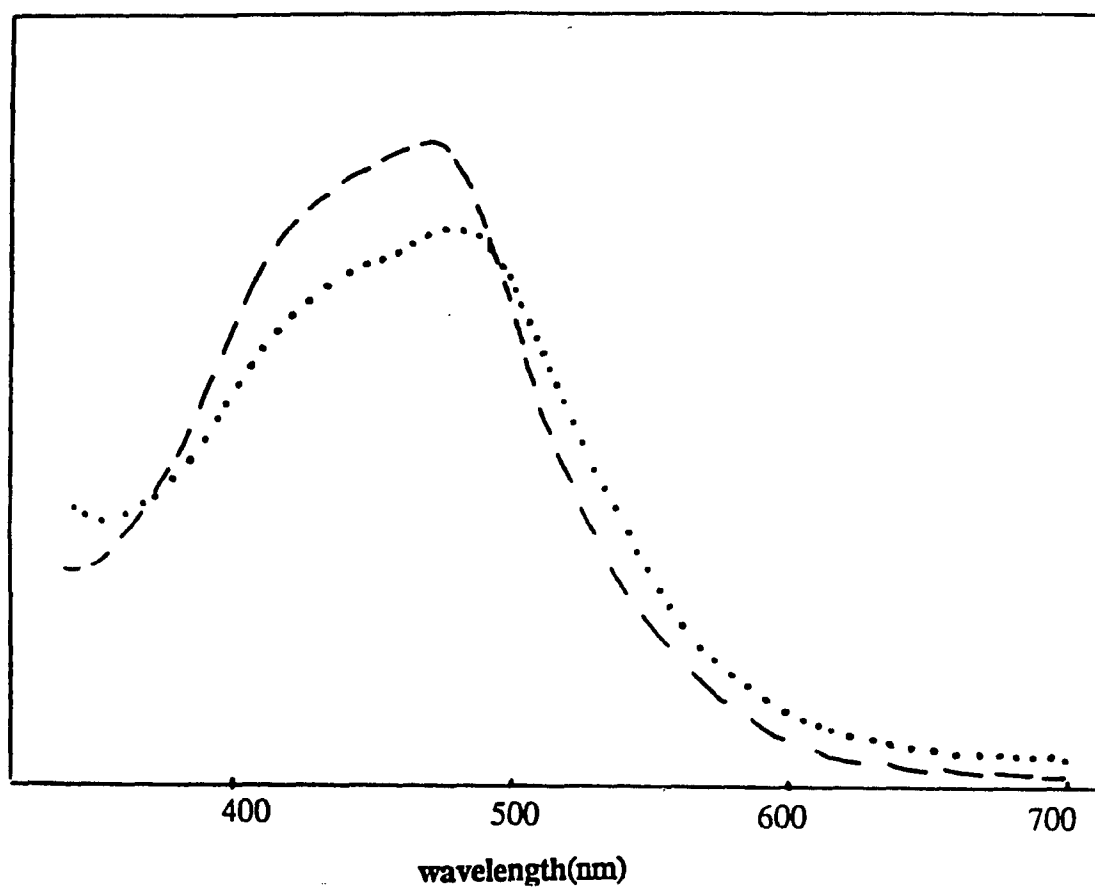


Figure 12a. Absorbance spectra of Ru(phen)₂Cl₂ in buffer R (---) and the same solution immediately after addition of calf thymus DNA (···). The nucleotide to ruthenium ratio was 20:1.

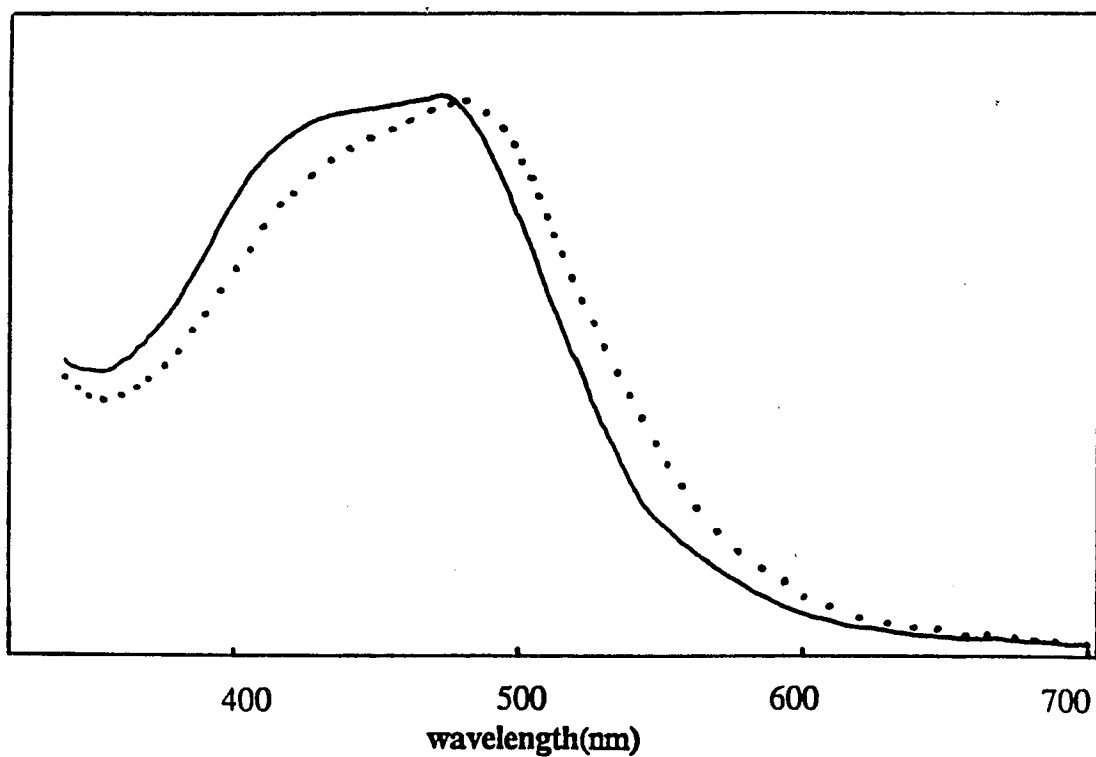


Figure 12b. Absorbance spectrum of Ru(phen)₂Cl₂ immediately after addition of calf thymus DNA at a 20:1 nucleotide to ruthenium ratio (···) and after 12 hours of incubation of the solution at room temperature (—). It is estimated that 50% of the ruthenium complex is coordinated to the DNA in the latter solution.

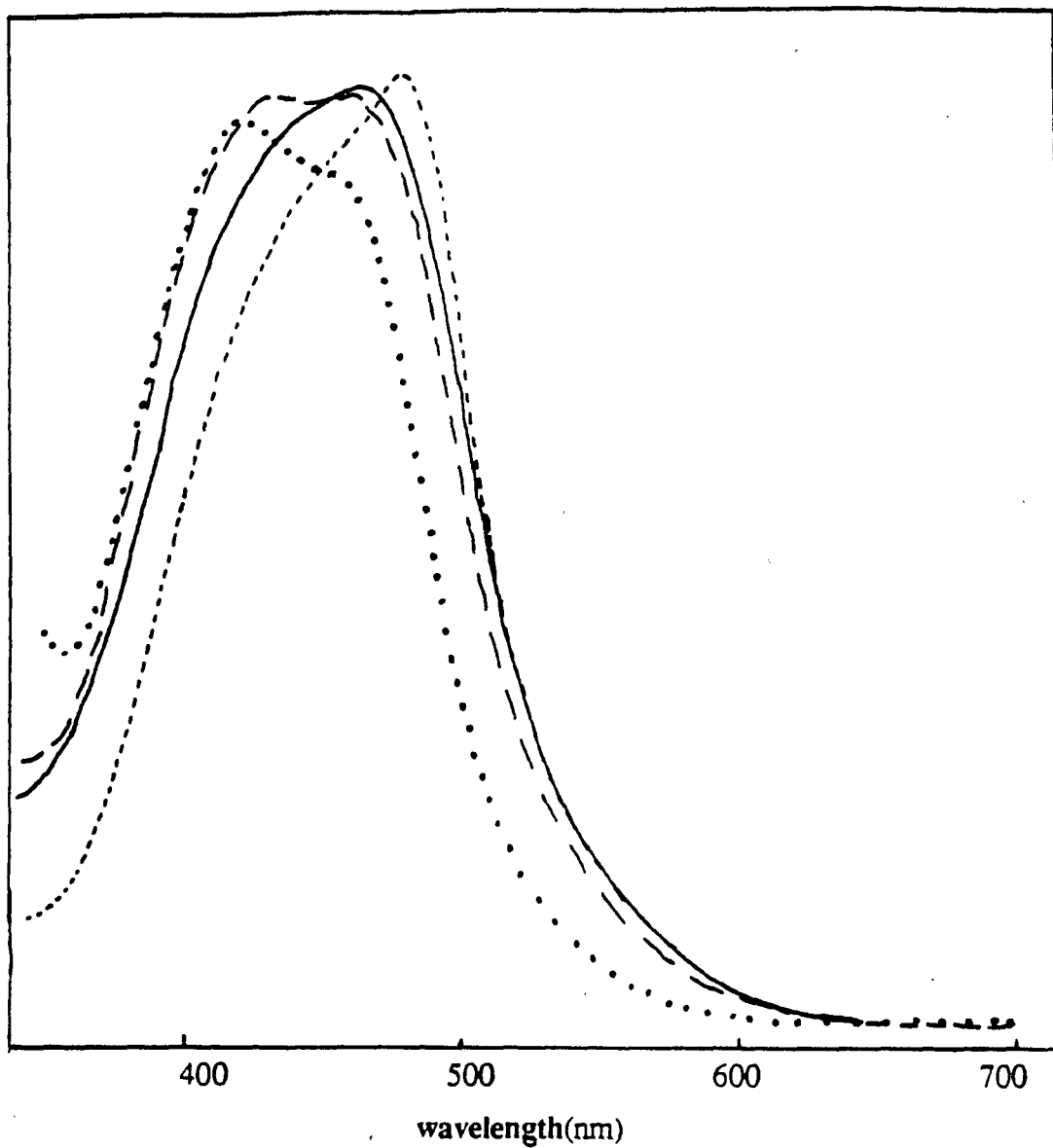


Figure 13. Absorbance spectra of complexes of the type $\text{Ru}(\text{phen})_2(\text{L})_2$ illustrating the blue shift as a function of the non-chromophoric ligands. $\text{Ru}(\text{phen})_2\text{Cl}_2$ dissolved in buffer R (—), $[\text{Ru}(\text{phen})_2\text{pyCl}]^+$ dissolved in buffer R (••), $\text{Ru}(\text{phen})_2(\text{NH}_3)_2^{2+}$ (----) and $\text{Ru}(\text{phen})_2(\text{guanosine})^{2+}$ (- -).

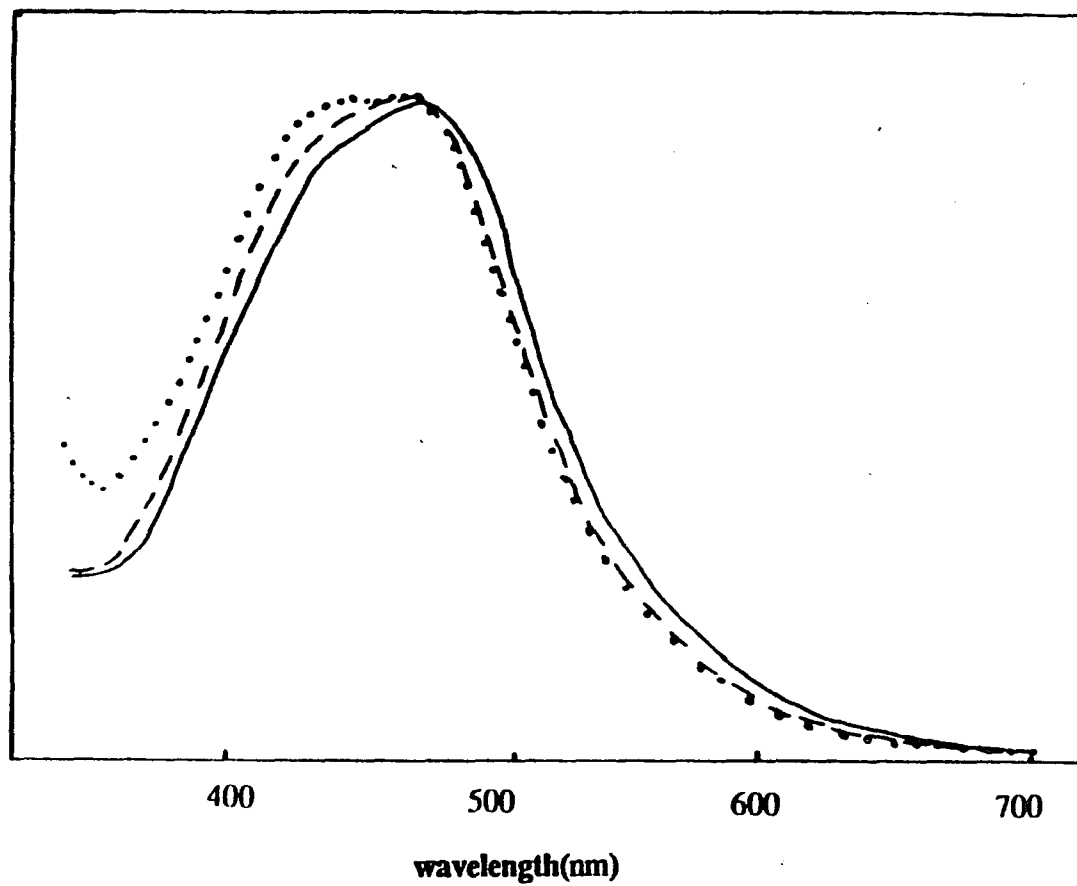


Figure 14. Effect of chloro vs. aquo ions on the absorbance spectrum of Ru(phen)₂Cl₂ dissolved in aqueous solution. Ru(phen)₂Cl₂ from an ethanol stock, immediately after dilution into aqueous solution (—), 2 hours after dilution into the aqueous solution (- -), and after treatment with AgNO₃ to remove all chloride ligands (· ·).

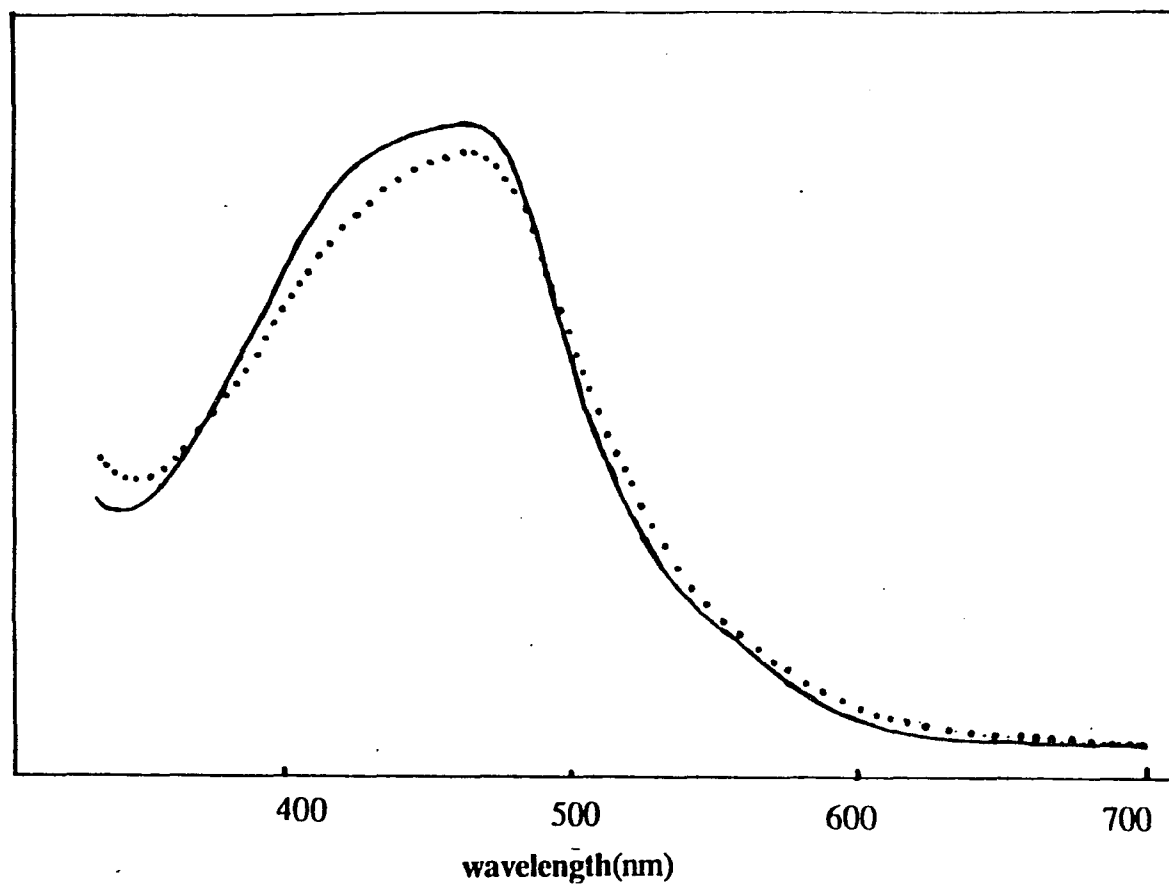


Figure15. Absorbance spectra of Ru(phen)₂Cl₂, in buffer R (—) and in phosphate buffer (···) after 12 hours at room temperature.

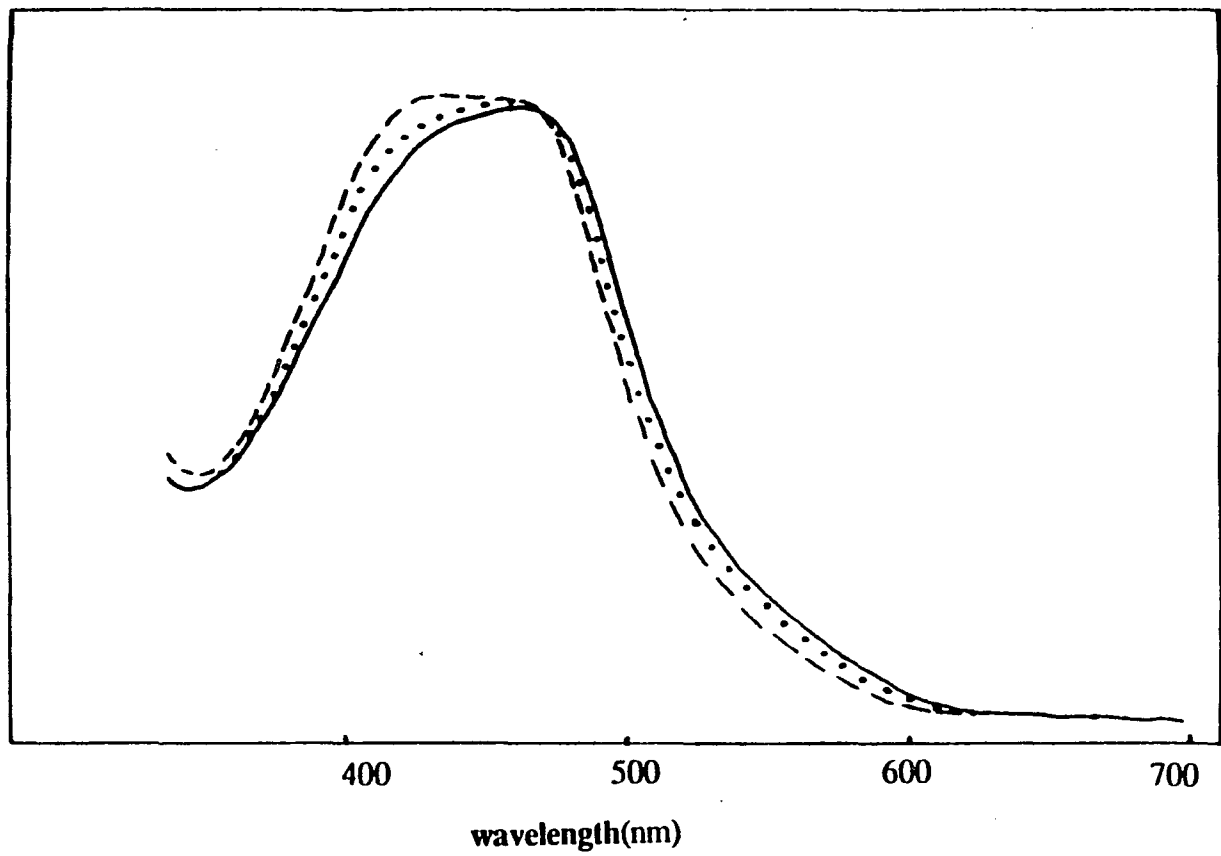


Figure 16. Absorbance spectra of Ru(phen)₂Cl₂ (—), Ru(phen)₂Cl₂ incubated with guanosine(···) and Ru(phen)₂Cl₂ incubated with guanosine 5' monophosphate (- - -). All solutions were incubated for 12 hours in buffer R at room temperature.

guanosine . We were not able to isolate a single species. The absorbance spectrum of the mixture shows a similar effect as was seen for $\text{Ru(phen)}_2\text{Cl}_2$ bound to DNA. The small blue shifts in the spectra of these complexes (relative to that of $\text{Ru(phen)}_2\text{Cl}_2$ in buffer R) is consistent with coordination of the metal at a weakly backbonding ligand such as an endocyclic nitrogen on the nucleotide. (See discussion.) Moreover, the similarity of the spectral shifts observed with GMP and with guanosine and the lack of any blue shift of $\text{Ru(phen)}_2\text{Cl}_2$ in phosphate containing buffer suggest that the ruthenium is not coordinating at a phosphate group on the DNA.

Binding of $\text{Ru(phen)}_2\text{Cl}_2$ to poly(dG-dA) poly(dC-dT)

As is shown in Table 2 poly(dG-dC)·poly(dG-dC) is the only polynucleotide, of those examined, with a preference for the Δ enantiomer. One possible explanation for this opposite enantioselectivity in binding to poly(dG-dC)·poly(dG-dC) is the formation of an intrastrand G-G adduct not possible in the cases of the other synthetic polynucleotides. To test this possibility we monitored the enantioselectivity of the binding reaction. with the polymer poly(dG-dA)·poly(dC-dT). Unlike in the case of poly(dG-dC)·poly(dG-dC), the Λ enantiomer was preferred in binding, indicating that the potential for an intrastrand adduct does not by itself cause a preference for the Δ enantiomer.

Binding of $\text{Ru(phen)}_2\text{Cl}_2$ to Z-DNA and the effect on the B to Z transition.

Since poly(dG-dC)·(polydG-dC) is known to adopt a Z conformation in the presence of certain metal ions we wanted to determine if a Z conformation induced by the ruthenium might explain the observation that poly(dG-dC)·(polydG-dC) is the only sequence with a preference for the Δ enantiomer. The following experiments were done to determine if this is the case. 1.

The relative affinity of $\text{Ru(phen)}_2\text{Cl}_2$ to B and Z DNA and 2. The effect of $[\text{Ru(phen)}_2\text{Cl}_2]$ binding on the B to Z transition of poly(dG-dC)·poly(dG-dC) were determined.

DNA in the Z conformation was prepared from poly(dG-dC)·poly(dG-dC) in 10 mM NaCl, 5 mM tris and 30 μM $\text{Co(NH}_3)_6^{3+}$, pH 7.5. B-DNA was prepared in the same buffer without $\text{Co(NH}_3)_6^{3+}$. Figure 17 illustrates the difference in binding of $\text{Ru(phen)}_2\text{Cl}_2$ to poly(dG-dC)·poly(dG-dC) in the two buffer systems. A much smaller amount of binding is seen when $\text{Co(NH}_3)_6^{3+}$ is present. Control experiments were done to assess the effect of the presence of $\text{Co(NH}_3)_6^{3+}$ on binding, regardless of the DNA conformation. Two types of control experiments were done. In the first experiment, the effect of $\text{Co(NH}_3)_6^{3+}$ concentration on the binding of $[\text{Ru(phen)}_2\text{Cl}_2]$ to calf thymus DNA was examined. A 30 μM $\text{Co(NH}_3)_6^{3+}$ concentration considerably reduces the binding of $\text{Ru(phen)}_2\text{Cl}_2$ to calf thymus DNA. The difference in binding in the presence and absence of $\text{Co(NH}_3)_6^{3+}$ however is not quite as great as that observed for poly(dG-dC)·poly(dG-dC). The second experiment was done by taking advantage of the fact that the B to Z transition driven by $\text{Co(NH}_3)_6^{3+}$ does not occur instantaneously. The binding of $\text{Ru(phen)}_2\text{Cl}_2$ to poly(dG-dC)·poly(dG-dC) was compared for samples to which $\text{Co(NH}_3)_6^{3+}$ was added three hours prior to addition of $\text{Ru(phen)}_2\text{Cl}_2$ (which allows time for the polymer to adopt the Z conformation) and those to which $\text{Co(NH}_3)_6^{3+}$ was added immediately prior to the addition of $\text{Ru(phen)}_2\text{Cl}_2$. A smaller amount of binding is observed for the case in which DNA has been converted to the Z conformation before addition of the $\text{Ru(phen)}_2\text{Cl}_2$.

The B to Z transition can be driven by the presence of high NaCl concentration. The time course of the B to Z transition was monitored for samples of poly(dG-dC)·poly(dG-dC) containing various amounts of bound ruthenium by adding 4M NaCl to poly(dG-dC)·poly(dG-dC) which had first been incubated with $\text{Ru(phen)}_2\text{Cl}_2$ for increasing time intervals. The

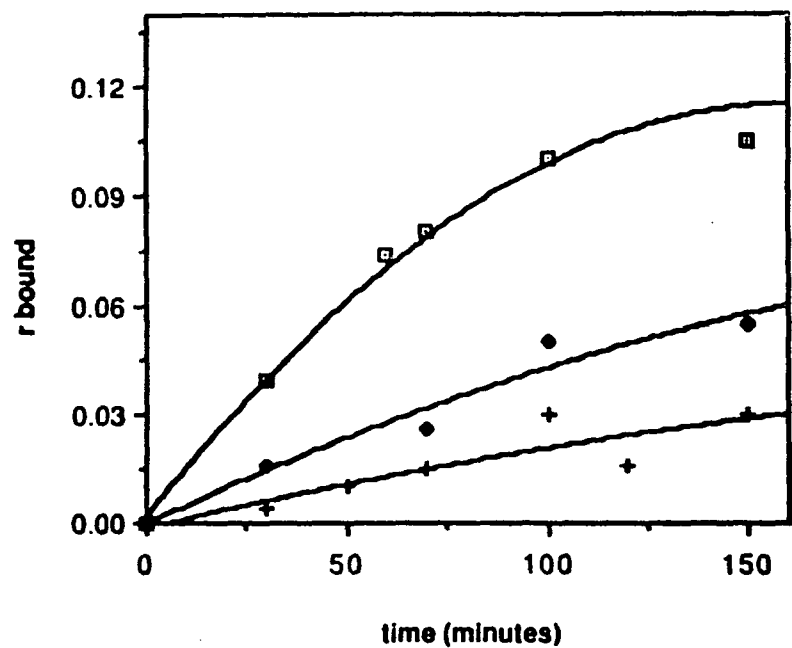


Figure 17. Effect of the presence of $\text{Co}(\text{NH}_3)_6^{3+}$ on the degree of binding of $\text{Ru}(\text{phen})_2\text{Cl}_2$ to poly(dG-dC)-poly(dG-dC). The points depicted represent represent binding experiments done in the presence of no $\text{Co}(\text{NH}_3)_6^{3+}$ (\square), 20 μM $\text{Co}(\text{NH}_3)_6^{3+}$ added to the DNA simultaneously with the $\text{Ru}(\text{phen})_2\text{Cl}_2$ (\blacklozenge), and 20 μM $\text{Co}(\text{NH}_3)_6^{3+}$ added to the DNA 3 hours prior to the addition of the $\text{Ru}(\text{phen})_2\text{Cl}_2$ (+). The concentrations of the DNA and the ruthenium complex were 20 μM and 100 μM respectively.

total ruthenium complex in solution was therefore identical while the amount coordinated was increased with each time point. The transition was monitored by observing the absorbance of the DNA at 295 nm. DNA in the Z conformation has a larger extinction coefficient at this wavelength than DNA in the B-conformation. (See Figure 13) As is shown in Figure 19, the approach to the absorbance characteristic of the Z-conformation following addition of NaCl slows or stops as the concentration of bound ruthenium increases, indicating an inhibition of the transition.

The conformational transitions were also monitored by the C.D. spectra of poly(dG-dC)·(polydG-dC). Figure 20 illustrates the C.D. spectra of poly(dG-dC)·(polydG-dC) and of poly(dG-dC)·(polydG-dC) bound to Ru(phen)₂Cl₂ (r=.1) each in the presence and absence of 4M NaCl. Again, the bound ruthenium appears to be inhibiting the conformational transition.

Binding experiments with derivatives of Ru(phen)₂Cl₂

In order to try to maximize the enantioselectivity of the binding reaction and to investigate which positions on the phenanthroline are most responsible for the steric hindrance which leads to enantioselectivity, ruthenium(II) complexes containing derivatives of phenanthroline were used in binding experiments similar to that shown in Figure 1. The compounds compared to Ru(phen)₂Cl₂ were: Ru(5,6-dimethylphenanthroline)₂Cl₂ and Ru(5-phenylphenanthroline)₂Cl₂. The binding of these complexes to DNA is illustrated in Figure 15. It is seen that greater amounts of binding to both calf thymus DNA and poly(dG-dC)·poly(dG-dC) occurs for Ru(5,6-dimethylphenanthroline)₂Cl₂ as compared to Ru(phen)₂Cl₂. Slightly smaller amounts of binding were observed for Ru(5-phenylphenanthroline)₂Cl₂.

Optical rotations at 270 nm for the enantiomerically enriched solutions of the unbound ruthenium complexes as a function of r are graphed in Figures 21 and 22. The modification of

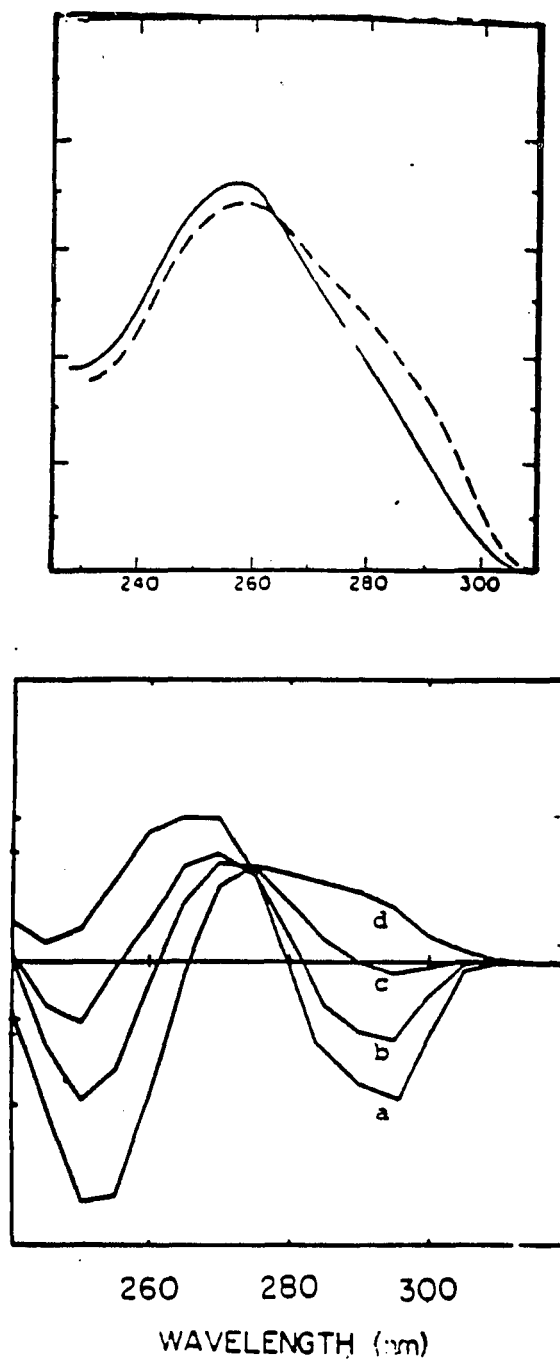


Figure 18. Top: Absorbance spectra of B(---) and Z(---) DNA. Bottom: C.D. spectra of 100% B-DNA(d), 66% B-DNA (c), 33% B-DNA (b) and 100% Z-DNA (a).

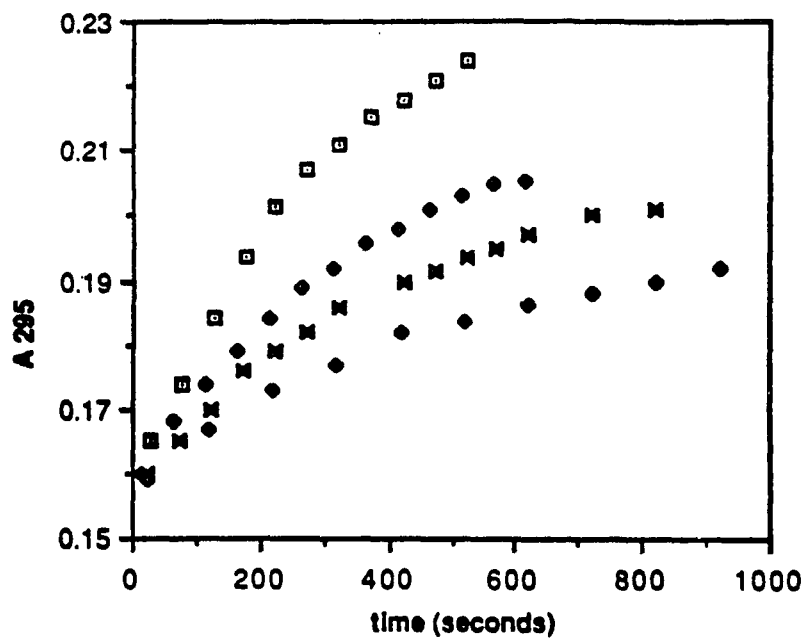


Figure 19. Effect of the bound $\text{Ru}(\text{phen})_2\text{Cl}_2$ complex on the B to Z transition as monitored by the absorbance of the DNA at 295 nm. The transition was induced by the addition of 4M NaCl subsequent to incubation with $\text{Ru}(\text{phen})_2\text{Cl}_2$. Increasing time of incubation with $\text{Ru}(\text{phen})_2\text{Cl}_2$ prior to the addition of NaCl causes an inhibition of the conformational transition. 0', \square ; 12', \blacklozenge ; 26', $*$; 80', \circ .

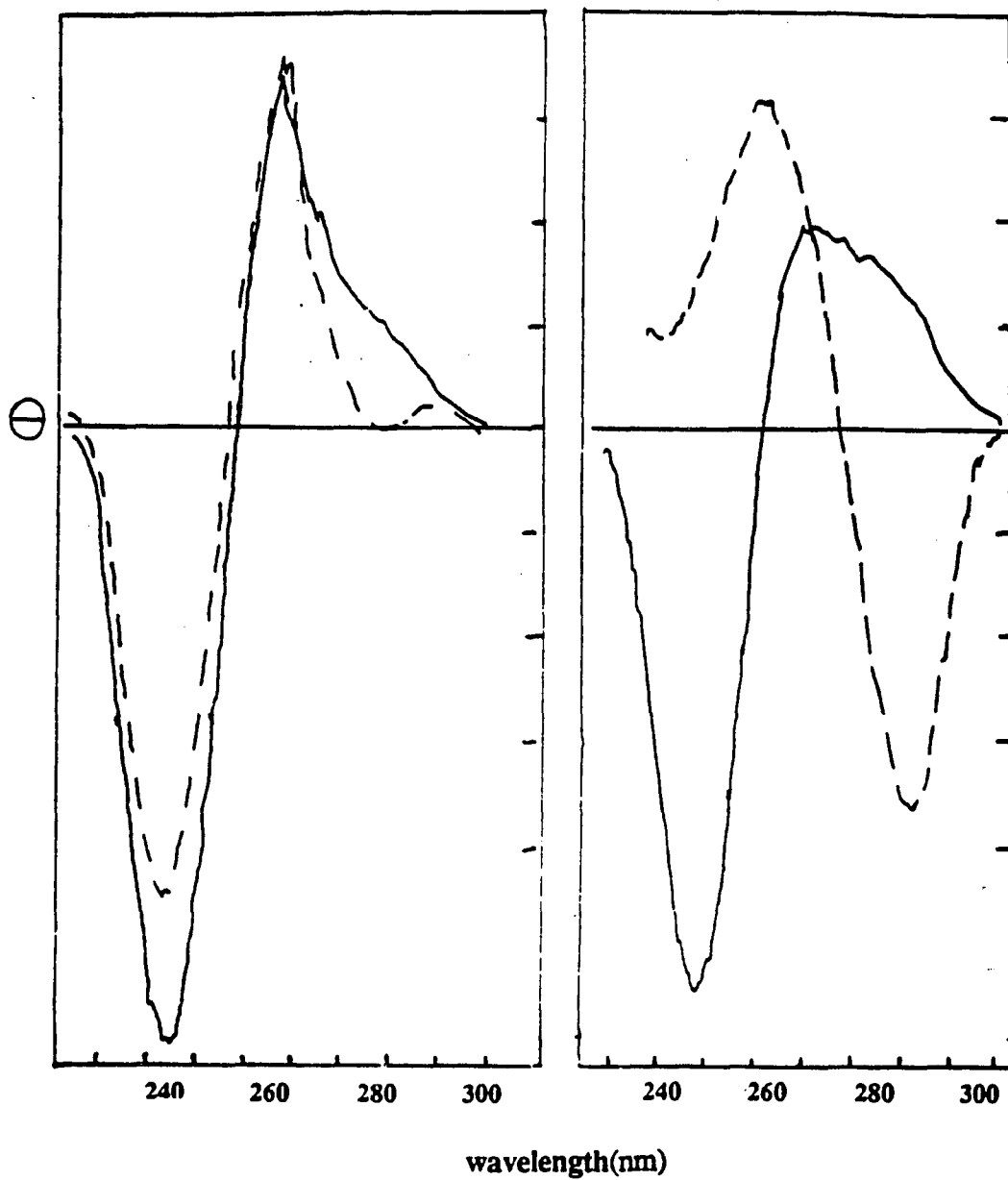


Figure 20. Effect of the bound ruthenium complex on the B to Z transition as monitored by the C.D. spectra. Right: 100 μ M unbound poly(dG-dC)·poly(dG-dC) in the presence of 50 mM NaCl (—) and 4M NaCl (- -). left: 100 μ M poly(dG-dC)·poly(dG-dC) which had first been incubated with 20 μ M Ru(phen)₂Cl₂ for 4 hours ($r_{\text{bound}} = .1$) in the presence of 50 mM NaCl (—), 4 M NaCl (- -).

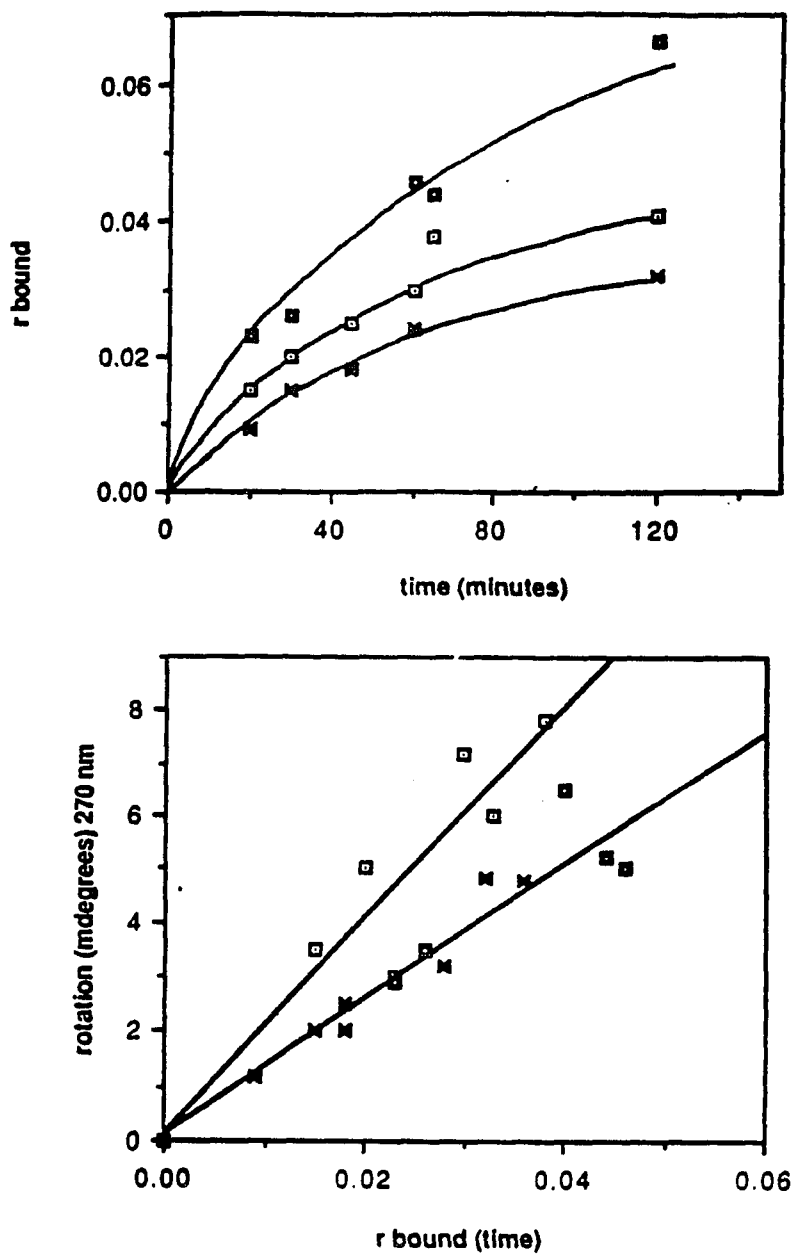


Figure 21. Binding (top) and enrichment of the Λ enantiomer (bottom) as a function of time for the reactions of $\text{Ru}(\text{phen})_2\text{Cl}_2$ (□), $\text{Ru}(5,6\text{ dimethylphen})_2\text{Cl}_2$ (■) and $\text{Ru}(5\text{phenylphen})_2\text{Cl}_2$ (*) with calf thymus DNA.

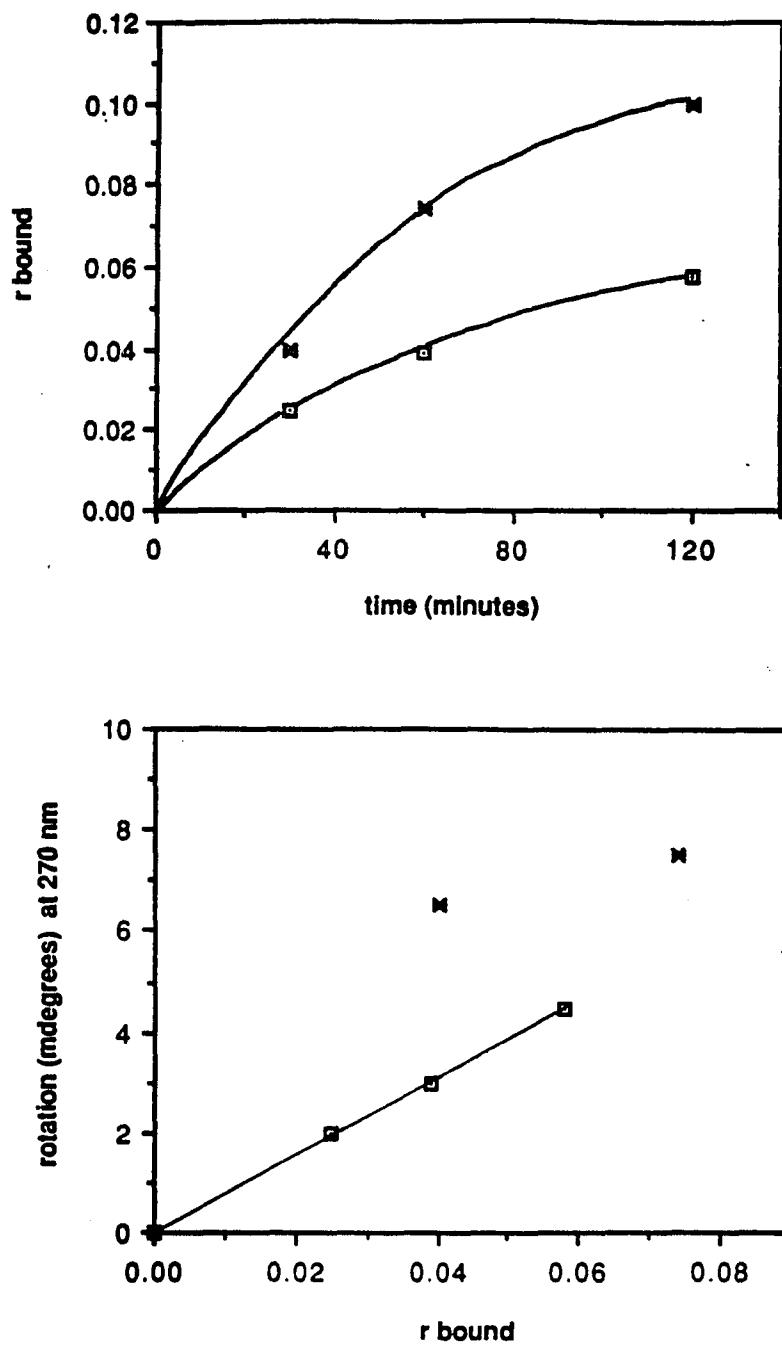


Figure 22. Binding (top) and enrichment of the Δ enantiomer (bottom) as a function of time for the reactions of Ru(phen)₂Cl₂ (□) and Ru(5,6-dimethylphen)₂Cl₂ (✱) with poly(dG-dC)·poly(dG-dC).

the 5 and 6 positions was not effective in increasing enantioselectivity with calf thymus DNA. A small increase in enantioselectivity is observed for Ru(5,6-dimethylphenanthroline)₂Cl₂ compared to Ru(phen)₂Cl₂ in the binding reaction with poly(dG-dC)·poly(dG-dC). The magnitudes of the optical rotations were not determined for all of these complexes. Based on the known magnitudes of the optical rotations of similar complexes containing 3,4,7,8-dimethylphenanthroline and 4,7-diphenylphenanthroline as ligands, we are assuming that the magnitude of the optical rotations of the complexes discussed above are not less than 60% that of Ru(phen)₂Cl₂.

Effect of Ru(phen)₂Cl₂ on the Exonuclease Reaction with DNA

In order to identify sites of Ru(phen)₂Cl₂ binding on DNA the effect of the bound complex on the pattern of cleavage by the enzyme exonuclease III was analyzed by gel electrophoresis. Lanes 3-8 in Figure 23 illustrate that Ru(phen)₂Cl₂ does inhibit exonuclease cleavage. Higher concentrations of Ru(phen)₂Cl₂ incubated with the DNA result in darker bands within the lanes which correspond in most part to those in the G reaction. (Bands result from incomplete reaction of the enzyme.) Longer incubation periods of the DNA with the ruthenium complex also result in darker bands. This effect is illustrated by the comparison of lanes 3, 5 and 7 with lanes 4, 6 and 8 respectively. The observed effects support the notion that ruthenium binds at guanine nucleotides on the DNA. However, as is also illustrated in lane 1, the enzyme itself has many stopping points on this fragment. The activity of ExoIII is least efficient at the 3' end of guanine nucleotides²⁴ and this is may be the reason for the similarity of the G reaction to the ExoIII reaction. A general inhibition of the enzyme by ruthenium could conceivably increase or modify these already existing bands. It is difficult to distinguish between a local inhibition caused by binding to a particular site on the DNA and a general inhibition or modification of the reaction caused by binding of the ruthenium to the

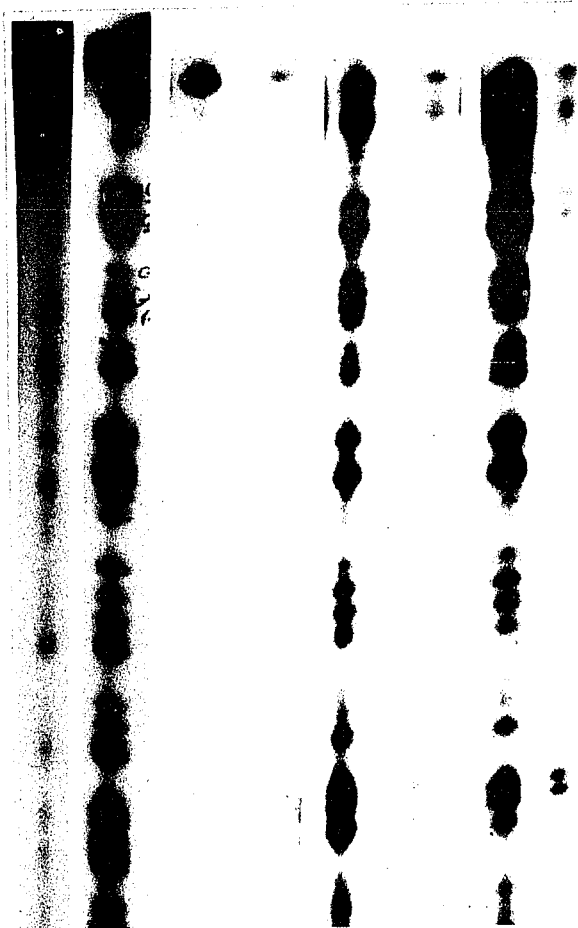


Figure 23. Effect of $\text{Ru(phen)}_2\text{Cl}_2$ on the reaction of Exonuclease III with SV40 DNA (0-300). $\text{Ru(phen)}_2\text{Cl}_2$ was incubated with the DNA (calf thymus DNA was used as carrier). Free $\text{Ru(phen)}_2\text{Cl}_2$ was then removed by ethanol precipitation and the samples were resuspended and treated with the enzyme. lane 1, no $\text{Ru(phen)}_2\text{Cl}_2$, 30 U Exo III ; lane 2, Maxam Gilbert G reaction.; lane 3, $r_{\text{free}} = .006$, incubation time with $\text{Ru(phen)}_2\text{Cl}_2 = 1$ minute; lane 4, $r_{\text{free}} = .006$, incubation time with $\text{Ru(phen)}_2\text{Cl}_2 = 3$ hours ; lane 5, $r_{\text{free}} = .06$, incubation time with $\text{Ru(phen)}_2\text{Cl}_2 = 1$ min. ; lane 6, $r_{\text{free}} = .06$, incubation time with $\text{Ru(phen)}_2\text{Cl}_2 = 3$ hours; lane 7, $r_{\text{free}} = .2$, incubation time with $\text{Ru(phen)}_2\text{Cl}_2 = 1$ min., lane 8, $r_{\text{free}} = .2$, incubation time with $\text{Ru(phen)}_2\text{Cl}_2 = 3$ hours. DNA in lanes 3-8 was treated with 150 U ExoIII.

enzyme.

Discussion

Sequence dependencies of binding and enantioselectivity

In order to determine the sequence preferences of $\text{Ru}(\text{phen})_2\text{Cl}_2$ for binding to DNA, binding experiments were carried out with the synthetic polynucleotides $\text{poly}(\text{dG-dC})\cdot\text{poly}(\text{dG-dC})$, $\text{poly}(\text{dG})\cdot\text{poly}(\text{dC})$, $\text{poly}(\text{dA-dT})\cdot\text{poly}(\text{dA-dT})$ and $\text{poly}(\text{dA})\cdot\text{poly}(\text{dT})$. A dependence on G-C content is observed. The most binding is seen to polymers containing G-C base pairs. Though synthetic polynucleotides are a simple way to measure sequence dependencies of a reaction, because of their repeating nature one must consider the possibility that they might regularly take on conformations uncharacteristic of natural DNA. Such conformational differences could conceivably account for the different amounts of binding to each polynucleotide. However, these types of conformational differences have been shown to be as much a function of base sequence as base composition.²⁵ Therefore, the observation that both alternating and homopolymers containing GC sequences are preferred over both alternating and homopolymers containing AT sequences and that calf thymus DNA has an intermediate degree of binding between the two sequences leads to the conclusion that variations in binding do arise because of the sequence composition (i.e., G-C preferences) rather than any anomalous conformations.

Many of the soft transition metals for which binding to DNA has been observed display a preference for N-7 of guanine.² Binding at N-7 is therefore one likely explanation for the dependence of binding on G-C content. Conceivably, there may be a preference for another functional group on G or C nucleotides.^{4a,4c,26} Preferences arise because of a combination

of effects including that of the basicity of the site, inductive effects and steric interactions (favorable or unfavorable) on the thermodynamics and the kinetics of the reaction. It has been noted that the binding of $[\text{Ru}(\text{NH}_3)_5\text{Cl}]^+$ to N-7 of guanine on DNA is governed by a mix of kinetic and equilibrium controls.²⁷

Chiral molecules are employed in our studies with the goal that differences in binding of the two enantiomers will reflect the structures of the binding sites. For this reason we compared the enantioselectivities of the various polynucleotides. They are listed in Table 2. The data illustrate that poly(dG)-poly(dC) is the most similar to calf thymus DNA in terms of the enantioselectivity of its binding reaction. This observation plus the fact that the greatest amount of binding to $\text{Ru}(\text{phen})_2\text{Cl}_2$ is observed for poly(dG)-poly(dC) leads us to propose that a site similar in sequence or conformation to the one found on this polynucleotide (i.e. a homopurine site containing guanine nucleotides) is a primary binding site on naturally occurring DNA.

Figure 24 illustrates a model of one possible mode of binding. In this model the metal is coordinated to the endocyclic nitrogen, N-7 of guanine. The model suggests an explanation for the preference for the Λ enantiomer observed in most cases. First we note that if the metal is oriented to coordinate to either one or two of the central guanines in the major groove the phenanthrolines on the Λ enantiomer follow the orientation of the helix, whereas the ligands on the Δ enantiomer oppose that orientation. Specifically, for the Λ enantiomer, one ligand is positioned in the solvent and the other is positioned with its surface against the walls of the helix. In the case of the Δ enantiomer, one of the phenanthroline ligands is hindered by interactions with the phosphate backbone and the other by the column of bases. Further characterization of the adduct will be necessary to corroborate or modify this model.

We note from the results in Table 2 that the greatest enantioselectivity is observed for the binding reaction with calf thymus DNA, as compared with all the synthetic polynucleotides.

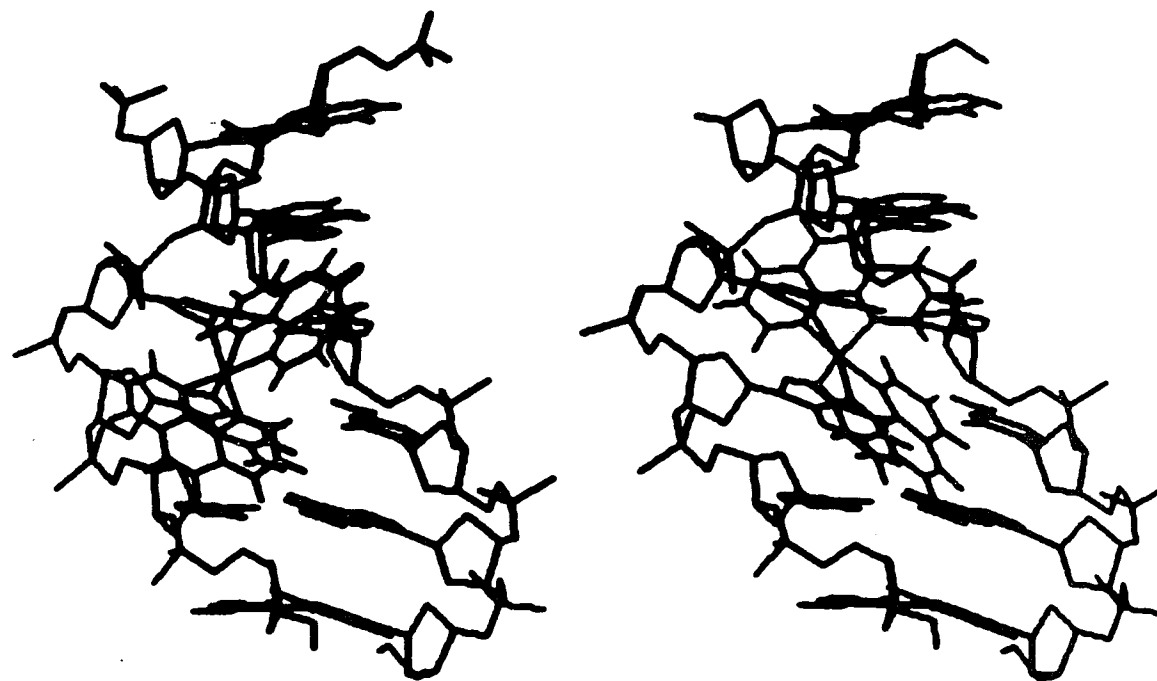


Figure 24. Proposed models of Λ (left) and Δ (right) $\text{cis-Ru(phen)}_2\text{Cl}_2$ coordinated to N-7 of guanine in B-DNA.

This fact may reflect secondary structures that the synthetic polynucleotides can adopt (eg: hairpins, strand slippage). Alternatively it is possible that a site on calf thymus not represented amongst the polynucleotides examined has the greatest enantioselectivity. For instance, some model building studies suggest to us that a site containing thymine and guanine nucleotides on one strand may be the most preferred for the Λ enantiomer. According to this model, if the ruthenium coordinates to the guanines and favorable hydrophobic interactions could occur between the methyl groups on thymine and the phenanthroline ligands.

Spectroscopic Studies of $\text{Ru}(\text{phen})_2\text{Cl}_2$ bound to DNA and related complexes

The energies of the charge transfer bands of ruthenium(II) complexes have been demonstrated to correlate with the difference in potentials between the oxidation of the metal and the reduction of the ligand.²⁸ For example, the more stabilized the ruthenium(II) state of a complex, the higher in energy is its metal to ligand charge transfer (MLCT) transition. Insofar as the non-chromophoric ligands (L_2 of $\text{Ru}(\text{phen})_2\text{L}_2$) affect the electron density at the metal center, their nature will be reflected by the energy of the charge transfer band. Data in the literature indicate that in the case of *cis*- $\text{Ru}(\text{bpy})_2\text{L}_2$ complexes, ligands in the L_2 positions that are capable of backbonding by accepting π electron density from the metal, stabilize the ruthenium(II) state and thereby raise the energy of the MLCT transition in these complexes.²⁹

The addition of DNA to $\text{Ru}(\text{phen})_2\text{Cl}_2$ causes an immediate decrease in absorbance of the band and a red shift of the maximum wavelength similar to that seen when DNA is added to $\text{Ru}(\text{phen})_3^{2+}$. This effect reflects the non-covalent binding of the complex to the DNA. The original red shift is followed by a gradual blue shift in the spectrum. The addition of GMP or of guanosine to $\text{Ru}(\text{phen})_2\text{Cl}_2$ also causes a blue shift in the spectrum over the course of several hours. (No immediate red shift is observed in these cases suggesting that non-covalent

associations with the metal complex are only characteristic of polynucleotides.)

We compared the effects on the absorbance spectrum of DNA or components of DNA binding to $\text{Ru}(\text{phen})_2\text{Cl}_2$ to the effects of having pyridine or amines as the non-chromophoric ligands. Both endocyclic nitrogens and amine groups are potential ligands on the DNA. Consistent with the notion that non-chromophoric backbonding ligands raise the energy of the MLCT transition, we find that the complexes containing pyridine ligands have spectra that are blue shifted compared to $\text{Ru}(\text{phen})_2\text{Cl}_2$ in our buffer system. Amines and water molecules on the other hand are not π bonding ligands. Amines coordinated to the metal have the effect of slightly red shifting the transition compared to the spectrum of $\text{Ru}(\text{phen})_2\text{Cl}_2$ dissolved in buffer R. (This shift may be a function of the better σ bonding ability of the NH_3 group). The removal of all the coordinated chloride ions from $\text{Ru}(\text{phen})_2\text{Cl}_2$ in aqueous solution by AgNO_3 also causes a blue shift in the spectrum, consistent with the chloride ions being π electron donating ligands. Dissolving $\text{Ru}(\text{phen})_2\text{Cl}_2$ in phosphate buffer has hardly any effect on the energy of the visible charge transfer band. A question relevant to our system is the degree of effectiveness of a nucleotide as a backbonding ligand. Clarke and Taube have studied ruthenium pentaammine-guanine complexes and have proposed, based on the reduction potential of their complex, that when ruthenium is bound to guanine at N-7 this ligand has some backbonding capabilities but is not nearly as strong a backbonder as pyridine.^{4b} The same conclusion was drawn based on the relative affinities of ruthenium(II) and ruthenium(III) for guanine.^{27b} The observed blue shift in the spectrum of the DNA bound complex (as well as the complexes bound to GMP or guanosine), intermediate between that of $\text{Ru}(\text{phen})_2\text{Cl}_2$ dissolved in buffer R and of $[\text{Ru}(\text{phen})_2(\text{py})\text{Cl}]^+$, (Figure 13) is consistent with binding of the $\text{Ru}(\text{phen})_2\text{Cl}_2$ at an endocyclic nitrogen on the nucleotide.

The lack of effect of phosphate buffer on the spectrum of $\text{Ru}(\text{phen})_2\text{Cl}_2$ and the similarity in shifts for $\text{Ru}(\text{phen})_2\text{Cl}_2$ binding to guanosine and to guanosine 5' monophosphate suggest

that binding to phosphates is not occurring on the DNA. Such a finding would not be surprising. Though ruthenium(III) compounds have been observed to bind to phosphate oxygens³⁰ and ruthenium(II) does coordinate to oxygens, such interactions are thermodynamically less favorable and kinetically more labile than interactions of ruthenium(II) with softer ligands.³¹ Given the proven preference toward N-7 for $\text{Ru}(\text{NH}_3)_5(\text{Cl})^+$ binding to DNA this site is the most likely possibility for the site of binding in our case as well.

Some reservations concerning the interpretations of the absorbance spectra remain, however. The bands we observe are very broad and the shifts among some of these complexes are small. In addition, the bonding of free amines or free phosphates to $\text{Ru}(\text{phen})_2\text{Cl}_2$ may have a different spectroscopic effect than the bonding of these groups on the DNA. Finally, though we have interpreted the shift in the spectra in terms of π bonding, it is known that σ bonding also affects the energy of the MLCT transition.³² These considerations cause these spectra to fall short of being conclusive evidence of the type of site of metal binding. Some caution must also be used in drawing parallels between the ruthenium(II) amine complexes, whose adducts have been characterized, and the phenanthroline complexes. For example, backbonding of the phenanthroline ligands may affect the reactivity of the metal. Data indicate that backbonding ligands lower the rate of substitution of ruthenium(II) complexes and also lower the affinity of the metal for another backbonding ligand.³³ Moreover, the $\text{Ru}(\text{phen})_2\text{Cl}_2$ complex is relatively sterically hindered compared to the pentaamine complex and the DNA (or even a single nucleotide) is a quite bulky ligand. Amines or other groups not within the rings on the nucleotides would be more accessible to the metal than endocyclic nitrogens.

We also attempted to use resonance Raman spectroscopy to elucidate the nature of the adduct. However, these studies were unsuccessful because of the apparent insensitivity of the

spectrum to the non- chromophoric ligands. The charge transfer transitions are all localized on the phenanthroline ligands. Apparently, variations in the non-chromophoric ligands do not have effects on the vibrational energies of the phenanthroline ligands that are large enough to observe. Resonance Raman of the nucleotides in the UV region might be more successful, though more complicated since all the nucleotides and the phenanthrolines have large extinction coefficients in the U.V. region. A small amount of photoanation or photoaquation of the complexes may also have occurred during irradiation. Such reactions would of course be expected to render the various spectra more similar to each other.

Effect of the binding of Ru(phen)₂Cl₂ on the conformation of DNA

Coordination of metal complexes to DNA has been found to alter its conformation. Such an effect is demonstrated in our system by the changes that Ru(phen)₂Cl₂ binding has on the C.D. spectra and the electrophoretic mobility of DNA. The unwinding of the DNA by Ru(phen)₂Cl₂ as illustrated by the gel electrophoresis experiments (Figure7) reflect the perturbation that Ru(phen)₂Cl₂ binding has overall on the conformation of the DNA. Retardation of the supercoiled band reflects unwinding of the DNA and the faster migration of the nicked band reflects compaction of the DNA. Similar effects have been observed with platinum(II) complexes³³ whose major adduct involves the metal coordinated to N-7 of guanines and with benzo[a]pyrene diol epoxide which forms adducts at N-2 of G and N-6 of A.³⁴ Electron microscopy in the case of cis-DDP has illustrated shortening of the DNA as a function of r_{bound} .³⁴ It has been proposed that unwinding of supercoiled DNA and shortening of the nicked DNA may stem from disruption of hydrogen bonds between the bases. In any case such effects on the migration of the DNA must reflect a change in orientation of the phosphodiester backbone by a non-dissociating (or slowly dissociating) species.

Of the various polynucleotides examined, only the alternating polymer poly(dG-

dC)·poly(dG-dC) displays a preference in binding to the Δ enantiomer of Ru(phen)₂Cl₂ (Table 1). Various explanations can be proposed for this observation. One possibility is that this polynucleotide offers different potential connectivities than any of the other polynucleotides. Specifically, interstrand crosslinks or intrastrand crosslinks between two non-adjacent guanine (or cytosine) nucleotides are possible. For example, in the reaction of cis-DDP with poly(dG-dC)·(polydG-dC) a major adduct that forms is that of the central platinum coordinated to two non-adjacent guanines on the same strand.³⁵ The effect of the potential for an intrastrand crosslink on enantioselectivity was investigated by the binding experiment with poly(dG-dA)·poly(dC-dT). As indicated in Table 2, The Λ enantiomer is preferred in the binding reaction with this polynucleotide. Therefore we conclude that the potential for an intrastrand cross-link is not the cause of preference in poly(dG-dC)·(poly(dG-dC) binding to the Δ enantiomer.

A second possible explanation for the reversed enantioselectivity observed in binding to poly(dG-dC)·poly(dG-dC) involves the propensity of this polymer to adopt the Z conformation. The presence of metal ions can drive this transition³⁶. Molecules that bind to DNA can also affect the B to Z conformational transition.³⁷ If Ru(phen)₂Cl₂ is inducing this conformational change, the bound adduct on this polynucleotide would be different from those on the other polynucleotides. Several methods were used to determine the effect of Ru(phen)₂Cl₂ binding on the B to Z transition. 1. The relative amounts of binding of Ru(phen)₂Cl₂ to B and Z DNA were measured. A greater degree of binding to one form or the other would be expected to drive the transition in the direction of the favored conformation. 2. The effect of the binding of Ru(phen)₂Cl₂ to B and Z DNA on their C.D. spectra were monitored. 3. The effect of covalent binding of Ru(phen)₂Cl₂ on the B to Z transition of poly(dG-dC)·poly(dG-dC) induced by 4M NaCl was monitored by the absorbance spectra and the C.D. spectra of the DNA.

Less binding is observed for poly(dG-dC)·poly(dG-dC) in the Z conformation than in the B conformation (Figure 11). The interpretation of these results, however, are made ambiguous because of the large effect that the $\text{Co}(\text{NH}_3)_6^{3+}$ (which is necessary to stabilize the Z-DNA) has on the binding of $\text{Ru}(\text{phen})_2\text{Cl}_2$ to DNA (see Figure 17). Since $\text{Co}(\text{NH}_3)_6^{3+}$ binds to phosphate oxygens, N-7 of guanine and O-6 of guanine, a site specific competition is likely to occur between the two metal complexes. Moreover, since $\text{Co}(\text{NH}_3)_6^{3+}$ drives the transition to Z-DNA, it is probable that it binds more strongly to this form than to B-DNA. Therefore it may compete even more effectively with $\text{Ru}(\text{phen})_2\text{Cl}_2$ when the DNA is in the Z conformation than when it is in the B conformation. In summary, though more binding is observed for poly(dG-dC)·poly(dG-dC) in the B conformation than in the Z conformation, this may be more of a reflection of the effectiveness of $\text{Co}(\text{NH}_3)_6^{3+}$ as a competitor of $\text{Ru}(\text{phen})_2\text{Cl}_2$ than of which conformation is favored in binding to the ruthenium complex.

The immediate effect that $\text{Ru}(\text{phen})_2\text{Cl}_2$ binding has on the C.D. spectrum of B-DNA is a decrease at 290 nm and an increase at 270nm (Figure 8). This difference spectrum has some characteristics of a Z-DNA spectrum. However, since a similar effect is observed for the non-covalent binding to calf thymus DNA this effect cannot be interpreted as a B to Z conformational transition. Increasing amounts of covalent binding of $\text{Ru}(\text{phen})_2\text{Cl}_2$ cause a qualitatively different type of change in the C.D. spectrum (i.e., unlike that of B or Z DNA) with no further decrease at 290 nm (Figure 9).

The B to Z transition of poly(dG-dC)·poly(dG-dC) can be followed by monitoring the absorbance of the DNA at 295 nm or the C.D. spectrum of the polynucleotide in this region. Figure 13 illustrates that the more $\text{Ru}(\text{phen})_2\text{Cl}_2$ covalently bound to the DNA the less effective is 4M NaCl at causing an increase in absorbance at 295 nm. This result indicates that $\text{Ru}(\text{phen})_2\text{Cl}_2$ does not drive the transition of DNA to the Z conformation being

enhanced by $\text{Ru}(\text{phen})_2\text{Cl}_2$. Kinetics of the B to Z transition are such that nucleation sites created by a molecule which binds and locally stabilizes one of the conformations should increase the rate of the transition to that conformation driven by another agent.³⁸ Although it is not possible to tell from this experiment whether $\text{Ru}(\text{phen})_2\text{Cl}_2$ is completely inhibiting the transition or just slowing it, either explanation is inconsistent with $\text{Ru}(\text{phen})_2\text{Cl}_2$ driving an overall transition to Z-DNA.

The effect of the coordination of the ruthenium complex on the conformational transition was also monitored by C.D. spectroscopy. The $\text{Ru}(\text{phen})_2\text{Cl}_2$ was bound to DNA to an r_{bound} value of about .1 and then 4M NaCl was added to induce the B to Z transition. The comparison of the C.D. spectrum of this DNA that of Z DNA formed in the absence of $\text{Ru}(\text{phen})_2\text{Cl}_2$ (Figure 12) leads us to suggest that the transition to Z DNA is partially inhibited by the ruthenium complex. By calculating the expected $\Delta\epsilon$ value at 292 nm for an uninhibited transition we determine that 20-25% of the DNA did undergo a transition to Z-DNA. This represents 3-5 base pairs inhibited for every $\text{Ru}(\text{phen})_2\text{Cl}_2$ bound. Of course one must consider the possibility that the spectra of Z-DNA will not be the same once $\text{Ru}(\text{phen})_2\text{Cl}_2$ is covalently bound. However, since both the absorbance spectra and the C.D. spectra indicate an inhibition of the B to Z transition and since these spectra are not so drastically modified by the binding of the ruthenium complex in the case of B-DNA, it is reasonable to conclude from the absorbance and C.D. spectra that the B to Z transition is inhibited by the bound ruthenium complex.

Based on these results we conclude that binding of $\text{Ru}(\text{phen})_2\text{Cl}_2$ does not drive an overall transition to Z-DNA. However, we do not rule out the possibility that local conformational changes at the binding site may be induced by the metal complex. Such local conformational changes have been observed for the binding of cis-DDP to poly(dG-dC)·poly(dG-dC). In that

case, as well, the binding of the metal complex inhibits an overall transition to Z-DNA.^{39,40} Binding of cis-DDP to poly(dG-dC)·poly(dG-dC) causes a C.D. spectrum uncharacteristic of B-DNA or Z-DNA.^{41b} Based on antibody binding studies however, the Pt-DNA adduct has been found to have some characteristics of the Z conformation⁴¹. Proton NMR spectra of the trinucleotide d(G-C-G)⁴² bound to cis-DDP have shown the coordinated guanosine to be in the syn conformation, characteristic of Z-DNA and this may be the structure that the antibodies recognize.

It has been proposed that the inhibition of a B to Z transition can be caused by an adduct that does not allow for a movement of the bases necessary for the transition to occur.⁴⁰ Steric inhibition of the movement necessary for the transition may be the inhibiting factor in our case. Preliminary evidence has indicated that the Z to B as well as the B to Z transition is inhibited by binding of the ruthenium complex. In that sense binding of Ru(phen)₂Cl₂ may be stabilizing whatever conformation the DNA originally adopts.

Binding experiments with complexes containing derivatized phenanthrolines.

Some model building studies suggested to us that the 5 and 6 positions on the phenanthroline may be integral in the steric hindrance of the Δ enantiomer. However, no increase in selectivity was observed for the binding of Ru(5,6-dimethylphen)₂Cl₂ or Ru(5-phenylphen)₂Cl₂ to calf thymus DNA. The enantioselectivity of poly(dG-dC)·poly(dG-dC) for the Ru(5,6-dimethylphenanthroline) derivative is however slightly increased as compared to the enantioselectivity of this polynucleotide for Ru(phen)₂Cl₂, suggesting once again the different nature of this adduct as compared to that of calf thymus DNA.

The net enantioselectivity observed is of course affected by the many variables which contribute to the stereochemistry of the adduct with either enantiomer. These factors are

difficult to predict particularly because the effect of the binding of the complex on the structure of the DNA is unknown. It is clear however that binding does cause structural perturbations as discussed in the above sections.

The methyl substituted compounds show greater amounts of binding (Figures 16,17). Two explanations for this effect can be proposed. The methyl groups may be donating electron density to the ruthenium center which increases the substitution rate.⁴³ Alternatively, the methyl groups could have hydrophobic interactions with the DNA which may render their interactions with it more favorable.

In summary, the model we propose explains the preference of $\text{Ru}(\text{phen})_2\text{Cl}_2$ for G-C containing sequences, the Δ enantioselectivity of the binding reaction, the similarity between the hydrodynamic effects of $\text{Ru}(\text{phen})_2\text{Cl}_2$ with those of platinum(II) complexes and the spectroscopic features of the ruthenium complexes. Further characterization of the adduct is necessary in order to corroborate or modify the proposed model.

References

1. a) Barton, J.K., Basile, L.A., Danishefsky, A.T., Alexandrescu, A. (1984) Proc Nat Acad Sci **81** 1961- 65. b) Kumar, C.V., Barton, J.K., Turro, N.J. (1985) J. Am. Chem. Soc.
2. a) Martin, B.R. (1985) Acc Chem Res **18** 32-8. b) Barton, J.K., Lippard, S.J. (1980) Metal Ions in Biol. **1** 32-113. c) Marzilli, L.G., Kistenmacher, T.J., Eichorn, G.C. ibid. 180-250.
3. Fichtinger-Schepmann, A.J., van der Veer, J.L., den Hartog, J.H.J., Lohman, P.H.M., Reedjik, J. (1985) Biochem. **24** 707-13.
4. a) Clarke, M.J., Buchbinder, M., Kelman, A.D. (1978) Inorg. Chim. Acta **27** L87-88. b) Clarke, M.J., Taube, H. (1974) J. Am Chem. Soc. **96** 5413-19. c) Clarke, M.J. (1980) Metal Ions in Biol. Syst. **11** 231-83.
5. Gidoni, D., Dynan, W.S., Tijan, R. (1984) Nature **312** 409-13.
6. Cowies, A., Kamen, R.J. (1986) J. Virol **57** 505-14
7. a) Sakonju, S., Bogenhagen, D.F., Brown, D.D. (1980) Cell **19** 13-25. b) Bodenhausen, D.F., Sakonju, S., Brown, D.D. (1980) Cell **19** 27-35.
8. McCall, M., Brown, T., Hunter, W.N., Kennard, O. (1986) Nature **322** 661-4.
9. Smith, D. Martinez, A.M., Ratliff, R.L. (1970) Anal Biochem **38** 85-9.
10. Felsenfeld, G., Hirschman, S.Z. (1965) J. Mol. Biol. **13** 407-27.
11. Wells, R.D., Larson, J.E., Grant, R.C., Shortle, B.E., Cantor, C.R. (1970) J.Mol Biol **54** 465-97.
12. Inman, R.B., Balwin, R.C. (1962) J. Mol. Biol. **5** 172-184.
13. Sullivan, B.P., Salmon, D.J., Meyer, T.J. (1978) Inorg Chem **17** 3334-41.
14. Barton, J.K., Lolis, E. (1985) J. Am. Chem. Soc. **107** 708-9.
15. Bryant, G.M., Fergusson, J.E., Powell, H.K.J. (1971) Aust. J. Chem. **24** 257-73.
16. Kumar, C.V., Barton, J.K., Turro, N.J., Gould, I.R. (1987) Inorg. Chem. **26** 1455-7
17. Maniatis, T., Fritsch, E.F., Sambrook, J. (1982) Molecular Cloning a Laboratory Manual p.124 Cold Spring Harbor.
18. Bowler, B.E., Lippard, S.J. (1986) Biochemistry **25** 3031-8.
19. Maxam, A.M., Gilbert, W. (1977) Proc. Nat. Acad. Sci. **74** 560-4.
20. Dwyer, F.P., Goodwin, H.A., Gyrfas, E.C. (1963) Aust. J. Chem. **16** 544-8.

21. Allen, L.R., Craft, P.P., Durham, B., Walsh, J. (1987) Inorg. Chem. **26** 53-6.
22. a) Mason, S.F., Peart, B.J. (1973) J. Chem. Soc., Dalton Trans. 949-955.
23. Bosnich, B., (1969) Acc. Chem. Res. **2** 266-73.
24. Linxweiler, W., Horz, W. (1982) Nucl. Acid Res. **10** 4845-59.
25. Leslie, A.G.W., Arnott, S., Chandrasekaran, R., Ratliff, R.L. (1980) J. Mol. Biol. **143** 49-72.
26. a) Clarke, M.J., Taube, H. (1975) J. Am. Chem. Soc. **97** 1397-1403. b) Clarke, M.J. (1977) Inorg. Chem. **16** 738-744. c) Clarke, M.J. (1978) J. Am. Chem. Soc. **100** 5068-5075.
27. a) Taube, H. (1981) Comm Inorg Chem **1** 17-31. b) Brown, G.M., Sutton, J.E., Taube, H. (1978) J. Am. Chem. Soc. **100** 2767-2774.
28. Dodsworth, E.S., Lever, A.B.P. (1985) Chem. Phys. Lett. **119** 61-60.
29. a) Bryant, G.M., Fergusson, J.E., Powell, H.H.J. (1971) Aust. J. Chem. **24** 257-73. b) Long, C., Vos, J.G. (1984) Inorg. Chim. Acta **89** 125-131. c) Haga, M.A. (1980) Inorg. Chim. Acta **45** L183-4. d) Brown, G.M., Weaver, T.R., Keene, F.R., Meyer, T.J. (1976) Inorg. Chem. **15** 190-6.
30. Mayer, B.E., Salmon, J.E. (1962) J. Chem. Soc. 2018-2020.
31. Stritar, J., Taube, H. (1969) Inorg. Chem. **8** 2281- 92.
32. a) Rillema, P.D., Allen, G., Meyer, T.J., Conrad, D. (1983) Inorg. Chem. **22** 1617-1622. b) Crutchley, R.J., Lever, A.B.P., (1982) Inorg. Chem. **21** 2276. c) Krause, R.A., Krause, K. (1982) Inorg. Chem. **21** 1714.
33. a) Cohen, G.L., Bauer, W.R., Barton, J.K., Lippard, S.J. (1979) Science **203** 1014-16. b) Scovell, W.M., Collart, F. (1985) Nucl. Acid Res. **13** 2881-95. c) Merkel, C.M., (1983) Ph.D. thesis, Columbia University.
34. Gamper, H.B., Straub, K., Calvin, M., Bartholomey, J.C. (1980) Proc. Nat. Acad. Sci. **77** 2000-4.
35. a) Brouwer, J., van der Putte, P., Fichtinger Schepman, A.M.J., Reedijk, J. (1981) Proc. Nat. Acad. Sci. **78** 7010-7014. b) Marcelis, A.T.M., den Hartog, J.H.J., Reedijk, J. (1982) J. Am. Chem. Soc. **104** 2664-5.
36. a) Zacharias, W., Larson, J.E., Klysik, J., Stirdivant, S.M., Wells, R.D. (1982) J. Biol. Chem. **257** 2775-2782. b) Behe, M., Felsenfeld, G. (1981) Proc. Nat. Acad. Sci. **78** 1619-23. c) Taboury, P.A., Bourtayre, P., Liquier, J., Taillandier, F. (1984) Nucl. Acid Res. **12** 4247- 4258.
37. Rich, A., Nordheim, A., Wang, A.H.-J. (1984) Ann. Rev. Biochem. **53** 791-846.
38. a) Pohl, F.M., Jovin, T.M. (1972) J. Mol. Biol. **67** 375-96. b) Mirau, P.A., Kearns, D.R. (1983) Nucleic Acids Res. **11** 1931-41.

39. Malfoy, B., Hartmann, B., Leng, M. (1981) Nucl. Acid Res. 9 5659-69.
40. Ushay, H.M., Santella, R.M., Caradonna, J.P., Grunberger, D., Lippard, S.J. (1982) Nucl. Acid Res. 10 3573-88.
41. a) Malinge, J., Leng, M. (1984) Eur. J. Mol. Biol. 3 1273-9. b) Malinge, J.M., Ptak, M., Leng, M. (1984) Nucl. Acid Res. 12 5767-78.
41. den Hartog, J.H.J., Altona, C., van Boom, J.H., Marcelis, A.T.M., van der Marel, G.A., Rinkel, L.J., Wille-Hazeleger, G., Reedijk, J. (1983) Eur. J. Biochem. 134 485-9.
43. Taube, H., (1973) Surveys Prog. Chem. 6 1-46.

Chapter 4

Photochemical Reactions of $\text{Ru}(\text{phen})_2\text{Cl}_2$ and $\text{Ru}(\text{phen})_3^{2+}$ with DNA

Introduction

The excited state properties of polypyridyl complexes of ruthenium(II) have been the subject of much research in inorganic chemistry.¹ The excited states of $[\text{Ru}(\text{bpy})_3]\text{Cl}_2$ can undergo oxidation², reduction³ and photosubstitution⁴ reactions not available to the ground state. Polypyridyl ruthenium(II) complexes have therefore been investigated for use as photocatalysts and photosensitizers. One interesting example is the investigation of the photoredox reactions of these complexes as catalysts in energy conversion schemes involving the decomposition of H_2O .⁵ Several aspects of photosubstitution reactions have also been studied. Interesting synthetic routes for the preparation of complexes unobtainable by thermal reactions, have been elucidated.⁶

Studies of the photophysics of these complexes have led to the determination of some properties of excited states from which the photoreactions occur. (A diagram of the excited state model for $[\text{Ru}(\text{bpy})_3]\text{Cl}_2$ shown in Figure 1. Excitation of the visible charge transfer band is followed by formation of short lived $^1\text{MLCT}$ ⁷ excited states which undergo efficient intersystem crossing to $^3\text{MLCT}$ excited states.⁸ Experimental observations are best interpreted as the MLCT states being in thermal equilibrium with LF states from which photosubstitution can occur.^{4a,b}

Complexes of the type $\text{Ru}(\text{bpy})_2\text{L}_2$, where L is a monodentate ligand, share with the tris chelate complexes the ability to undergo photosubstitution reactions following optical excitation of the charge transfer band. Though they share some characteristics of the

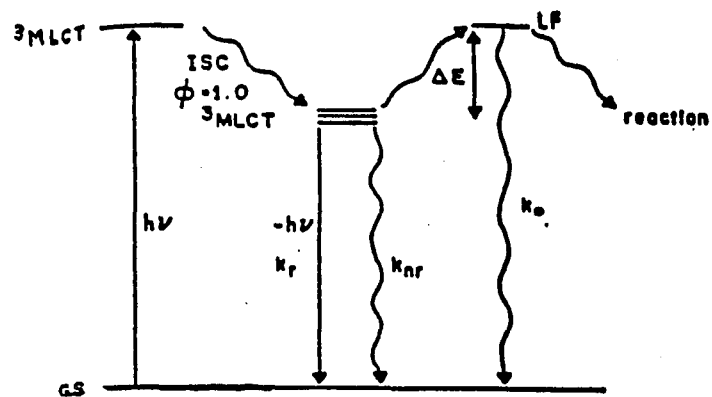


Figure 1. Photophysical properties of $\text{Ru}(\text{bpy})_3^{2+}$ (from reference 1b).

tris(polypyridine)ruthenium(II) complexes, the photochemical mechanisms of the bis(polypyridyl) complexes are not as well understood.^{9,10}

The spectral properties of these ruthenium complexes, that have been exploited for the photophysical investigations, are also useful for studying the interactions of the complexes with biological molecules. Extensive spectroscopic investigations have been carried out in our laboratory to examine the binding of $[\text{Ru}(\text{phen})_3]\text{Cl}_2$ ¹¹ and $[\text{Ru}(\text{dip})_3]\text{Cl}_2$ ¹² to DNA. (See Chapter 2.) These complexes bind non-covalently to DNA and can serve as probes for its structure. In Chapter 3 studies of $\text{Ru}(\text{phen})_2\text{Cl}_2$, which can coordinate to DNA via substitution of one of the non-phenanthroline ligands, are described.

In this chapter some photoreactions of the ruthenium complexes with DNA are described. We have observed a photosubstitution reaction of $\text{Ru}(\text{phen})_2\text{Cl}_2$, in which the binding of this complex to DNA is significantly increased over that of the thermal reaction. Based on comparisons of some physical and spectroscopic feature of the two substitution reactions, the photoreaction appears to be qualitatively similar to the thermal reaction. Photoracemization of $\text{Ru}(\text{phen})_2\text{Cl}_2$ has also been observed and its efficiency is compared with that of the photosubstitution reaction. Photocleavage of DNA in the presence of $[\text{Ru}(\text{phen})_3]\text{Cl}_2$ and $\text{Ru}(\text{phen})_2\text{Cl}_2$ are also described.

Experimental Procedures

Preparation of nucleic acids.

DNA was prepared by the procedures described in Chapters 2 and 3.

Preparation of ruthenium(II) complexes.

The synthesis of $[\text{Ru}(\text{phen})_3]\text{Cl}_2$ was described in Chapter 2 and that of $\text{Ru}(\text{phen})_2\text{Cl}_2$ was described in Chapter 3. Stock solutions of $\text{Ru}(\text{phen})_2\text{Cl}_2$, used in the binding experiments were prepared at a concentration of 1-2 mM by heating the solid in ethanol water solutions, in the dark for about 5 minutes. An extinction coefficient of $10,800 \text{ M}^{-1} \text{ cm}^{-1}$ at 500 nm in ethanol was used to determine concentrations.¹³ Stock solutions were kept in ethanol/water at 4° C when not in use. For the binding experiments, an aliquot of this solution was added to buffer R to yield the desired final concentration. In this buffer the ruthenium is partially aquated and the non-phenanthroline ligands are a mixture of water molecules and chloride ions.

Spectroscopic Instrumentation

All absorbance spectra were recorded on a Cary 219 spectrophotometer. C.D. Spectra were recorded on a Jasco J-40 automatic recording spectropolarimeter. Emission experiments were performed on a Perkin Elmer LS-5 spectrofluorimeter in line with a Perkin Elmer Data Station.

Irradiation of solutions.

Irradiations were performed using either an Oriel model 6140, 1000 W Hg/Xe lamp at 460 nm, or a Liconix He/Cd laser at 442 nm. The power obtained from both of these sources was approximately 18 mW. The lamp was equipped with a monochromator and the slit width during the experiments was set at + 15 nm. Unless otherwise specified the solutions were not deoxygenated. All solutions were at ambient temperature. All samples were contained in a volume of 1 ml. except for samples which were irradiated in preparation for gel electrophoresis. For these experiments 5ul samples were irradiated. Subsequent to irradiation

absorbance spectra were monitored to determine if any qualitative changes occurred to the Ru(phen)₂Cl₂ samples

Substitution reactions of [Ru(phen)₂Cl₂] with DNA.

In order to carry out the substitution reactions, an aliquot from a concentrated Ru(phen)₂Cl₂ stock solution was added to buffer R, followed by an aliquot of DNA from a concentrated stock solution. For the thermal substitution reactions this solution was incubated in the dark at room temperature for the allotted period of time. For the photoreactions, addition of DNA was immediately followed by irradiation. Incubation was followed by ethanol precipitation of the DNA with the bound ruthenium complex and centrifugation of the precipitate. Bound ruthenium concentrations were determined by the visible absorbance of the supernatant (free Ru(phen)₂Cl₂).

Agarose gel electrophoresis.

Gel electrophoresis of SV40 DNA bound to Ru(phen)₂Cl₂ were run in 1% agarose type V purchased from Sigma Chemicals. The running buffer contained 50 mM Tris-HCl, 18mM NaCl, 18mM Na acetate, pH 7.0. The gels were stained in ethidium bromide solutions and the densities of the bands were quantitated on an LKB 2202 laser densitometer.

Determination of the quantum yield of photoracemization

Ru(phen)₂Cl₂ solutions enriched in the Δ enantiomer were prepared by incubating a racemic mixture with calf thymus DNA at a ratio of 10:1 nucleotides to ruthenium, for three hours at room temperature in buffer R. After this time the DNA and the ruthenium complex bound to it was precipitated with 70% ethanol. The solution was centrifuged and the supernatant, enriched in the Δ enantiomer was lyophilized and resuspended in buffer R. This

solution was stored in the dark, at -70°C when not in use. A $10\mu\text{M}$ solution of $\text{Ru}(\text{phen})_2\text{Cl}_2$, 5% enriched in the Δ enantiomer was irradiated for varying time intervals with 442 nm light. The concentration racemized per light absorbed was calculated for several points within a region where the concentration racemized was linear with time. Since the solutions irradiated for the photoracemization experiments were only 5% enriched in the Δ enantiomer the amount of light absorbed by the solution was calculated based on this 5%. (The determination of the $\Delta\epsilon$ value of $\text{Ru}(\text{phen})_2\text{Cl}_2$ used in these calculations is described in Chapter 3.)

Actinometry was done according to the method of Parker.¹⁴ An extinction coefficient of $1.1 \times 10^4 \text{ M}^{-1}\text{cm}^{-1}$ was used to determine concentrations of $\text{Fe}(\text{phen})_3^{2+}$. Irradiated solutions of ferrioxalate were at a concentration of .15M. A quantum yield of 1.0 was used for the ferrioxalate photoreaction at 442 nm. Samples were stirred with a magnetic stirrer during irradiation.

Results

Effect of irradiation on the substitution reaction of $\text{Ru}(\text{phen})_2\text{Cl}_2$ with DNA.

An increase in binding of $\text{Ru}(\text{phen})_2\text{Cl}_2$ to DNA as a function of irradiation is observed. The effect of irradiation with 460 nm light on the binding of $\text{Ru}(\text{phen})_2\text{Cl}_2$ to calf thymus DNA is shown in Figure 2. The amount of $\text{Ru}(\text{phen})_2\text{Cl}_2$ bound to DNA within 10 minutes in the presence of light is equal to the amount bound within two hours when the reaction takes place in the absence of light. Explanations for why the reaction is driven in the direction of binding to DNA are considered in the discussion section.

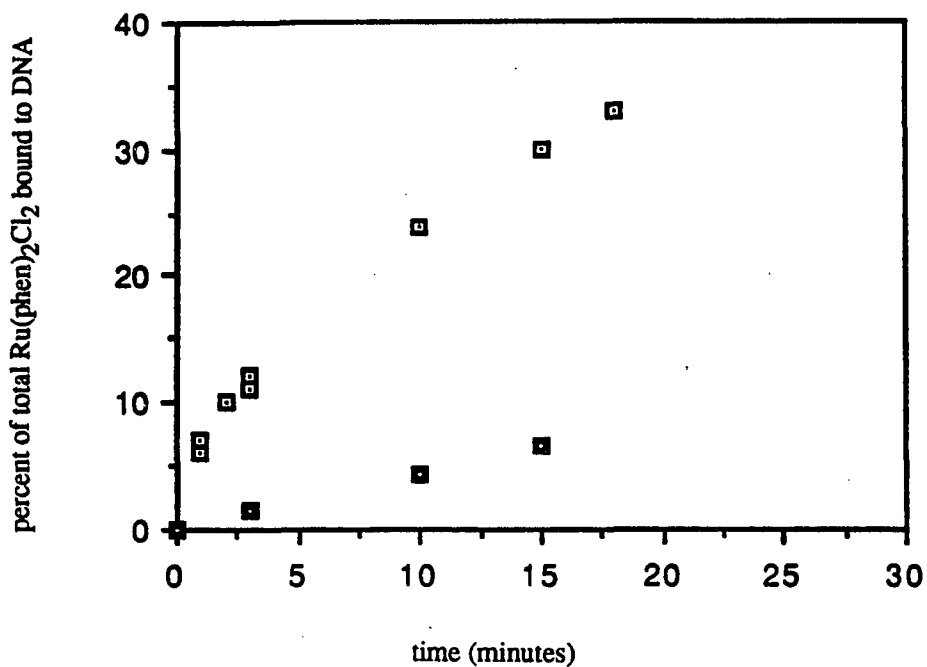


Figure 2. Effect of irradiation with 442 nm light on the binding of Ru(phen)₂Cl₂ to calf thymus DNA. ■, unirradiated samples □, irradiated samples. Irradiations were performed with an 18mW He/Cd laser. Concentrations in solution were 10uM and 100uM for the Ru(phen)₂Cl₂ and the DNA (in nucleotides) respectively.

Luminescence studies of Ru(phen)₂Cl₂ bound to DNA

Emission spectra can, in some cases, be useful for monitoring the binding of a complex to DNA. Therefore investigations were done to determine if emission can be detected for Ru(phen)₂Cl₂ bound to DNA. No emission was detected at temperatures as low as 4 C.

Physical and spectroscopic effects of the photosubstitution reaction of Ru(phen)₂Cl₂ with DNA.

In order to determine if the photosubstitution reaction is qualitatively similar to that of the thermal reaction some of the physical effects that the two reactions have on DNA were compared. In Chapter 3 we noted certain changes in the physical and spectroscopic properties of DNA that occur upon binding to Ru(phen)₂Cl₂. For example, in gel electrophoresis experiments the mobility of the supercoiled DNA band (form I) was retarded while the mobility of the nicked DNA band (form II) was increased. The graphs in Figure 3 illustrate that a similar effect is seen for the photosubstitution reaction. SV40 DNA was first incubated in the absence of light with varying amounts of Ru(phen)₂Cl₂. The figure illustrates that higher ruthenium:nucleotide ratios lead to increased unwinding of the supercoiled band. These same samples were then exposed to one half minute and two minutes of irradiation with 460 nm light from a Hg/Xe lamp (18mW) and the electrophoretic mobility of the supercoiled bands were further monitored. The irradiation causes further unwinding of the supercoiled band. The largest effect was observed for the sample with a ratio of 5:1 nucleotides:ruthenium.

It was also shown in Chapter 3 that over the time course of DNA binding to Ru(phen)₂Cl₂, changes are observed in the U.V. region of the C.D. spectra. Spectra of

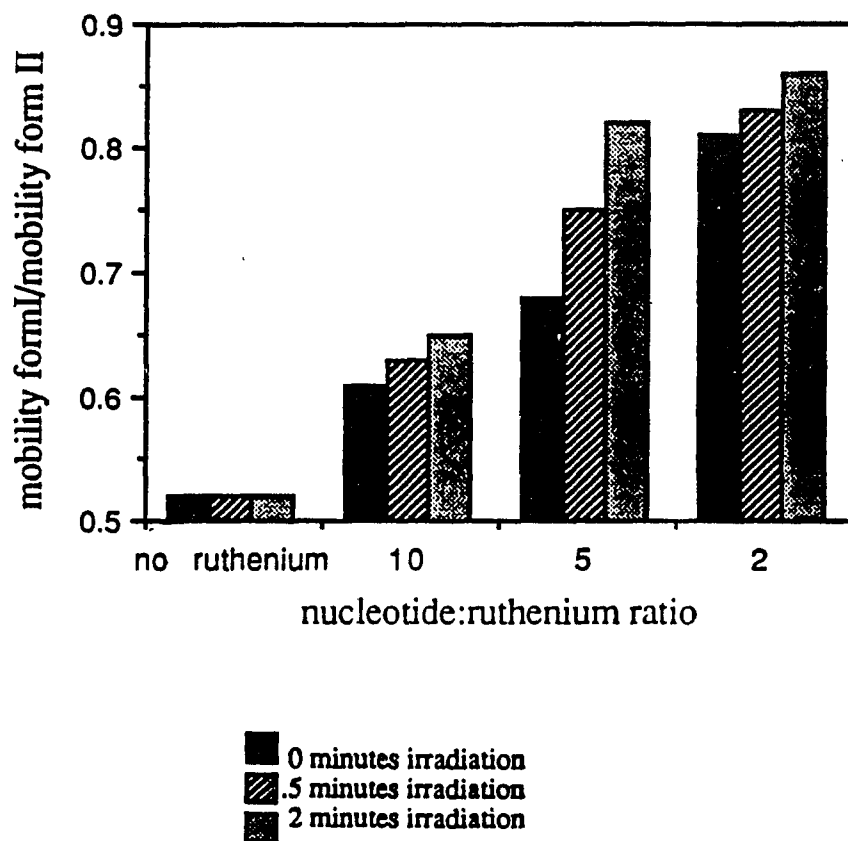


Figure 3. Effect of irradiation with 460 nm light, in the presence of $\text{Ru}(\text{phen})_2\text{Cl}_2$, on the electrophoretic mobility of SV40 DNA. All samples were first incubated in the absence of light for 3 hours. They were then irradiated with 460 nm light from a Hg/Xe lamp for the time periods indicated. The concentration of $\text{Ru}(\text{phen})_2\text{Cl}_2$ was equal to $50\mu\text{M}$

poly(dG-dC)·poly(dG-dC) in both B-DNA and Z-DNA forms bound to Ru(phen)₂Cl₂ are shown in Chapter 3, Figures 9 and 10. The C.D. difference spectra of poly(dG-dC)·poly(dG-dC) before and after 3 minutes of irradiation in the presence of Ru(phen)₂Cl₂ are shown in Figure 4. The effect of the binding of the ruthenium complex on the C.D. spectrum is identical for the thermal reaction and the photoreaction.

Photoracemization of Ru(phen)₂Cl₂ enantiomers - comparison of rate to increased rate of binding to DNA.

We have observed photoracemization of Ru(phen)₂Cl₂ in enantiomerically enriched solutions. (In contrast no racemization is observed for up to 24 hours when the solution is kept at room temperature in the absence of light.) We measured the relative efficiencies of the photosubstitution reaction and the photoracemization reaction under our conditions. This experiment was done in order to determine firstly, if the photosubstitution reaction we observe may be occurring by a similar mechanism as photoracemization and secondly, if we could expect to carry out photosubstitution reactions on enantiomeric Ru(phen)₂Cl₂. The graph in Figure 5 depicts the concentration of Ru(phen)₂Cl₂ that racemizes in a sample absorbing 3×10^{-10} (+ 5×10^{-11}) Einsteins per second. The quantum efficiency calculated for this reaction is $.05 \pm .02$. The graph in Figure 6 depicts the concentrations of Ru(phen)₂Cl₂ that binds to DNA for a sample absorbing 5.5×10^{-7} (+ 5×10^{-8}) Einsteins per minute. The quantum yield calculated for this reaction was $.0015 \pm .0002$.

Photocleavage of DNA by Ru(phen)₂Cl₂ and Ru(phen)₃Cl₂

Irradiation in the region of the visible charge transfer band of Ru(phen)₃²⁺ in the presence of DNA causes cleavage of the DNA. This effect is shown in Figure 7. The following

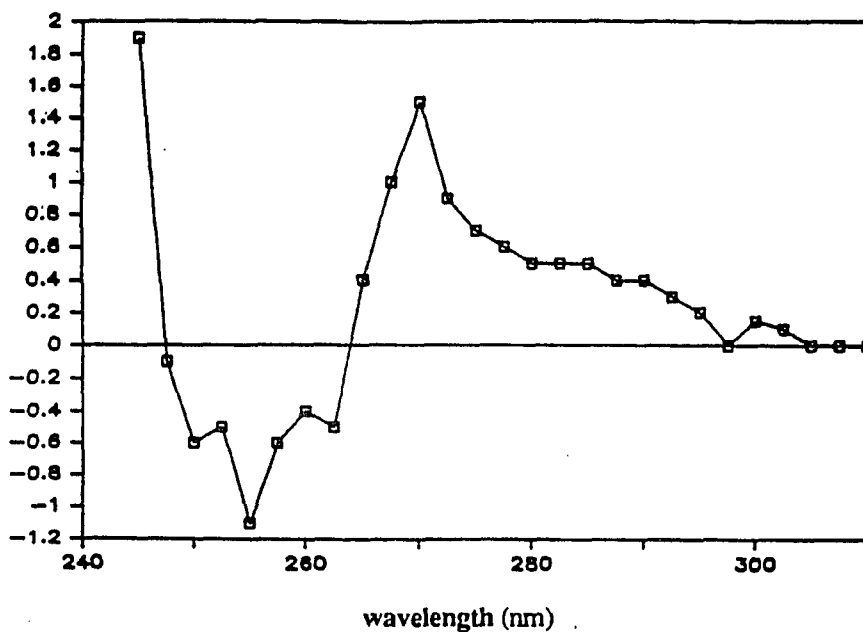


Figure 4a. Difference C.D. spectrum of poly(dG-dC)·poly(dG-dC) in 1/5x buffer R before and after 3' of irradiation at 460 nm in the presence of Ru(phen)₂Cl₂. The concentrations Ru(phen)₂Cl₂ and DNA were 20 μM and 100 μM respectively.

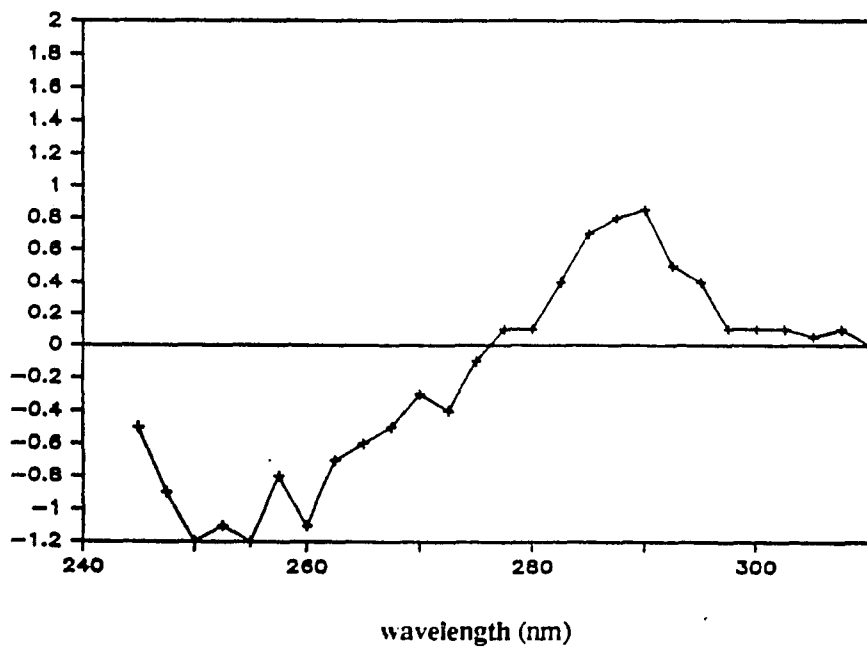


Figure 4b. Same experiment as figure 4a. except that 30 μM cobalt hexamine is present in the buffer to maintain the Z conformation of poly(dG-dC)·poly(dG-dC).

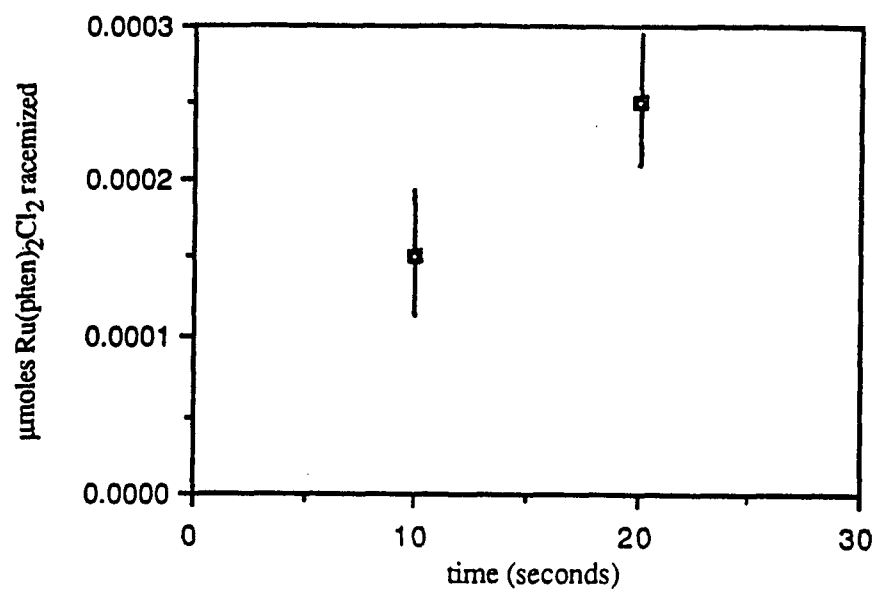


Figure 5. Racemization of Δ Ru(phen)₂Cl₂ as a function of time irradiated with 442 nm light. The total Ru(phen)₂Cl₂ concentration was 10 μ M, 5% enriched in the Δ enantiomer. The light absorbed per second by the excess Δ enantiomer was approximately equal to 3×10^{-10} einsteins. The quantum yield of racemization calculated from this experiment is equal to $.05 \pm .02$.

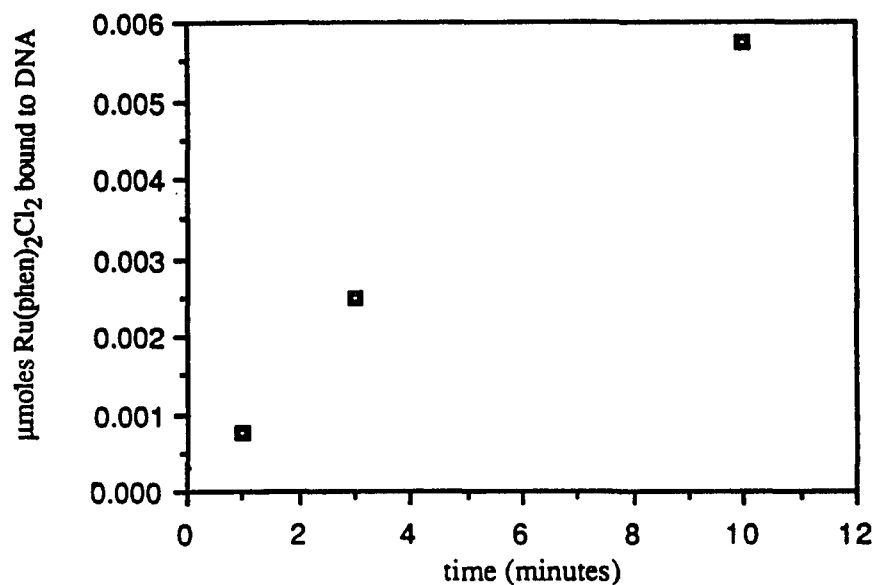


Figure 6. Concentration of Ru(phen)₂Cl₂ bound to DNA as a function of time irradiated with 442 nm light. The concentrations of the DNA and the ruthenium complex were 100uM and 10uM respectively. The light absorbed by the Ru(phen)₂Cl₂ per minute was equal to 5.5×10^{-7} einsteins per minute. The quantum yield for the photosubstitution reaction under these conditions was calculated, from this experiment, to be $.0015 \pm .0002$.

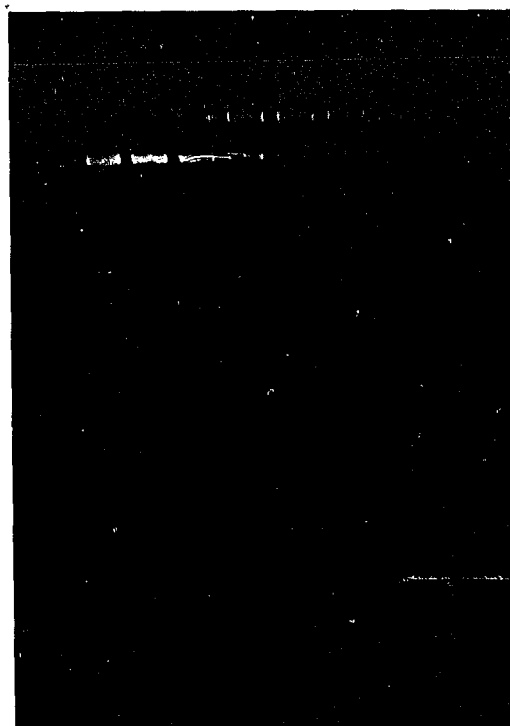


Figure 7. Cleavage of DNA in the presence of $\text{Ru}(\text{phen})_3^{2+}$ as a function of time irradiated with 460 nm light. Lanes, from left to right, depict increasing time periods of irradiation. 1, 10' (no ruthenium); 2, 30"; 3, 1'; 4, 3'; 5, 5'; 6, 5'; 7, 10'; 8, 15'. The samples in lanes 2-8 contained 50 μM $\text{Ru}(\text{phen})_3^{2+}$. The samples in all the lanes contained 250 μM DNA (in nucleotides).

experiments were done to investigate the possibility that singlet oxygen produced by the excited state of $\text{Ru}(\text{phen})_3^{2+}$ in the presence of oxygen may be causing the cleavage reaction.¹⁵ The effect that the presence of D_2O , which enhances the lifetime of singlet oxygen¹⁶ has on the rate of the cleavage reaction is illustrated in Figure 8. Samples were irradiated in buffer R containing 85% D_2O . The presence of D_2O enhances cleavage. The earliest time point shows a 1.8 fold enhancement of cleavage in the presence of D_2O . The reaction has clearly proceeded further than the region in which the reaction is linear with time, however. (After 2 minutes 66% of the product has already formed.) The 1.8 fold enhancement then is a minimum limit of the D_2O enhancement effect. Figure 9 illustrates the effect of O_2 on the $\text{Ru}(\text{phen})_3\text{Cl}_2$ photocleavage reaction. The presence of O_2 enhances the photocleavage reaction as compared to air or N_2 . The least efficient cleavage is observed in the presence of N_2 .

Photocleavage of DNA has also been observed in the presence of $\text{Ru}(\text{phen})_2\text{Cl}_2$, as illustrated in Figure 10. The figure also illustrates that the efficiency of this reaction can be slightly enhanced by alkaline conditions.

Discussion

Photosubstitution reactions of polypyridyl complexes of ruthenium(II) were first noted by Bosnich and Dwyer.¹⁷ Since that time numerous studies of these reactions have elucidated several of their features. In our work, we observe that irradiation of $\text{Ru}(\text{phen})_2\text{Cl}_2$ in the presence of DNA significantly increases its rate of binding to DNA. In order to use this photoreaction in binding experiments of this or similar compounds, it is important to consider some of the characteristics of this reaction. Firstly, the question of whether the photoreaction



Figure 8. Effect of the presence of D_2O on the photocleavage of DNA by $Ru(phen)_3^{2+}$. Samples in the even numbered lanes contained 85% D_2O in buffer R. Time periods of irradiation of the samples increase from left to right on the gel as follows: lanes 1 and 2, 0'; lanes 3 and 4, 2'; lanes 5 and 6, 5'; lanes 7 and 8, 10'.

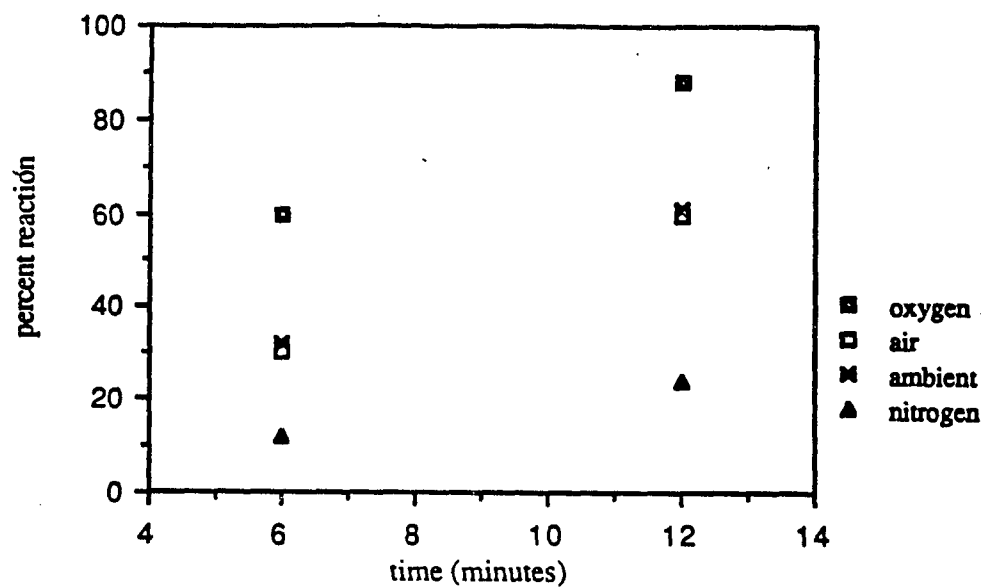


Figure 9. Effect of the presence of O_2 on the photocleavage of DNA by $Ru(phen)_3^{2+}$. Samples represented by the symbols for oxygen, air and nitrogen were irradiated in the presence of those gasses. Samples represented by the symbol for ambient conditions were irradiated in open tubes.

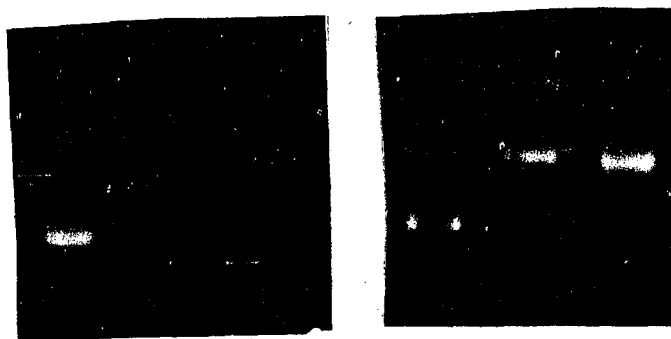


Figure 10. Cleavage of DNA in the presence of $\text{Ru}(\text{phen})_2\text{Cl}_2$ as a function of time of irradiation with 460 nm light. The samples were irradiated for the following time periods: lanes 1 and 4, 0'; lanes 2 and 5, 3'; lane 4 and 6, 15'. Samples in lanes 4-6 were incubated at 50°C, pH 11 for 1 hour following irradiation. Densitometric scans indicate that the percent form II DNA in the samples were as follows: 1.6%; 2.11%; 3.45%; 4.22%; 5.50%; 6.66%.

is qualitatively similar to the thermal reaction is addressed. Secondly, the relative efficiencies of the photoracemization and photosubstitution are compared. This point is important if one wants to employ photosubstitution in the reaction of chiral probes similar to $\text{Ru}(\text{phen})_2\text{Cl}_2$ with DNA. Thirdly, we consider possible explanations for the direction of the photoreaction.

Comparison of characteristics of thermal and photosubstitution reactions

Two physical effects that are observed for the thermal binding reaction are unwinding of the bound DNA on agarose gels and changes in the C.D. spectra over the course of binding. Both of these features were compared for the thermal reaction and the photoreaction. The similarity of the effect on the C.D. spectra and on the mobility of the DNA on gel electrophoresis for the thermal reaction and the photoreaction are consistent with a similar mode of binding for the two reactions.

Comparison of the time course of photosubstitution and photoracemization reactions.

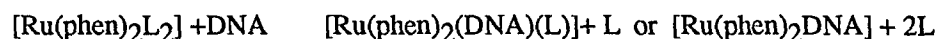
An important aspect of our studies with the DNA binding complexes has been the monitoring of the enantiomeric selectivity of the DNA for the two enantiomers of the chiral complexes (see Chapters 2 and 3). If we are to use photoreactions in binding our complexes to DNA it is important to know at what rate photoracemization occurs relative to the photosubstitution reaction. Durham et. al.^{4c} have concluded that the five coordinate intermediate that forms during the photoreaction of tris chelate complexes has a chiral intermediate. If this is the case it should be possible for the molecule to undergo a photosubstitution reaction without undergoing racemization. However, the relative efficiencies of the substitution and racemization reactions indicate that the photosubstitution reaction with DNA under our conditions occurs much more slowly than the photoracemization reaction. It may be that photosubstitution is slower than racemization because the binding to DNA is

rate limiting. That is, the efficiency of capture of the intermediate by the DNA may be the slowest step. If this is the case it may be interesting to investigate increasing the efficiency of this step by increasing the DNA concentration or lowering the salt concentration or using ligands other than phenanthroline in order to increase the affinity of the metal complex for the DNA thereby maximizing the efficiency of capture by the DNA.

Consideration of the direction of the photosubstitution reaction

The observation that irradiation affects the rate of binding of $\text{Ru}(\text{phen})_2\text{Cl}_2$ to DNA is consistent with the data reported in the literature for other bis(polypyridine)ruthenium(II) systems.^{4,6,17-20} Evidence suggests that photoanation reactions of compounds of the type $\text{Ru}(\text{bpy})_2\text{L}_2$ (where L is a monodentate ligand) occur via a five coordinate intermediate that is formed from a LF excited state. (A schematic of the excited states is shown in Figure 1.)

However, it is not always the case in these systems that the product of the photoreactions and the thermal reactions are equivalent. Therefore the direction in which the reaction:



is driven by irradiation deserves consideration. (L in this case represents coordinating solvent or anion molecules i.e., water or chloride ions in our system.)

Some of the observed characteristics of bis(polypyridine)ruthenium(II) photoanation reactions are listed below. 1. Monodentate ligands are more efficiently displaced than chelated ligands. 2. In coordinating solvents, the incoming ligand is often the solvent molecule. 3. In low dielectric constant, non-coordinating solvents, incoming ligands are counteranions or "contaminating" water molecules.

4. Neutral ligands are not favored as incoming ligands unless they are in large excess, whereas coordinating anions are observed to substitute for neutral ligands even at stoichiometric metal to anion concentrations. The fact that the charge on the incoming ligand is particularly

crucial in these reactions is suggested by the observation that even anions that are usually non-coordinating in thermal reactions (eg. nitrate anions) do coordinate by photoreactions. 5. The equilibrium state reached by the photoreaction will obviously also be determined by the relative efficiencies of the photoanation of the reactant and product. An example of a case in which this effect is clearly illustrated is the cis trans photoisomerization of $[\text{Ru}(\text{bpy})_2(\text{H}_2\text{O})_2]^{2+}$.¹⁷ The first four characteristics listed illustrate the importance of the effect of local concentration of the incoming ligand. Solvent molecules, anions in solvents with low dielectric constants, and chelated ligands are all at a high effective concentration near the metal and will therefore be trapped by the five coordinate intermediate.

Several of the phenomena suggest possible explanations for our observations of DNA as an incoming ligand in the photoreaction. Firstly since photosubstitution reactions favor coordination to anionic ligands one possibility is that the metal may be coordinating at a phosphate anion on the DNA. We do not consider this a very likely possibility since coordination of ruthenium(II) is more favored at the softer ligands on DNA.²¹ However, there is a negative electrostatic field surrounding the DNA even in the groove away from the phosphate backbone, (according to some calculations the negative potential at the groove appears to be even greater than that of the potential at the backbone²²) this negative field may have enough of an effect to increase binding to neutral substituents on the bases within the groove. Both of the above explanations imply that photosubstitution onto the DNA occurs because of a higher local concentration of the ruthenium near the DNA. The higher local concentration is presumably not only a function of the opposite charges of the DNA and the ruthenium complex but also a function of hydrophobic interactions between the two. In any case, it is known that these complexes bind non-covalently to DNA with a K_{eq} between 10^3 - 10^4 M^{-1} . Therefore regardless of whether the interactions are ionic or hydrophobic, the end result is a higher local concentration of the ruthenium complex near the DNA.

A second possible explanation for the direction of the photosubstitution reaction is that a five coordinate intermediate that resembles, or is identical to, the transition state for the thermal reaction may be produced by decay of the LF excited state. The production of such an intermediate would effect the rate of the reaction, but not the direction. A proposal such as this one has been offered to explain some of the photosubstitution reactions observed for chromium(III) ammines.²³

A third possible explanation is that the efficiency of the photoanation of the Ru(phen)₂-DNA complex may be lower than the efficiency of the photoanation of the free Ru(phen)₂(L)₂ complex (L in this case represents water or chloride ligands.) The proposal of this possibility was prompted by some results of an investigation by Pinnick and Durham¹⁸ in which the quantum yield of photoanation was measured in dichloromethane for several compounds of the variety Ru(bpy)₂L₂. In their investigation it was found that the quantum yield of photoanation for [Ru(phen)₂(imidazole)₂] was lower than that for most of the other complexes tested. It has been noted in the literature that as is the case for many other soft transition metals a primary site of binding of ruthenium(II) and ruthenium(III) compounds on DNA is N-7 of guanine.²¹ Since this site resembles the coordination site on imidazole, it seemed possible that photoanation from this site would be less efficient than from water or chloride molecules, causing the photoreaction to be driven in the direction of binding to the DNA. However, the spectral properties of the Ru(phen)₂-DNA complex are not similar to the spectral characteristics of the Ru(bpy)₂(imidazole)₂ complex described by Pinnick and Durham. Consistent with their imidazole complex having a low quantum yield of photoanation, is the fact that it emits as strongly as Ru(bpy)₃²⁺ at room temperature.¹⁰ (Photoanation and non-radiative decay are presumed to both occur via the LF state). In contrast we find that there is no detectable emission at room temperature (or as low as 4° C) for the Ru(phen)₂²⁺-DNA complex. Therefore, there is less reason to suspect that the

quantum yield of photoanation of this complex will be as inefficient as that of the imidazole complex. The most likely explanations for the direction of the photoreaction therefore are the first two possibilities proposed above.

Photocleavage reaction

Cleavage of DNA in the presence of $\text{Ru}(\text{phen})_2\text{Cl}_2$ or $\text{Ru}(\text{phen})_3^{2+}$ was observed in our studies. In cases when cleavage occurs at the DNA binding site such a reaction would be useful to map the site of binding of these complexes on DNA. Such work is presently in progress in Dr. Barton's laboratory.

Since $\text{Ru}(\text{phen})_3^{2+}$ is known to generate singlet oxygen and singlet oxygen is known to promote cleavage of DNA,¹⁵ several experiments were done to determine if this is the mechanism of cleavage in this case. The lifetime of singlet oxygen is enhanced by D_2O ,¹⁶ so a reaction dependent on singlet oxygen should be increased in the presence of D_2O . An enhancement of the cleavage reaction in the presence of D_2O is observed (Figure 6).

Of course, D_2O may affect the cleavage reaction through effects other than enhancement of the lifetime of singlet oxygen. Therefore, further experiments were done to determine the effect of oxygen on cleavage of DNA. Figure 7 illustrates the effect of oxygen on the efficiency of the photocleavage reaction. Photocleavage is enhanced in the presence of O_2 and decreased when the samples are partially degassed with N_2 . Additional experiments by M. Fleisher in our laboratory have demonstrated that when O_2 is completely purged no cleavage occurs. Also consistent with a singlet O_2 mechanism is the observation by H.Y. Mei that histidine, a singlet O_2 quencher decreases the efficiency of this cleavage reaction.

The elucidation of the mechanism of cleavage of $\text{Ru}(\text{phen})_2\text{Cl}_2$ awaits further experiments. We would like to note, however, that it is possible that the effect of irradiation in this case may simply be to increase binding. It may be that binding itself causes a low level of

cleavage of DNA which becomes more detectable when the reaction is driven quickly to completion. Furthermore, given the tendency of bis(polypyridyl) complexes of ruthenium(II) to undergo photosubstitution reactions, it is also possible that a product of such a reaction is responsible for the DNA cleavage.

References

1. a) Meyer, T.J. (1986) Pure and Appl. Chem. **58** 1193-1206. b) Watts, R.J., (1983) J. Chem. Ed. **60** 834-42.
2. Gafney, H.D., Adamson, H.W. (1972) J. Am. Chem. Soc. **94** 8238-9.
3. Anderson, C.P., Salmon, D.J., Meyer, T.J., Young, R.C. (1977) J. Am. Chem. Soc. **99** 1980-2.
4. a) Van Houten, J., Watts, R.J. (1976) J. Am. Chem. Soc. **98** 4854-9. b) Van Houten, J., Watts, R.J. (1978) Inorg. Chem. **17** 3381-85. c) Durham, B., Caspar, J.V., Nagle, J.K., Meyer, T.J. (1982) J. Am. Chem. Soc. **104** 4803-10.
5. Creutz, C., Sutin, N. (1975) Proc. Nat. Acad. Sci. **72** 2858-62.
6. Durham, B., Walsh, J.L., Carter, C.L., Meyer, T.J. (1980) Inorg. Chem. **19** 860-5.
7. a) Lytle, F.E., Hercules, D.M. (1969) J. Am. Chem. Soc. **91** 253-7. b) Klassen, D.M., Crosby, G.A. (1968) J. Chem. Phys. **48** 1853-58.
8. Demas, J.N., Taylor, D.G. (1979) Inorg. Chem. **18** 3177-79.
9. a) Wacholz, W.M., Auerbach, R.A., Schmehl, R.H., Ollino, M., Chery, W.R. (1985) Inorg. Chem. **24** 1758-60. b) Elfring, W.H., Crosby, G.A. (1981) J. Am. Chem. Soc. **103** 2683-7.
10. Pinnick, D.V., Durham, B. (1984) Inorg. Chem. **23** 3841-2.
11. a) Barton, J.K., Goldberg, J.M., Kumar, C.V., Turro, N.J. (1986) J. Am. Chem. Soc. **108** 2081-88. b) Barton, J.K., Danishefsky, A., Goldberg, J.M. (1984) J. Am. Chem. Soc. **106** 2172-6.
12. a) Kumar, C.V., Barton, J.K., Turro, N.J. (1985) J. Am. Chem. Soc. **107** 5518-23. b) Barton, J.K., Basile, L.A., Danishefsky, A., Alexandrescu, A. (1984) Proc. Nat. Acad. Sci. **81** 1961-5.

13. Barton, J.K., Lolis, E. (1985) J. Am. Chem. Soc. **107** 708-9
14. Parker, C.A. (1956) Proc. Royal. Acad. Sci. **235** 518.
15. Hallett, F.R., Hallett, B.P., Snipes, W. (1970) Biophysical J. **10** 305-315.
16. Merkel, P.B., Wilson, R. (1972) J. Am. Chem. Soc. **94** 1030-31.
17. Bosnich, B., Dwyer, F.P. (1966) Aust. J. Chem. **19** 2229-33.
18. Pinnick, D.V., Durham, B. (1984) Inorg. Chem. **23** 1440-5.
19. Crutchley, R.J., Lever, R.B.P. (1982) Inorg. Chem. **21** 2276-82.
20. Durham, B., Wilson, S.R., Hodgson, D.J., Meyer, T.J. J. Am. Chem. Soc. **102** 600-7.
21. Clarke, M.J. (1980) Metal Ions in Biological Systems **11** 231-83.
22. Matthew, J.B., Richards, F.M. (1984) Biopolymers **23** 2743-2759.